Title
Calcium, cyclic GMP metabolism and light adaptation in rods of the bullfrog

Author
McCarthy, Sean Thomas

Publication Date
1993

Peer reviewed|Thesis/dissertation

Calcium, Cyclic GMP Metabolism and Light Adaptation in Rods of the Bullfrog

by

Sean Thomas McCarthy

DISSERTATION

Submitted in partial satisfaction of the requirements for the degree of

DOCTOR OF PHILOSOPHY

in

Bioengineering

in the

GRADUATE DIVISION

of the

UNIVERSITY OF CALIFORNIA
Berkeley &
San Francisco

PREFACE

Less than six years ago I had money, a good job and leisure time - then I became a graduate student. It was an awkward transition but, in the end, I am glad of my choice. I shall be forever thankful to all my friends and colleagues who urged me to pursue a Ph.D. and to those who similarly encouraged me to return to college during my undergraduate hiatus.

There is no way I could thank any others before first expressing my gratitude to Dr. James Younger and Professor W. Geoffrey Owen.

Beyond generously contributing his sweat and editorial prowess to the completion of my thesis, James shared data without which critical parts of the Fura-2 and calcium regulation stories could not be told. Less tangible but more important are his friendship and the hours we spent discussing science and other equally important matters.

Geoff is the master of the "phototransduction frown" - a face that we both wore when phototransduction seemed more like the Blob than a more prosaic bit of physiology. Measuring calcium in rods with Fura-2 was an idea which was conceived by Geoff in collaboration with Dr. Roger Y. Tsien. Geoff must also take credit for his encouragement and considerable intuition which played no small part in the evolution and completion of this work.

Life in the lab would not have been so interesting or educational if it were not for its other denizens. I thank Dr. Roger Miller for his *bonhomie*, generosity and for being so kind as to write his thesis as I wrote mine - misery loves company. Dr. William Hare's stories of electrodes, bicycles, EGAINT and fish are legendary. I am glad he shared his uniqueness with me. I also thank Dr. Angela Wang for helping me learn to patch-clamp and for the mantra, "ok. 1, 2, 3 ... now! BEEP". Ms. Sharareh Movafagh and Mr. Kang-Cheng (Kenny) Chen honored me by allowing me to be involved in their work and helped me to learn how to teach.

Graduate school is often paved with fiscal and bureaucratic obstacles. A graduate program which is administered jointly by two graduate divisions creates novel confusion. I am indebted to Ms. Debra Harris of the Bioengineering program for her expert help in

avoiding pitfalls. I also thank everyone else who has made the bioengineering program work, especially, Drs. Steven Lehmann and Edwin Lewis who were always enthusiastic with their assistance.

I also have a deep appreciation for Professors Juan Korenbrot, Edwin Lewis, David Copenhagen and Harold Lecar for reading this thesis and their very helpful comments. In particular, conversations I had with Juan Korenbrot and Ted Lewis about the biochemistry and specialization of sensory receptors were influential in my decision to study phototransduction in earnest.

Dr. Gian-Michele Ratto must be hailed for constructing the fluorescence apparatus and for working out many of the Fura-2 techniques that James and I later adopted. Drs. Robert Zucker and Yan-Yi Peng were very helpful when I was imaging retinal slices.

Late nights in the lab would have been unendurable if not for the lyricism of the Irish musical group Planxty (*Slainte!*), two flamenco guitarists (*gracias*), assorted opera stars (*grazie*) and a few dead composers (*danke*).

Thanks also to Dirk and especially Paul for art, politics and carousing; Margot and Malia for more art and for being my friends during a particularly bad time; and Liz "the Whiz" and Dan for encouragement and for introducing me to Jane Brody, Scout, Clio and an entirely likeable sort of lawyer.

Of course, I am also always grateful to my mother, Kathy, my sister, Colleen, my brothers, Brian and Denis, and the shorter ones Caroline, Molly, Michael and Alison who will yet get to see my potions.

Finally, thanks to the frogs.

Calcium, Cyclic GMP Metabolism and Light Adaptation in Rods of the Bullfrog

by

Sean Thomas McCarthy

ABSTRACT

A rod's response to illumination is shaped by the interplay of cGMP and calcium. I report the results of an extensive investigation of the regulation of calcium and calcium's role in phototransduction in intact rods and retinas of the bullfrog (*Rana Catesbeiana*). I show that Fura-2, the fluorescent indicator dye I employed to measure calcium, has unusual properties in the rod (existing in at least two forms) but remains a capable calcium sensor. In the dark, $[Ca^{2+}]_i$ is 100-200 nM. Suction electrode experiments demonstrated that calcium flows across the outer segment plasma membrane only through the cGMP-gated channels and the Na^+; Ca^{2+}, K^+ exchanger, whose rate is proportional to $[Ca^{2+}]_i$ near the membrane. Steady-state $[Ca^{2+}]_i$ is thus proportional to the steady-state circulating current with 20-30% of the current flowing through the cGMP-gated channels being carried by calcium ions. $[Ca^{2+}]_i$ changes sluggishly when cGMP-gated channels are shut, taking up to 15 seconds to fall to a few nanomolar during saturating illumination. The calcium kinetics, which are described by the sum of two exponentials during bright illumination, reflect the fact that less than 1% of the accessible calcium is free but also the fact that a calcium ion's movements are less hindered in the periphery of the outer segment than elsewhere. Nevertheless, the calcium dynamics can be calculated from the time course of the circulating current. Contrary to expectations, I find no evidence that calcium influences cGMP synthesis. Instead, it sharply inhibits PDE activation (K_M = 35-70 nM, Hill coefficient of 4). This effect is consistent with a calcium-triggered onset of recovery of the photocurrent after a flash. There is also an acceleration in the rate of recovery of current during prolonged illumination but it is not well correlated with changes in the cytosolic free calcium concentration. In a separate analysis of the cGMP cascade, I conclude that the second of the two transducin molecules required to activate a PDE fully has much more impact than the first.

TABLE OF CONTENTS

LIST OF FIGURES

INTRODUCTION

Photoreceptors are arrayed in a dense mosaic at the distal margin of the retina. They are the cells that capture photons - they transduce light into a neural response. In frogs, as in most vertebrates, there are several types of photoreceptor. The main classes are cones, which are important in daylight, and rods, which dominate after twilight when it is darker. Both classes are expected to have similar physiology; in this thesis I investigated only rods.

When a rod has been in the dark for a while it has a remarkable ability to respond to the capture of a single photon. When ambient illumination is brighter, the rod loses this acute sensitivity in order to respond to larger changes in light intensity. But they continue to remain responsive even when several tens of thousands of photons are captured per second. This pliancy to feast and famine is termed light adaptation.

A rod is only sensitive to changes in illumination when a current circulates between its inner and outer segment. The majority of the current flowing into the outer segment passes through cyclic-GMP gated channels and is carried by cations (Na^+, K^+, Ca^{2+} and Mg^{2+}). The remainder of the current is generated by the Na^+; Ca^{2+}, K^+ exchanger. Light interrupts the cyclic GMP-gated current, resulting in a hyperpolarization of the rod.

How light modulates the circulating current has been the subject of intense scrutiny for more than 15 years. It is now known that a train of enzymatic reactions - called the cyclic GMP cascade - is triggered when the photopigment rhodopsin absorbs a photon, converting its 11-*cis*-retinal chromophore to all-*trans*-retinal. An activated rhodopsin molecule catalyzes a GTP-for-GDP exchange on a number of G-proteins (transducins) which in turn transform cyclic GMP phosphodiesterase molecules into their highly active, cyclic GMP-hydrolyzing state (see Lamb and Pugh, 1993, for the most recent and complete review.) Thus, when photons are captured, the cytosolic cyclic GMP concentration is reduced and the mean number of open cyclic GMP-gated channels goes down.

Cyclic GMP is the diffusible second-messenger in photoreceptors, but calcium is no mere bystander. Yoshikami and Hagins (1973) demonstrated that extracellular calcium has a striking effect on rods - enough for them to propose that calcium itself was the intracellular second-messenger. That cyclic GMP has now been found to play this role does not mean that cytosolic calcium can be dismissed from the proceedings, a fact that was made even more certain by two studies I return to many times in this thesis: the delayed recovery of rods incorporating the calcium chelator BAPTA (Torre *et al.*, 1986) and the freezing of light adaptation in rods in which changes in the cytosolic free calcium concentrations were curtailed (Matthews *et al.*, 1988).

Calcium has been called the messenger of light adaptation although its mode of

action has not been completely determined. Several authors have proposed that cyclic GMP synthesis by guanylate cyclase is highly dependent on calcium concentrations, and such a mechanism has been offered as the determining factor in both the recovery of a rod after illumination and in the process of light adaptation (see for example Koch and Stryer, 1988).

In my investigation I do not find evidence in support of a strong effect of calcium in the physiological concentration range on the rate of cyclic GMP synthesis. Rather, low calcium concentrations in the rod outer segment interfere with how effectively an activated rhodopsin molecule can influence the rate at which cyclic GMP can be hydrolyzed. This effect, which I refer to as the "calcium latch", has a calcium dependence much like the calcium dependence that has been ascribed to cyclic GMP synthesis. In fact, the "calcium latch" can explain more of the classic traits of light adaptation than calcium-dependent cyclic GMP synthesis could. The data and considerations which lead to this hypothesis are contained in Chapter 5.

Calcium dynamics and cyclic GMP synthesis and hydrolysis are intertwined. Chapters 3 and 4 untangle some of the strands. I used the fluorescent calcium-indicator dye Fura-2 to measure cytosolic free calcium concentrations in rod outer segments. Fura-2 is not, however, an easy dye to use. Its properties in the retina are not what one would expect based on its design (Grynkiewicz *et al.*, 1985). Chapter 3 is, unfortunately though necessarily, a dense account of my examination of Fura-2's characteristics. Briefly, there

are at least two forms of Fura-2 but only one of these is dominant in my usual experiments. More important, cytosolic calcium concentrations can still be measured accurately.

Chapter 4 examines the regulation and dynamics of light-induced changes in calcium concentrations. Extensive use is made both of calcium measurements with Fura-2 in intact retinas and of currents recorded from intact but isolated rods. Thus, the conclusions are expected to be physiologically realistic. Of the several novel findings, the fact that the exchange current (and the cytosolic free calcium concentration) has kinetics that are much slower than previously reported (Yau and Nakatani, 1985, Hodgkin *et al.*, 1987) is perhaps the most critical. Just as instructive are the data that show that the kinetics during saturating illumination are unexpectedly described by two exponentials rather than one. A model is presented, with some physical justification, to account for the data. The important result is that the model is also predictive of calcium concentrations that are measured during the recovery of the rod from illumination and when the rod adapts to non-saturating illumination.

An important part of the work described in this thesis is highlighted in Appendix B but only referred to in the chapters (Chapters 4 and 5). It is an investigation of the activation kinetics of the cyclic GMP cascade. Similar to the work of Lamb and Pugh (1992), it differs in several important aspects. Some of these aspects allow me to separate the circulating current from the exchange current during bright illumination. Others are

critical in the identification of the "calcium latch".

I describe one more aspect of light adaptation, but this one does not appear to depend on calcium in an easily describable way. The rate at which a rod recovers after illumination changes with time, becoming faster as illumination is prolonged. The data which show this phenomenon are included in Chapter 5.

CHAPTER TWO: METHODS AND MATERIALS

Dissection

Retinas were obtained from large bullfrogs, *Rana Catesbeiana*. Frogs were killed by decapitation and double-pithed in dim red light after overnight dark adaptation. Eyes were enucleated and all remaining procedures carried out under infra-red illumination or in the dark. Retinal halves were prepared and placed separately into vials containing 2 ml of the control solution described below supplemented with 12.5 μM Fura-2 AM (Molecular Probes, Eugene OR, 97402), 0.015% Pluronic F-127 (BASF Wyandotte), and 1.9% fetal calf serum. The vials were then placed in light-tight containers and transferred for one hour to a gently stirred water-bath pre-heated to 24° C. Isolated rods were obtained from loaded retinas by gently stroking the photoreceptor layer with fine forceps and then sucking up approximately 200 μl of solution from above and around the tissue.

Fluorescence Experiments

The apparatus used to measure the fluorescence of loaded retinas is substantially the same as described by Ratto *et al.* (1988) and Younger (1991) (Fig. 1 and Fig. 2). Briefly, loaded retinas were mounted receptor-side up on black filter paper and placed into the recording chamber. A circular patch, 5.5 mm in diameter encompassing approximately 200,000 rods, was illuminated by alternating between 340 nm and 380

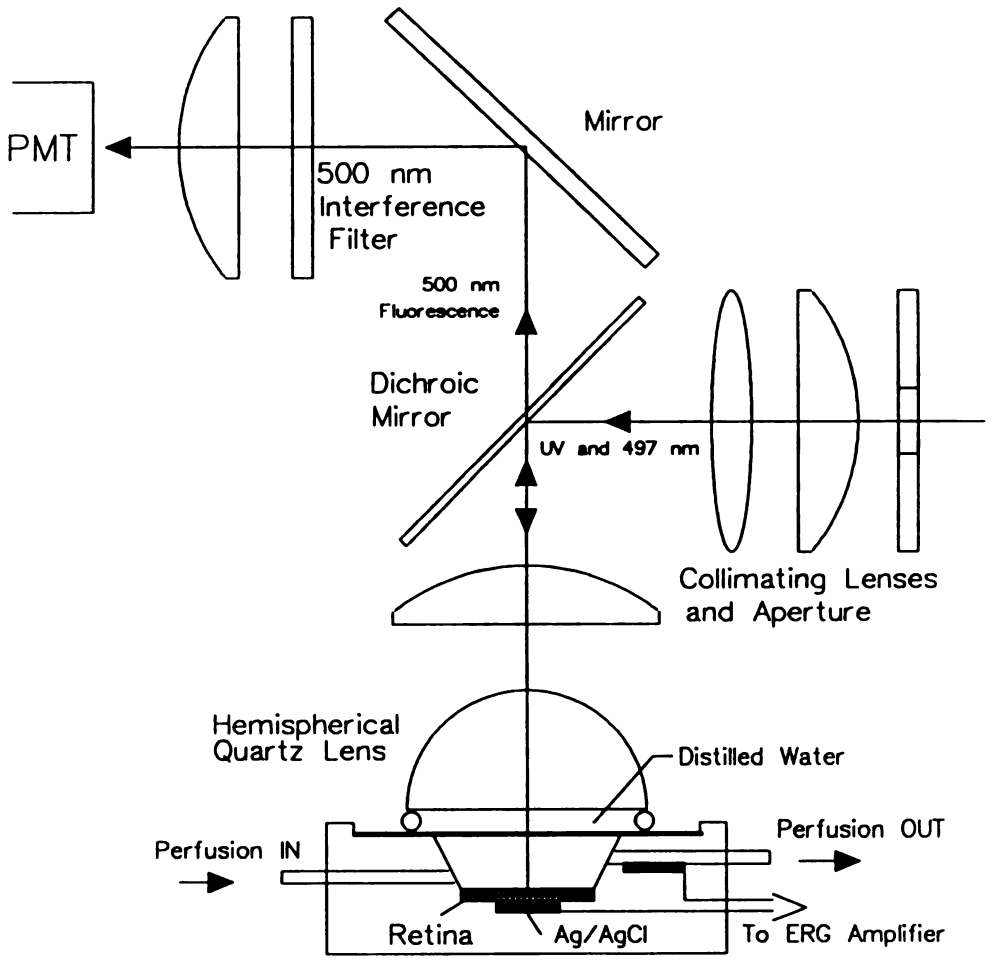

Figure 1. The arrangement inside the Faraday cage for illuminating the retina while perfusing and recording the electroretinogram. Incident UV light passes through a system of collimating lenses and is reflected down onto the retina by a dichroic mirror, passing through a hemispherical quartz lens. The lens is separated from a coverslip by a neoprene O-ring; the space between them is filled with distilled water. Ag/AgCl electrodes record the transretinal potential. Fluorescence, at around 500 nm, is passed by the dichroic mirrors and arrives at the photomultiplier (PMT) after passing through a bandpass filter centered around 500 nm and a weak lens. Adapting light at 497 nm is only weakly reflected by the dichroic mirror, but a fraction does reach the retina.

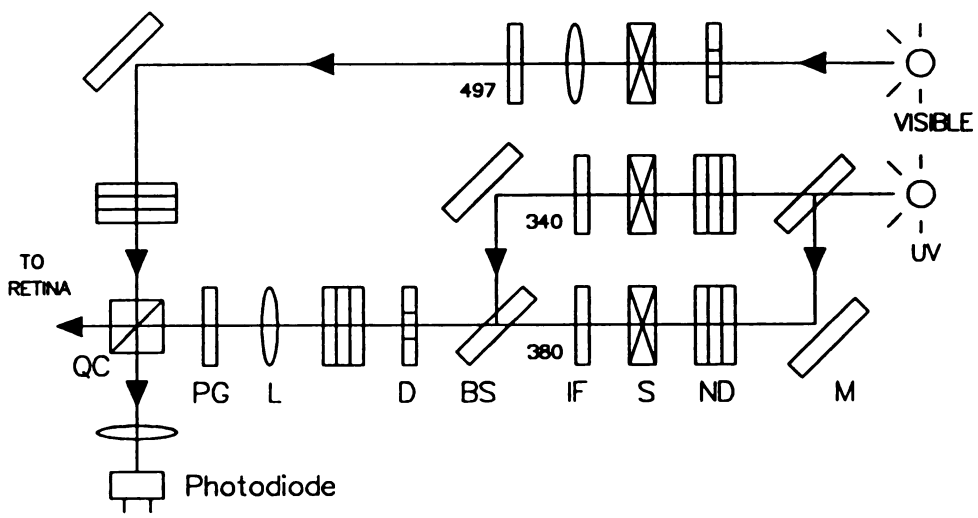

Figure 2. Layout of the optics delivering actinic and visible light to the retina in the Faraday cage. Each beam is controlled by an electronic shutter (S) and an interference filter (IF). Neutral density filters could be inserted at various points (ND). UV light from a xenon-arc source is split by a beam-splitter (BS), one resultant is bandpass filtered at 340 ± 5 nm, the other at 380 ± 5 nm. The beams are recombined by mirrors (M) and a second beamsplitter. This beam then passes through a diaphragm (D), a collimating lens (L) and a purple glass filter (PG), which cuts-out visible light. The beam of light from a quartz-halogen bulb at 497 ± 5 nm is merged with the UV beam by a quartz beamsplitter (QC). A photodiode monitored the intensity of each wavelength.

nm light. Ultraviolet illumination served both to stimulate Fura-2 fluorescence and isomerize approximately 10,000 rhodopsin molecules per second (see Younger, 1991, for a discussion of the collecting area of the rods). Visible, adapting illumination (497 nm) was delivered to the retina via the same optics. Absolute stimulus intensities were determined on a number of occasions by placing a calibrated photometer (International Light Research Radiometer, IL-1700) in the position of the retina within the recording chamber. During an individual experiment, the stimulus intensities were continuously monitored with a UV-sensitive diode (Hamamatsu, S-1226) placed in the path of light reflected from the main stimulation beam.

Up to six different solutions could be delivered to the retina during an experiment. Perfusion was driven by gravity and changes were essentially complete within one minute. Autofluorescence was measured after quenching Fura-2 fluorescence with manganese. Quenched retinas were indistinguishable from unloaded retinas in their fluorescent properties. Manganese had no effect on unloaded retinas. Photoresponses were monitored via the aspartate isolated pIII component of the electroretinogram (ERG), (Furakawa and Hanawa, 1955).

The free salt of Fura-2 was calibrated *in vitro* using the same recording chamber and stimuli described above. Fura-2 was dissolved to 1 μM in 110 mM KCl, 12 mM NaCl. The calcium-free solution contained 5 mM EGTA (ethylene glycol-bis(β-aminoethyl(ether) N,N,N',N'-tetraacetic acid). The high calcium solution contained 1.5

mM $CaCl_2$. An additional solution was used to test the validity of the calibrations. It typically contained about 100 nM free calcium using a mixture of added calcium and EGTA with appropriate corrections for pH (Martell and Smith, 1974). All solutions were buffered to pH 7.6 with HEPES (N-2-[hydroxyethyl]piperazine-N'-[-2-ethanesulfonic acid]) and N-methyl d-glucamine. Calibrations in which the expected and measured value of free calcium for the validating solution differed markedly were not used.

The calibration parameters are $R_o = 1.02 \pm 0.01$, $R_m = 41.9 \pm 2.7$ and $F = 17.5 \pm 1.5$. All values in this paper are reported mean ± s.e.m. R_o, R_m and F are used throughout this paper to represent R_{min}, R_{max} and F_o/F_s, respectively, of Grynkiewicz, *et al.*, (1985). R_o is the ratio of the fluorescence elicited by 340 nm illumination to that elicited by 380 nm illumination in the absence of calcium. R_m is the equivalent ratio measured at high calcium concentrations. F is the ratio of the fluorescence elicited by 380 nm illumination in the absence of calcium with respect to that measured at high calcium concentrations.

Suction Electrode Experiments

Photocurrents were recorded with the virtual ground/suction electrode method developed by Baylor *et al.* (1979a). Suction electrode experiments were performed in the same room and under the same conditions as fluorescence experiments, usually with cells of the same animal and often at the same time.

Suction electrodes were fabricated from cleaned, non-heparinized hematocrit tubes (Fisher Scientific, 02-668-68). Double-pulled tubes were scored with a diamond knife and then snapped to produce tips which were clean-cut and had outside diameters of 15 - 20 µm. The tips were then melted so that they were smooth and possessed an inner diameter of approximately 6 µm. Melting was accomplished by bringing the tip of the rough electrode to within 15 µm of a glass-coated platinum wire which had been heated to a dull red. Successfully prepared electrodes were placed in a bell jar within a pre-heated oven and baked at 300°C. After 30 minutes, the oven was turned off and 10 µl of silane (γ-methacryloxypropyltrimethoxysilane) was injected into the bell jar. Electrodes remained within the bell jar and oven until they cooled to room temperature. Completed electrodes were stored in covered containers and were re-used for as long as they gave satisfactory recordings.

Isolated photoreceptors were squirted into the suction electrode recording chamber and allowed to settle for approximately 15 minutes. Perfusion of this chamber was also driven by gravity and changes were complete within a few minutes. Effluence was removed from the chamber with a filter-paper wick. Depending on the objectives of an experiment, either the inner segment or outer segment of a rod was gently sucked into an electrode. The pressure within the electrode was controlled with a screw-driven, 250 µl syringe. Pressure variations were monitored via a transducer connected to the syringe. Electrical connections were made via agar bridges (2-3% wt/wt) connected to calomel electrodes which I constructed. Details of the recording chamber and electrical

connections are shown in Fig. 3.

Photocurrents were low-pass filtered at 9.8 Hz and recorded at least every 25 milliseconds. The basic design of the current monitor (Fig. 4) was a gift from Dr. Vincent Torre. I have, however, redesigned several components. I have removed a filtering capacitor from the headstage and introduced buffers to transmit the output of the virtual ground and the common ground from the headstage to a central differential amplifier in order to decrease common-mode interference. I have also employed a simple follower to control the bath potential. I found this form of active feedback reduced low-frequency drift. I suspected that the original, more sophisticated and more usual feedback circuit introduced drift as a result of fluctuations in the voltage offsets of the constituent operational amplifiers (one microvolt corresponds to approximately 0.5 pA in the experiments). Noise at 60 Hz was virtually eliminated by driving the bath at 60 Hz but 180° out-of-phase with the noise. Ultimately, fluctuation of the resistance of the seal between the rod and electrode was the largest source of extraneous noise.

A schematic representation of the optical arrangement for the suction electrode experiments is shown in Fig. 5. Stimuli illuminated a 150 μm by 50 μm rectangular area centered on an isolated rod with 565 nm light from narrow band LEDs. Each LED could be controlled independently and was extremely linear. Infra-red illumination, which did not adapt rods, allowed cells to be viewed on a video monitor. The video camera was placed outside of the Faraday cage in order to reduce electrical noise. Absolute stimuli

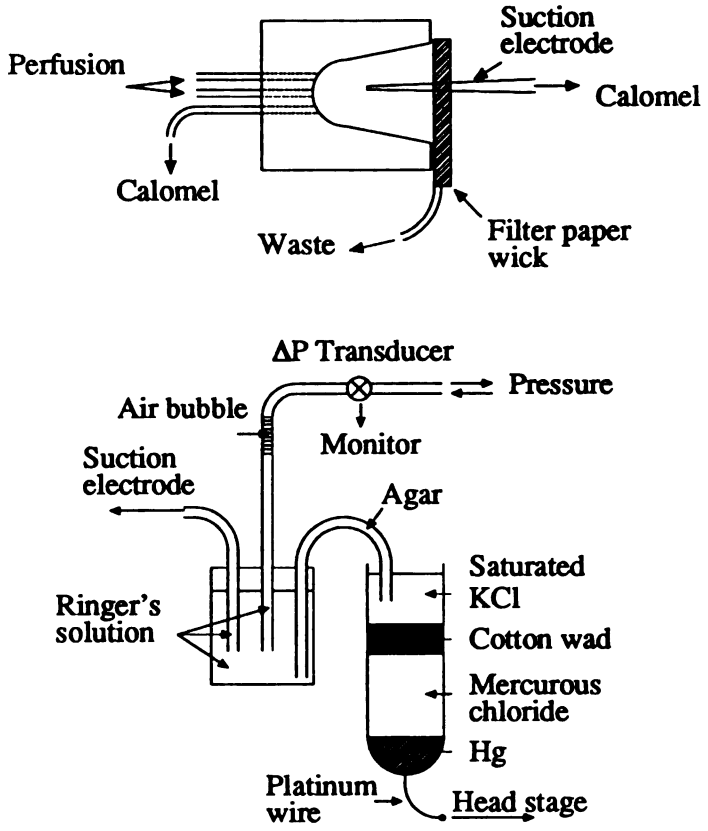

Figure 3. The recording chamber and electrical connections for suction electrode experiments. The chamber was machined from black PVC and glued to a glass slide which had been coated with silane. A cover slip on top of the chamber retained the solution and aided in focusing the stimulus. The bath and suction electrode were connected to calomel electrodes (Cobbold, 1974) via reservoirs of Ringer's solution and agar bridges (only one reservoir/calomel electrode pair is shown). The pressure within the suction electrode was controlled with a screw-driven syringe attached to the Ringer's reservoir. An air bubble between the syringe and reservoir helped to reduce antenna pick-up.

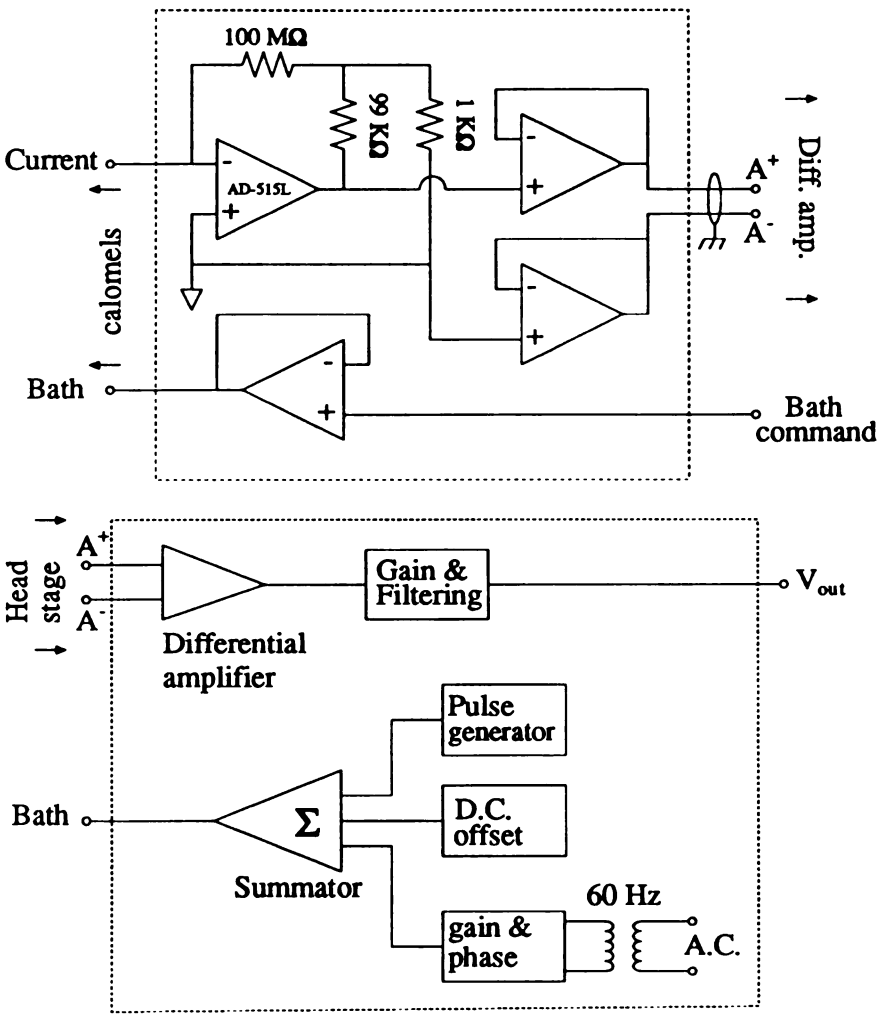

Figure 4. Virtual ground amplifier and bath control. The output of the AD-515L (MOSFET) was 10 mV/pA. Additional amplification, as well as low-pass filtering, were performed at a later stage. The bath potential was controlled by an operational amplifier follower. Its command was the sum of a DC potential, to offset junction potentials, and a manually controlled 60 Hz feedback. The pulse generator was used to measure the resistance of the suction electrode before and after sucking in a rod.

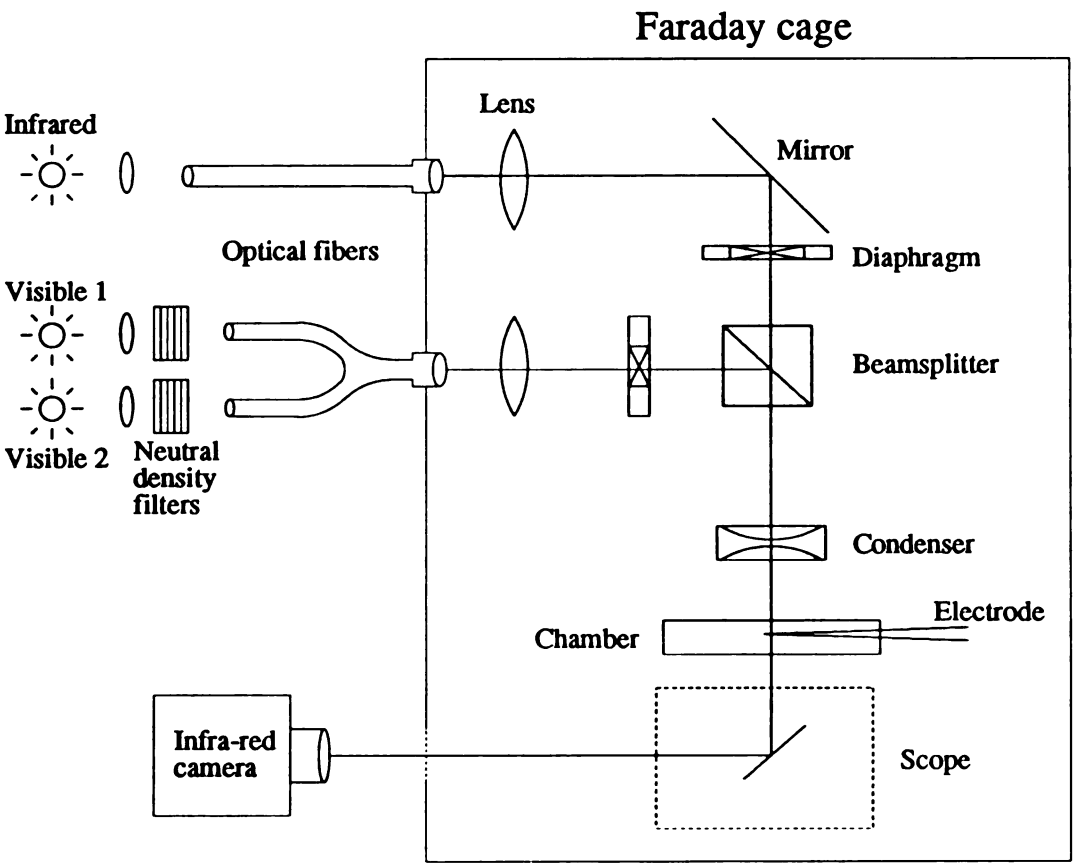

Figure 5. The arrangement for stimulating and visualizing rods in the suction electrode experiments. Illumination in all cases was derived from light-emitting diodes focused onto fiber optic cables. Merging the output of the two visible LEDs (565 nm), which were controlled independently, allowed me to deliver steady illumination and flashes of vastly different intensities. Neutral density filters could be added and removed as desired. Attenuation factors of 0 to 5 O.D. were typical. An infra-red sensitive camera, which was placed outside the Faraday cage to reduce noise, collected the image of the cells that was directed at it by the inverted microscope. Experiments were performed in a very dark room. All sources of extraneous light (computer screens, pilot lights, etc.) were either made opaque or covered with red film.

intensities were determined with the IL-1700 photometer mentioned previously.

Imaging

Fluorescence imaging of retinal slices and isolated rods was performed with the dynamic ratio imaging system described by Tsien and Harootunian (1990). Slices and isolated cells were prepared from loaded retinas. Light intensities required for satisfactory images were many times brighter and longer in duration than those required for calcium measurements in intact retinas. In addition, it was impractical to shield the cells from the dim ambient lighting of the imaging apparatus. Under these conditions, rods are expected to be completely light adapted. However, whole retinas exposed to the same conditions for comparable times remained reddish pink, indicating that extreme bleaching of rhodopsin did not occur.

Solutions

Solutions were made anew for each day's experiments. The control solution contained 94 mM NaCl, 27 mM $NaHCO_3$, 3.5 mM KCl, 0.6 mM $MgCl_2$, 0.6 mM $MgSO_4$, 1 mM CsCl, 1.5 mM $CaCl_2$, 9 mM glucose, 1 mM ascorbic acid, 1 mM Na-pyruvate, 10 mM Na-aspartate and 3 mM HEPES. Caesium, which blocks the voltage-dependent channels of the rod inner segment (Bader *et al.*, 1982), was added in order to resolve exchange currents better. Aspartate abolished light responses in all retinal neurons except

photoreceptors, as confirmed by recording the pIII component of the ERG (the late receptor potential) (Furakawa and Hanawa, 1955). The Ca^{2+}-free solution was identical to the control solution except for the exclusion of $CaCl_2$ and inclusion of 5 mM EGTA. The Fura-2 quenching solution was also identical to the control solution but with the substitution of 5 mM $MnCl_2$ for $CaCl_2$ and addition of 500 µM IBMX (3-isobutyl-1-methylxanthine). In later experiments, IBMX was omitted from the quenching solution without significant effect. The normal/IBMX solution was the control solution with 500 µM IBMX and, in some instances, 10 µM of the calcium ionophore, ionomycin. The guanidinium/IBMX solution contained 134 mM CH_5N_3-HCl, 1.5 mM $CaCl_2$, 3.5 mM K-aspartate, 500 µM IBMX, 9 mM glucose and 3 mM HEPES. The isotonic calcium solution contained 88 mM $CaCl_2$, 10 mM hemi-magnesium aspartate, 500 µM IBMX, and the normal concentrations of ascorbic acid, glucose and HEPES. The membrane-permeable, heavy-metal chelator, N,N,N',N'-tetrakis(2-pyridylmethyl)ethylenediamine (TPEN), was added to the above solutions to a concentration of 50 µM, when noted. All solutions had a pH of 7.5 to 7.6. Solutions were titrated with N-methyl d-glucamine when necessary.

CHAPTER THREE: CYTOPLASMIC FREE CALCIUM CONCENTRATIONS DETERMINED IN THE PRESENCE OF MULTIPLE FORMS OF FURA-2 IN RODS OF THE BULLFROG

INTRODUCTION

Cytosolic free calcium in rod outer segments has been shown to mediate a powerful negative feedback in phototransduction. Torre *et al.* (1986) showed that slowing the rate of change of cytoplasmic calcium by incorporating the calcium chelator, BAPTA (1,2-bis(*o*-aminophenoxy)ethane-N,N,N',N'-tetraacetic acid), significantly altered the amplitude and retarded the recovery of dim flash responses. Matthews *et al.* (1988) reported similar results when a rod's ability to extrude calcium was blocked and calcium influx was minimized. The study by Matthews *et al.* (1988) also made it clear that normal calcium regulation is required for resetting flash sensitivity during sustained illumination. These findings strongly suggest that light-induced changes in the cytosolic free calcium concentration play an important part in light adaptation.

Proof of this hypothesis requires, of course, that the cytosolic free calcium concentration changes when rods are illuminated. Several studies have shown this to be true. Yau and Nakatani (1984) and Hodgkin *et al.* (1985) demonstrated that calcium is extruded during illumination in an electrogenic exchange for sodium. McNaughton *et al*,

(1986) measured the calcium concentration more directly with the luminescent photoprotein, aequorin, and set an upper limit of approximately 600 nM in the dark and lower than this during illumination. Using the more sensitive calcium probe, Quin-2, Korenbrot and Miller (1989) measured a cytosolic free calcium concentration in toad rods of 273 ± 129 nM in the dark and no less than 50 nM in bright light. Ratto *et al.* (1988) reported similar results using Fura-2. Their values were 220 nM in the dark and approximately 140 nM after about six seconds of bright illumination. Although all these studies demonstrate that illumination results in a reduction in the concentration of cytosolic free calcium in rods, the absolute concentrations reported are problematic.

The calcium concentrations measured, particularly the latter two, do not appear to be in complete concordance with the range of concentrations expected to influence phototransduction based on biochemical evidence. At least part of calcium's regulation of light adaptation is believed to occur via guanylate cyclase, which is modulated by calcium concentrations below 100 nM according to Lolley and Racz (1982), Pepe *et al.* (1986), Koch and Stryer (1988), or 200 nM according to Dizhoor *et al.* (1991). Early reports also suggest that calcium may have a regulatory action on phosphodiesterase, although Barkdoll *et al.* (1989) ruled out any effect below 10 μM of free calcium unless a soluble protein was also involved. More recently Kawamura and Murakami (1991) have suggested that just such a modulator protein causes a drastic change in the activity of phosphodiesterase between 30 nM and 1 μM of free calcium. Lagnado and Baylor (personal communication to W.G. Owen) have found that free calcium below 100 nM is

a strong regulator of phosphodiesterase activity. Yet another calcium-dependent effect has been recently reported by Hsu and Molday (1993). They reported that calmodulin influences the cyclic GMP-gated channel. This too would occur when the cytosolic free calcium is submicromolar. While the cytoplasmic free calcium concentrations reported for rods in the dark do not dispute the biochemical evidence, the concentrations reported for rods stimulated with bright light suggest that the full range of the potential influence of calcium is not utilized during light adaptation.

A more serious challenge to the reported cytosolic free calcium concentrations during bright illumination comes from the work of Cervetto *et al.* (1989). They convincingly demonstrated that potassium is extruded along with calcium by the exchange mechanism. During bright illumination, when all cyclic GMP-gated channels are shut (Baylor and Nunn, 1986), the Na^+; Ca^{2+}, K^+ exchanger is expected to reach equilibrium. The cytosolic free calcium concentration should be only a few nanomolar at this time: much lower than if only sodium and calcium were involved in the exchange process. This concentration is well below the values measured during the bright illumination of rods by either Korenbrot and Miller (1989) or Ratto *et al.* (1988).

The involvement of potassium in the exchange mechanism and the mismatch of the expected and measured calcium concentrations prompted first Younger (1991) and then me to examine more closely the concentration of free calcium in the cytosol of rod outer segments and the veracity of Fura-2 as a calcium indicator in this application. We

find that the concentration of cytosolic free calcium in the outer segment is, indeed, reduced to a few nanomolar during bright illumination. I also find that the behavior of Fura-2 loaded into rods is quite unexpected but that this behavior explains the high apparent calcium concentration during bright illumination reported by Ratto *et al.* (1988). My analysis of the properties of Fura-2 in rods, particularly its separation into at least two different calcium-sensitive pools, may be of value to any researcher utilizing Fura-2 for quantitative determinations of calcium concentration. More important, however, it has allowed me to measure the time course and magnitude of the light-induced changes in cytosolic free calcium concentration in rod outer segments.

RESULTS

Free Cytosolic Calcium is a Few Nanomolar in Bright Lights

Classical determinations of calcium concentrations with Fura-2 have used the fluorescence ratio method described by Grynkiewicz *et al.* (1991) The fluorescence ratio is defined as the fluorescence elicited by 340 nm illumination divided by the fluorescence elicited by 380 nm illumination after appropriate corrections for autofluorescence have been made. In Fig. 1*A* and Fig. 1*B*, I show the average time course of fluorescence elicited by each stimulus wavelength from three dark-adapted retinas. The resulting fluorescence ratio is shown in Fig. 1*C*. The corresponding photocurrent of seven isolated rods loaded with Fura-2, is shown in Fig. 1*D*. The stimulus in each case was a six-second step of illumination that isomerized 10,000 rhodopsin molecules per second. Within 250 ms of the onset of illumination, all cyclic GMP-gated channels are shut and a ratio of four is measured. During the next six seconds, cyclic GMP-gated channels remain shut and the exchange current and fluorescence ratio decline. If the same behavior continued, one would expect a final, steady-state fluorescence ratio of 2.5. In fact, experiments in which actinic stimuli were presented for 60 seconds demonstrated that this behavior does continue and final, steady-state ratios are achieved within approximately 15-20 seconds (Younger, 1991). The fluorescence data shown in Fig. 1 are similar in most respects to those reported by Ratto *et al.* (1988) and Younger (1991).

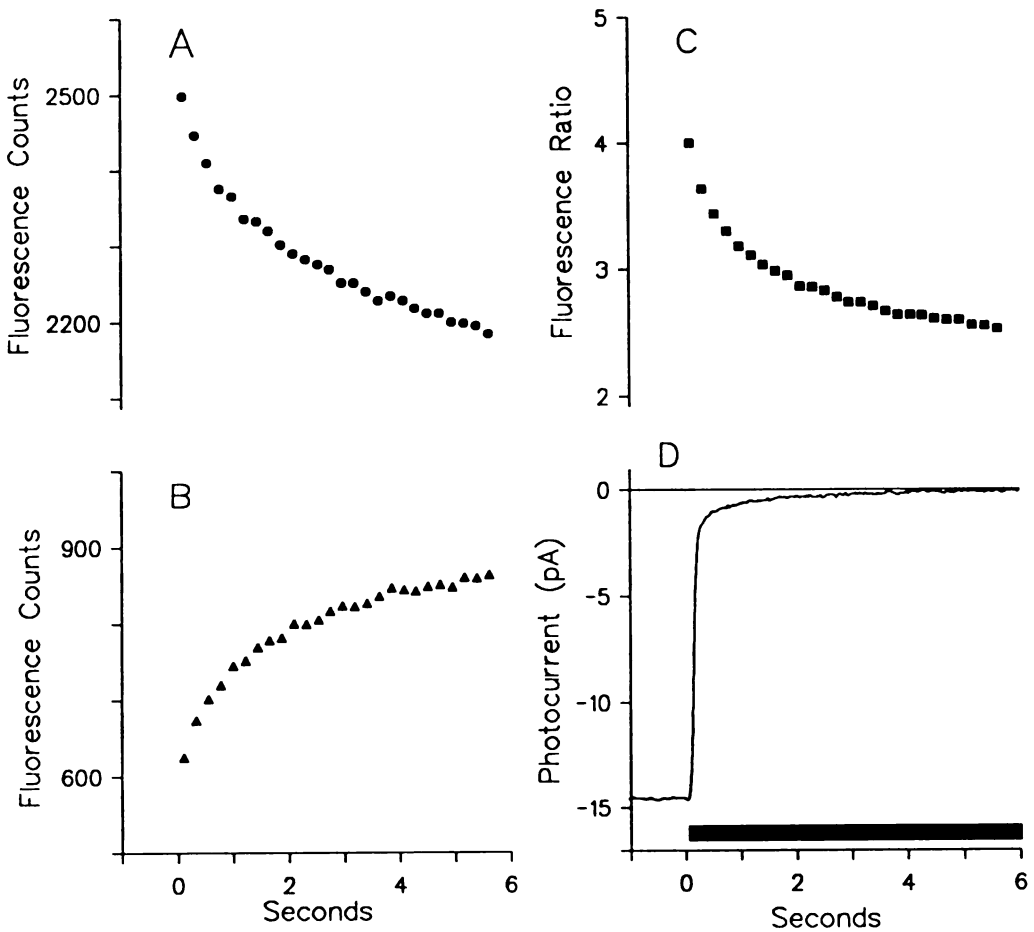

Figure 1. The fluorescence elicited from dark-adapted retinas and the photocurrent recorded from isolated, Fura-2 loaded rods. *A*, the fluorescence measured during 340 nm illumination and, *B*, during 380 nm illumination. Fluorescence is displayed as the number of counts recorded by a cooled photomultiplier tube during a period of 100 milliseconds. *C*, the ratio of the data displayed in *A* with respect to those displayed in *B*. The data shown are the average from three different retinas and a total of 165 trials. *D*, the average photocurrent recorded from seven isolated rods obtained from five different frogs: a total of 35 trials. The slow relaxation of the photocurrent to zero is a result of the action of the Na^+: Ca^{2+}, K^+ exchange mechanism. Stimuli isomerized approximately 10,000 rhodopsin molecules per rod per second for six seconds and were repeated every minute.

Based on the *in vitro* calibration parameters (Chapter 2), a final, steady-state ratio of 2.5 suggests that the cytoplasmic free calcium concentration is approximately 65% of the calcium dissociation constant of Fura-2 which is expected to be on the order of 100 nM in rods. However, as discussed above, the action of the Na^+: Ca^{2+}, K^+ exchange mechanism is expected to reduce the cytoplasmic free calcium concentration to a few nanomolar.

Younger (1991) and I tested whether the final, steady-state ratio truly reflects an absence of free calcium ions by exposing retinas and isolated rods to a Ca^{2+}-free perfusate. Soon after exposure, both the retinal ERG and light-suppressible current of isolated rods increased in magnitude. At the same time, the duration of the rising phase of the photocurrent - the time required to close cyclic GMP-gated channels - increased. Over the course of the next ten to fifteen minutes, the magnitudes of the ERG and photocurrent decreased to a level below the control value and the rising phase continued to slow, lasting slightly longer than one second at the end of the exposure. This behavior is consistent with a large increase in cytoplasmic cyclic GMP concentration brought about by a low cytoplasmic calcium concentration. The decrease in photocurrent observed is consistent with observations by Hodgkin *et al.* (1984) and is probably caused by diminished ionic gradients resulting from the high permeability of the outer-segment plasma membrane.

During exposure to the Ca^{2+}-free perfusate, no exchange current was observed in

isolated rods and no light-induced change in fluorescence was evident from Fura-2 loaded retinas. In Fig. 2*A*, I compare the average fluorescence ratio obtained from a retina in the control solution to that obtained after several minutes exposure to the Ca^{2+}-free solution. The projected final, steady-state ratio in bright light is the same as the ratio measured in the Ca^{2+}-free solution. In 14 additional experiments, the average fluorescence ratio measured for retinas perfused with the Ca^{2+}-free solution was 2.0 ± 0.1. The final, steady-state ratio in the control solution was 2.0 ± 0.1 in these same 14 retinas. In Fig. 2*B*, the ratios obtained in the Ca^{2+}-free solution are plotted with respect to the final, steady-state ratios obtained in the control solution for each retina. The correlation is clear. The least-squares regression line expressing the relationship has a slope of one, a negligible intercept and a squared correlation coefficient of 0.84 suggesting each ratio measures the same cytosolic free calcium concentration. These observations mean that the cytoplasmic free calcium concentration after approximately 15 seconds of bright illumination is no more than a few nanomolar.

I originally believed that the unexpectedly large value of the final, steady-state fluorescence ratio measured in bright light could be a consequence of the presence of zinc in the retina. Grynkiewicz *et al.* (1985) reported that the affinity of Fura-2 for manganese, iron and zinc is 50 to 100-fold greater than its affinity for calcium. While manganese and iron quench Fura-2 fluorescence, zinc-bound Fura-2 is similar to the calcium-bound form. The EGTA in the Ca^{2+}-free solution, however, also has a much greater affinity for zinc than for calcium. The correlation between the final, steady-state

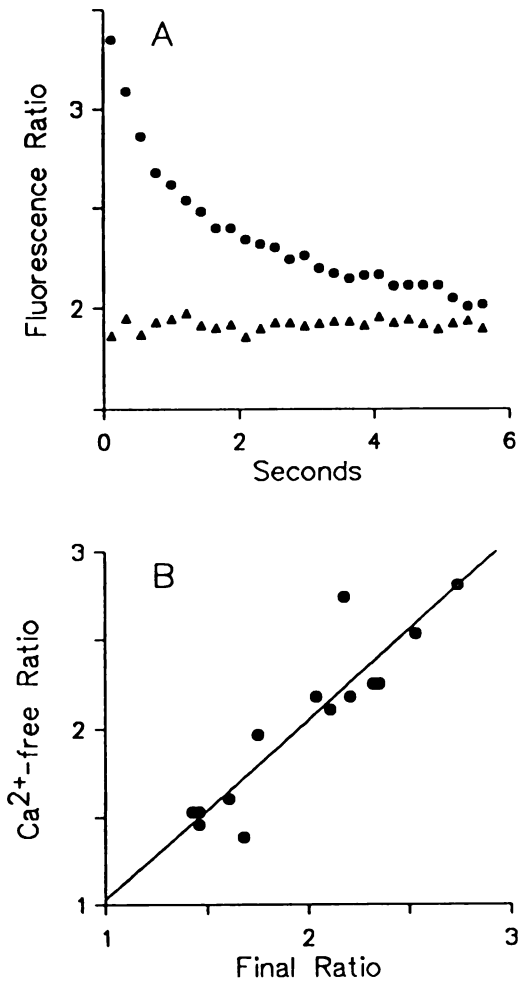

Figure 2. The equivalence of the final, steady-state fluorescence ratio projected for retinas exposed to the control solution and the fluorescence ratio measured for retinas exposed to the Ca^{2+}-free solution. *A*, the average fluorescence ratio measured for five trials with a single retina exposed to the control solution (circles) and five trials when the retina had been exposed to the Ca^{2+}-free solution for several minutes (triangles). *B*, the relationship between the final, steady-state ratio expected for 14 retinas exposed to the control solution and the fluorescence ratio measured for the same retinas while they were exposed to the Ca^{2+}-free solution. The regression line, determined by the least-squares method, has a slope of 1.02 and an intercept of 0.05 ($R^2 = 0.84$). The data shown in *B* were obtained by Dr. James Younger.

ratio measured in bright light and the fluorescence ratio measured in the presence of the Ca^{2+}-free solution suggests, therefore, that zinc does not account for the large value of either ratio. In addition, the data shown in Figures 1 and 2*A* were recorded from retinas that were perfused with solutions that contained the membrane-permeable, heavy-metal chelator, TPEN, first used in a similar application by Arslon *et al.* (1985). The fluorescence ratios recorded from retinas that were not exposed to TPEN were no different than those shown. Hence, the value of the fluorescence ratio in bright light, which is the *in situ* value of R_o, must be explained in some way other than as the consequence of heavy-metal contamination.

Classical Fura-2 Calibration in High Calcium

A number of experiments included procedures intended to measure the *in situ* values of R_m and F, in accordance with the classic ratio method of calcium determination. In each procedure, retinas were perfused with solutions designed to increase cytoplasmic free calcium concentrations. Most of these solutions contained the cyclic GMP phosphodiesterase inhibitor, IBMX. Some also included the calcium ionophore, ionomycin, which did not appear to have any additional effect (Younger, 1991). The estimates of the value of F are with respect to the 380 nm fluorescence elicited six seconds after the onset of stimulation from retinas bathed in the control solution. The fact that the calcium concentration at this time is still a few tens of nanomolar means, therefore, that the estimates of the value of F are slightly low. When Younger (1991)

exposed retinas to the normal/IBMX perfusate, the fluorescence ratio increased rapidly and averaged 13.0 ± 1.1 in eight such experiments. The apparent value of F for the same experiments was 2.0 ± 0.1. Six similar experiments with retinas perfused with the guanidinium/IBMX solution yielded an R_m of 11.5 ± 1.2 and an F of 2.1 ± 0.2 (Younger, 1991). The substitution of guanidinium for sodium ensured that the Na^+: Ca^{2+}, K^+ exchange mechanism could not extrude calcium from the rod outer segment (Yau and Nakatani, 1988). Exposure of retinas to an isotonic calcium/IBMX solution emulated the technique of Hodgkin *et al.* (1987). They exposed isolated salamander rods to an isotonic calcium/IBMX solution to measure the properties of the Na^+: Ca^{2+}, K^+ exchanger. With rapid solution changes, they estimated an increase in total calcium concentration of approximately one millimolar within ten seconds. My solution changes were not as rapid but I expected a similar elevation in calcium concentration. The estimated maximum ratio, R_m, in two retinas exposed to isotonic calcium/IBMX was 10 ± 1. The apparent value of F in this solution was approximately 0.5, a lower value than in the other solutions. A value of F below 1 means that the fluorescence elicited by 380 nm illumination paradoxically increased when I exposed the retina to the high calcium solution. No TPEN was present in these solutions and so the low value of F may be a consequence of competition between calcium and the heavy metals that normally quench Fura-2.

All three solutions yield similar results, more similar than would be expected if the cytoplasmic calcium concentrations they represent were very different in each case.

Yet all three parameters, R_o, R_m and F are significantly different *in situ* than *in vitro*. There are several ways in which this could occur. In the retina, one excitation wavelength could be absorbed by the retina more than expected. The value of F would be unchanged in this case, however, since it depends only on 380 nm stimulation. Another possibility is that there is some source of fluorescence for which I have not accounted. Fura-2 compartmentalization, such as within the disks of the rod outer segment, binding competition with some other element or intracellular component, or the presence within rods of multiple forms of Fura-2 all seem possible. It is also possible that the excitation spectrum of Fura-2 is significantly altered by intracellular factors such as polarity or viscosity (Roe *et al.*, 1990, Poenie *et al.*, 1990, Uto *et al.*, 1991). Each of these possibilities can be tested.

Fura-2 is not Significantly Compartmentalized in Rod Cells

Ratto *et al.* (1988) estimated that approximately 90% of the fluorescence elicited from the retina originates in the outer segment. This estimate was based on calculations of the fraction of the excitation and emission that is absorbed by rhodopsin in the outer segment and an extensive assay of the concentration and distribution of Fura-2 in the retina.

I used a fluorescence imaging system that allowed me to estimate the relative intensities elicited at each wavelength from retinal slices and isolated rods to make a more

direct estimate of the relative contribution from each region of the retina. By far the brightest region of slices were their photoreceptor layers. Fluorescence from the remainder of the retina was unmeasurable above background contributions, except for an occasional ganglion cell. The higher concentration of Fura-2 in rod cells is consistent with the expectation of Ratto *et al.* (1988) who noted that only photoreceptors and ganglion cells were in contact with the loading solution and that the rod's surface area is much greater than that of any other cell in the retina. Within isolated rod cells and in the photoreceptor layer of slices, the inner segment region was approximately three times brighter than the outer segment region for both 340 nm and 380 nm excitation. The difference in intensity might suggest that Fura-2 is several times more concentrated in the inner segment than in the outer segment. However, the cytosol accounts for only approximately half the total volume of an outer segment. The remainder of the outer segment is occupied by lipid bilayer disks. When absorption by rhodopsin in the outer segment is also considered, which I estimate to be approximately 10% when illuminated transversely, it seems that the concentration of Fura-2, with respect to cytosol, is only approximately 1.25-1.5 times greater in the inner segment than in the outer segment. From these measurements, I estimate that 80 to 90% of the total fluorescence observed in the usual experiments originates in the outer segment, in good agreement with Ratto *et al.* (1988).

It was hard to measure fluorescence ratios precisely with the imaging apparatus because of the difficulties encountered in measuring autofluorescence. Fura-2 quenching

never occurred rapidly enough for me to be confident of the results. However, when loaded slices were compared with unloaded slices, it was clear that a large fraction of the total fluorescence elicited from the photoreceptor layer of loaded slices was derived from Fura-2. My subsequent estimates of the fluorescence ratios were 1.5 for both the outer segment and inner segment. The ratio obtained for the calcium-free form of Fura-2 in this system was approximately 1. The results from the imaging apparatus are consistent with the fluorescence ratio observed in response to low calcium in my usual experiments (see also Younger, 1991). It also suggests, within the certainty of the estimates, that the intracellular properties of Fura-2 are the same in the inner and outer segments and that the potentially high calcium concentration within the outer-segment disks (Szuts and Cone, 1977, Schröder and Fain, 1984, Somlyo and Walz, 1985) is not significantly sensed by Fura-2.

Light-induced Change in Fluorescence Arises from the Outer Segment

The results of the imaging studies support the notion that most of the fluorescence measured in experiments using retinal halves derives from Fura-2 in the outer segments of rods. However, I have tested this hypothesis in another manner and, more importantly, resolved with surety that light-induced changes in fluorescence originate in outer segments.

In the usual experiments, retinas were mounted on circular pieces of filter paper

so that the photoreceptors are nearest the stimulus. This arrangement allows me to derive full benefit from rhodopsin screening. I altered this configuration in several experiments in a manner similar to that of Ratto *et al.* (1988). In these experiments, retinas were sandwiched between two filter-paper annuli. Experiments began with the photoreceptor layer nearest to the stimulus as in the usual experiment. Midway through the experiment, retinas were quickly but very carefully inverted so that the photoreceptor layer was now distant from the stimulus. The results of each such procedure with a loaded retina were compared to the results of the same procedure applied to an unloaded retina from the same frog. In both the photoreceptor-up and photoreceptor-down configuration, the fluorescence contribution from the outer segments should be nearly equivalent because the remainder of the retina is fairly transparent to the excitation and emission wavelengths. However, the contribution from the inner segments and other retinal neurons should be much greater when the photoreceptors point downward.

I found that the total fluorescence elicited from the retina was approximately three times brighter in the photoreceptor-down configuration than in the photoreceptor-up configuration, slightly greater than that found by Ratto *et al.* 1988. The greater total fluorescence in the photoreceptor-down configuration suggests that the shielding of Fura-2 in the inner retina by rhodopsin in the outer segment is significant. The light-induced change in fluorescence when the photoreceptors were distant from the stimulus was approximately 70% of the light-induced change in fluorescence recorded from the photoreceptor-up configuration. In both cases, however, the light-induced change in

fluorescence had the same time course (see Fig. 9 of Chapter 4). The decrease in intensity may be due to loss of rod cells incurred when flipping retinas or from ultraviolet absorption by the retina. The observation that the photoreceptor-down fluorescence had the same time course but was less intense than the photoreceptor-up fluorescence means that the light-induced change in fluorescence for each configuration originates in the outer segments of rods. This conclusion does not depend on corrections for autofluorescence.

Fluorescence Observed is Incompatible with the Ratio Method

One possible explanation of the results of the *in situ* calibration is that the fluorescent properties of Fura-2 are significantly altered by intracellular factors. There is a way, which I believe has not been presented previously, to test this possibility.

Fluorescence elicited by each excitation wavelength may be written as:

$$\phi = \phi_o + \phi_\beta \beta \qquad (1)$$

$$\psi = \psi_o + \psi_\beta \beta$$

where ϕ (ψ) is the Fura-2 fluorescence elicited by 340 nm (380 nm) illumination, ϕ_o (ψ_o) is the Fura-2 fluorescence that would be emitted if all available Fura-2 were in the calcium-free form, ϕ_β (ψ_β) is the difference between the Fura-2 fluorescence that would be emitted if all Fura-2 were in the calcium-bound form and the Fura-2 fluorescence that would be emitted if it were all in the calcium-free form. The variable β represents the

fraction of available Fura-2 that is in the calcium-bound form. Simple algebraic manipulation of eqn (1) results in an expression relating the fluorescence elicited by 340 nm illumination to that elicited by 380 nm illumination.

$$\phi = m\,\psi + (\phi_o - m\,\psi_o) \tag{2}$$

where I have defined a slope, m, as ϕ_β/ψ_β.

In the usual calibration of Fura-2, four observations, the fluorescence elicited by each excitation wavelength in low and high calcium, are used to determine three parameters, R_o, R_m and F. The slope, m, is a fourth parameter that may be determined from the classic calibration without additional information. Unlike the determination of the values of R_o, R_m and F, however, determination of m does not require corrections for background fluorescence or autofluorescence. An examination of eqn (2) makes it clear that background fluorescence only affects the intercept of the line relating the Fura-2 fluorescence elicited at each stimulating wavelength.

The slope, m, may be measured independently from R_o, R_m and F. It may also be predicted from those parameters.

$$m \equiv \frac{\phi_\beta}{\psi_\beta} = \frac{R_m - R_o F}{1 - F} \tag{3}$$

where

$$R_o = \frac{\phi_o}{\psi_o} \qquad R_m = \frac{\phi_o + \phi_\beta}{\psi_o + \psi_\beta} \qquad F = \frac{\psi_o}{\psi_o + \psi_\beta}$$

The *in vitro* calibration yields an expected slope of -1.5 (R_o = 1.02, R_m = 41.9 and F = 17.5). Calibration parameters reported by Grynkiewicz *et al.* (1991) yield an expected slope of -1.6. In experiments with retinas exposed to the control solution, the measured slope was normally between -1.4 and -1.6 and averaged -1.5. The average fluorescence elicited by 340 nm illumination from eight experiments is plotted with respect to the average fluorescence elicited by 380 nm excitation in Fig. 3. I have plotted a line with a slope of -1.5 through the data to demonstrate how well it is described. This strongly suggests that the light-induced change in fluorescence observed in retinas exposed to the control solution originates from a pool of Fura-2 that is very similar to the *in vitro* form.

The slope predicted from the *in situ* calibration is approximately -8, using R_o = 2.0, R_m = 12 and F = 2. This prediction is not consistent with the light-induced behavior of the fluorescence I measure. When I examined the fluorescence elicited from retinas perfused with the normal/IBMX solution, it became clear that the classical ratio method was not applicable to the data. The average total fluorescence measured by Dr. James Younger in eight experiments in response to 33 seconds of excitation is displayed in Fig. 4*A*. The same data is plotted in Fig. 4*B* but in the form of Fig. 3 The lower right portion of the data corresponds to last 10 seconds or so of excitation and is well described by a line with a slope of -1.5. The remainder of the data is obviously different. The failure

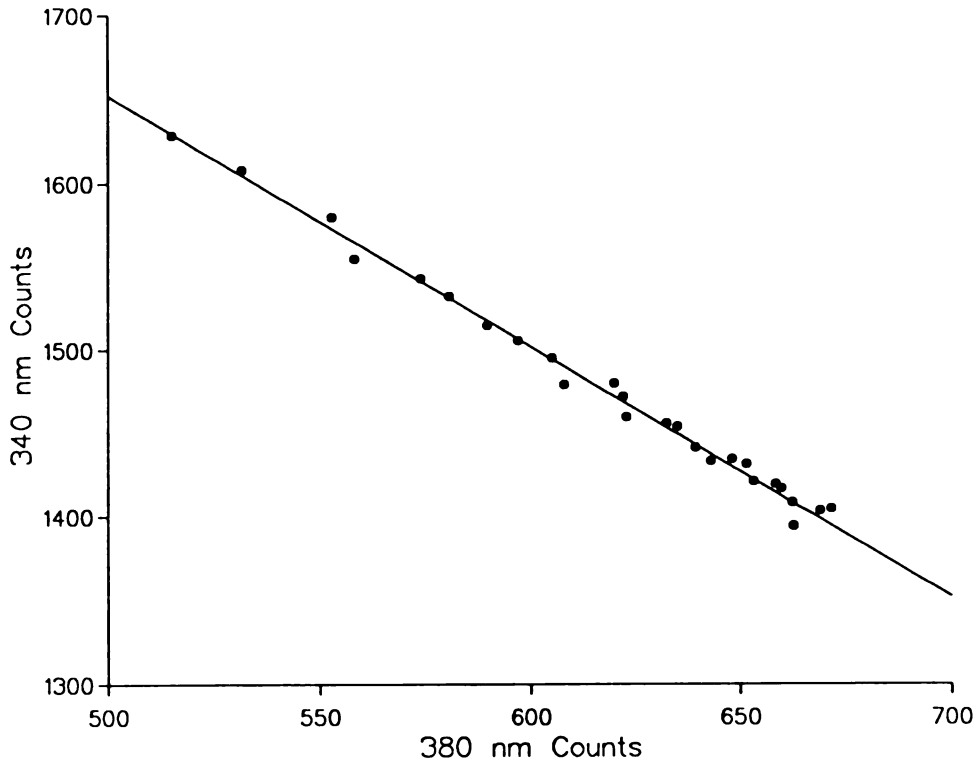

Figure 3. The relationship between the fluorescence elicited by 340 nm illumination to that elicited by 380 nm illumination. The data shown are the average of eight experiments of 10 trials each. The line through the data was drawn by eye and has a slope of -1.5. Most of these data were obtained by Dr. James Younger.

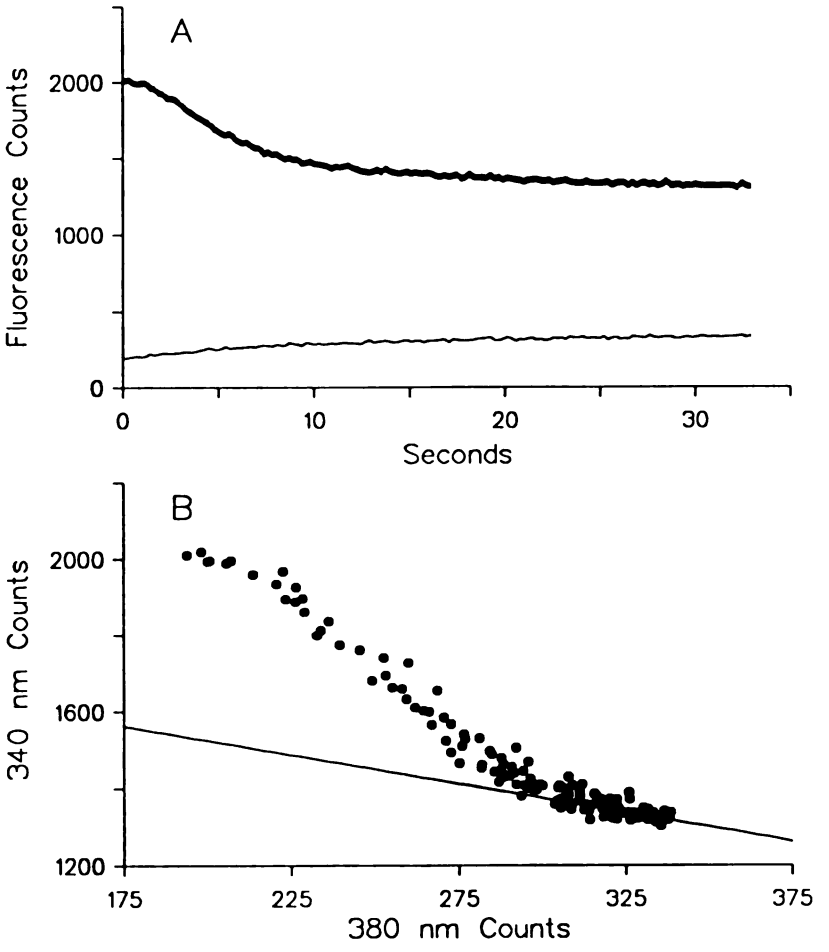

Figure 4. The average fluorescence elicited by 33 seconds of stimulation by 340 nm illumination (thick trace) and 380 nm illumination (thin trace) from eight retinas exposed to the normal/IBMX solution. The shape of the light-induced change in fluorescence was the same in each experiment. *A*, the time course of the measured fluorescence. *B*, the relationship between the 340 nm data with respect to the 380 nm data shown in *A*. The line through the lower portion of the data has a slope of -1.5 to demonstrate that the fluorescence measured during the tail of the response behaves the same as the light-induced change in fluorescence observed in retinas exposed to the control solution. Data recorded from these same retinas when they were exposed to the control solution would superimpose on the lower portion of the data shown. These data were obtained by Dr. James Younger.

of a straight line to describe the data is most simply explained by assuming that the light-induced change in fluorescence originates from more than one form of Fura-2 or that the fluorescent properties of Fura-2 change during excitation.

Evidence for Multiple Forms of Fura-2

During the course of an experiment, typically one to two hours, the total fluorescence elicited from a retina decreases substantially. At the same time, the fluorescence ratio increases. The data shown in Fig. 5 are the average results of the first five stimuli delivered in eight experiments and the last five stimuli delivered shortly before quenching Fura-2 fluorescence in the same experiments. In all cases, the retina was perfused with the control solution. In Fig. 5*A*, each data point represents the mean Fura-2 fluorescence measured during six seconds of illumination at 340 nm (circles) and 380 nm (triangles). In Fig. 5*B*, I show the average light-sensitive change in fluorescence, i.e., the difference between fluorescence elicited at the onset and cessation of each six-second stimulus. The ratio of the 340 nm data to the 380 nm data shown in Fig. 5*A* is displayed in Fig. 5*C*. Finally, the difference between the 340 nm and 380 nm data shown in Fig. 5*A* is illustrated in Fig. 5*D*.

An increase in the fluorescence ratio is typical of nearly all experiments. The cause of this is fairly evident in Fig. 5. The total fluorescence elicited by each stimulus wavelength decreases by approximately the same amount, roughly 1000 counts for the

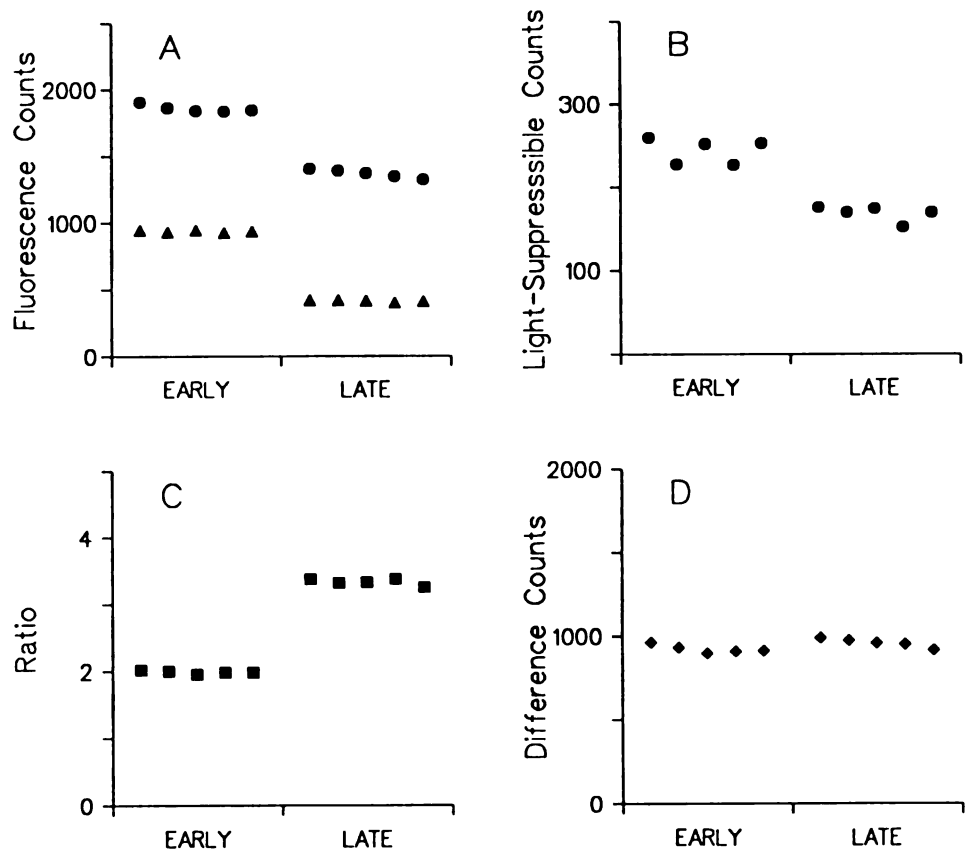

Figure 5. The loss of fluorescence and the increase in the fluorescence ratio during an experiment. *A*, the average total Fura-2 fluorescence elicited by 340 illumination (circles) and 380 nm illumination (triangles) from seven retinas. Each point in *A* represents the average fluorescence elicited during the standard six-second stimulus. The data have been corrected for residual fluorescence but this correction does not alter the conclusions. The first five data points were recorded from the first five stimulations of each retina. The last five were recorded shortly before each retina was quenched by exposure to manganese. *B*, the light-induced change in fluorescence elicited by 340 nm illumination. The light-induced change was determined by subtracting the fluorescence elicited by 340 nm illumination at the end of the six-second stimulation from the fluorescence elicited by the same wavelength at the beginning of the stimulation. *C*, the ratio of the 340 nm data with respect to the 380 nm data shown in *A*. *D*, the difference between the 340 nm data and the 380 nm data shown in *A*. Most of these data were obtained Dr. James Younger.

340 nm data and slightly more for the 380 nm data. This can be expressed as 25% change in the 340 nm data and a 55% change in the 380 nm data by the end of the experiments. At the same time, the light-induced change in fluorescence, Fig. 5*B*, has decreased by approximately 30%. If the total fluorescence and the light-induced change in fluorescence could be attributed to the same source, the percentage change in each case would be the same. The fact that it isn't implies that there are at least two pools of Fura-2.

One pool responds to the change in cytosolic free calcium induced by illumination. This pool is quenched at the end of an experiment. Although I do not show it here, the light-induced changes in fluorescence shown in Fig. 5*B* behave the same as the data shown in Fig. 3. That is, a line describing the fluorescence elicited by 340 nm illumination plotted with respect to the fluorescence elicited by 380 nm illumination has a slope of -1.5, the slope predicted by the *in vitro* calibration. Thus the pool of Fura-2 that is causing the light-induced change in fluorescence in the control solution is, in my belief, composed of Fura-2 that is free in the cytoplasm of the outer segment and is very similar to the Fura-2 described by Grynkiewicz *et al.* (1985).

The source of fluorescence that is responsible for the majority of the gross change in fluorescence during an experiment seems to be unhydrolyzed Fura-2 AM which is initially trapped within cells and the extracellular matrix of the retina. Unhydrolyzed dye would be expected to leak out of the tissue slowly. Fura-2 AM has a fluorescence ratio

of 1.0 in the apparatus and so would fluoresce as brightly for each stimulus wavelength. Thus the counts at 340 and 380 nm drop by similar amounts, approximately 1000 (Fig. 5*D*), even though this represents a dramatically different percentage of the overall signal at each wavelength. In addition, as Dr. James Younger and I gained experience with Fura-2 loading in the retina, we began to wait 15 to 20 minutes after mounting retinas in the recording chamber before beginning an experiment. In these later experiments, the decrease in total fluorescence was not as great as in earlier experiments, presumably because we allowed time for unhydrolyzed Fura-2 AM to wash out.

The rate at which Fura-2 is quenched at the end of an experiment suggests that at least one more pool of Fura-2 is present in rods and that this pool is quenched by manganese. When Fura-2 loaded retinas are exposed to the quenching solution, there is a significant decrease in fluorescence within the first few minutes, as shown in Fig. 6. The fluorescence elicited by 380 nm illumination is usually nearly eliminated in this period, while the fluorescence elicited by 340 nm is still substantial. Over the subsequent 30 minutes, the 340 nm fluorescence gradually decreases. Some Fura-2, which is probably Fura-2 that is free in the cytosol, is quenched rapidly. Another pool is quenched much more slowly. The second pool fluoresces more brightly at 340 nm than at 380 nm. It is my belief that this pool of Fura-2 is responsible for the deviation from the classic Fura-2 behavior when calcium is much higher than in the control conditions (Fig. 4).

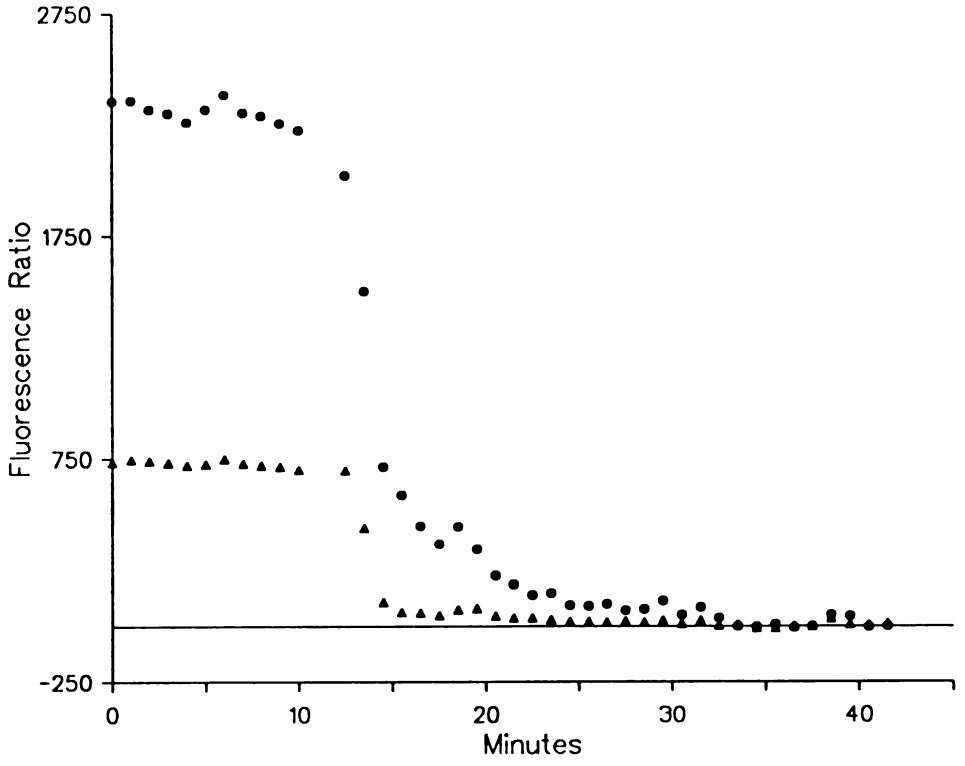

Figure 6. The two phases in the rate at which fluorescence elicited by each stimulus wavelength is quenched in the presence of manganese. The data representing the fluorescence elicited by 340 nm illumination (circles) and that representing the fluorescence elicited by 380 nm illumination (triangles) are each the averages of the fluorescence elicited from a retina during the standard six-second stimulation repeated every minute. The first eleven points were recorded while the retina was exposed to the control solution. The quenching solution was presented to the retina approximately one minute before the 12th pair of points were recorded. The data demonstrate that the majority of the fluorescence elicited by 380 nm illumination is quenched more rapidly than that by 340 nm.

The Effect of Fura-2 on Photoresponses

Exchange currents recorded from Fura-2 loaded rods exposed to the control solution are not noticeably different from those recorded from unloaded rods under the same conditions. In Fig. 7, I show the average exchange currents recorded from seven Fura-2 loaded rods and eight unloaded rods. They are different from the exchange currents reported by Yau and Nakatani (1985) and Hodgkin *et al.* (1987). Those researchers reported that the exchange current recorded from salamander rods had an initial magnitude of 1.5 pA which decayed with a single exponential time constant of 400 to 500 milliseconds. Although, I find that the initial magnitude of the exchange current in frog rods to be not very much different, it decays in a way that can be best described by two exponential time constants, 500 milliseconds and 4 seconds. The difference in my findings can probably be attributed to my longer stimuli resulting in a prolonged saturation phase and better resolution of the longer time constant.

The lack of influence of Fura-2 on the exchange current is surprising. Torre *et al.* (1986) showed that incorporation of the calcium chelator, BAPTA, at a concentration of approximately 10 mM in salamander rods significantly slowed the exchange mechanism. Fura-2 was expected to have similar, if less dramatic results. Ratto *et al.* (1988) reported that the total Fura-2 concentration in rods that were loaded in conditions identical to mine was 37-77 μM. For Fura-2 to have so little an effect on the exchange kinetics the native buffering capacity of frog rods would have to be many millimolar.

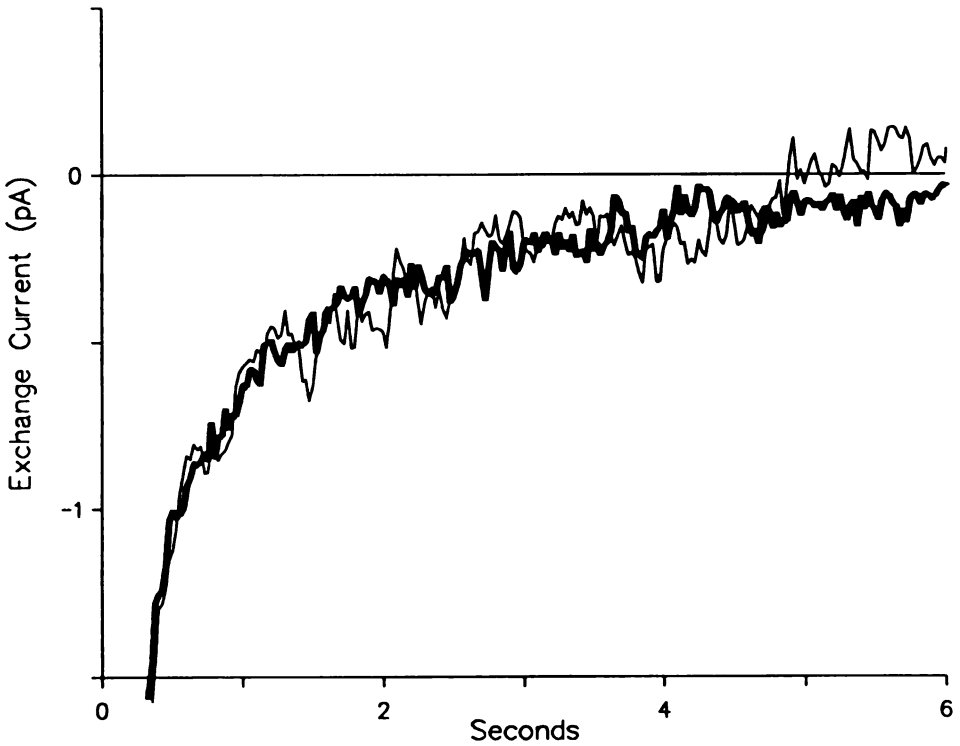

Figure 7. The exchange current recorded from Fura-2 loaded rods and unloaded rods. The average exchange current recorded from Fura-2 loaded rods, thick trace, is from the data shown in Fig. 1. It was recorded from seven rods. The exchange current for unloaded rods, thin trace, is the average of eight cells from five different animals. The total, light-suppressible current was 14.5 pA in both cases.

Rather, in light of my previous findings and the results reported by Konishi *et al.* (1988), who observed that up to 85% of Fura-2 loaded into myocytes may be bound to proteins, it seems more likely that most of the Fura-2 in rods is unable to bind cytoplasmic calcium. The portion of total Fura-2 that could bind calcium would then represent only a small fraction of the total buffering power of rod outer segments.

Fura-2 does, however, have an effect on the photoresponse. Fura-2 loaded rods always recover more slowly after a bright step of illumination than unloaded rods. In Fig. 8A, I show the average response of four Fura-2 loaded rods and four unloaded rods recorded on the same day. The stimulus in each case was a six-second step of illumination that isomerized 10,000 rhodopsin molecules per second. All cells were obtained from the same frog and perfused with the control solution. The responses shown in Fig. 8 are typical. The delayed recovery could be an effect of the added calcium buffering imposed by Fura-2. However, I have shown that the exchange mechanism is not significantly affected by the presence of Fura-2. In addition, I have demonstrated that the cytosolic free calcium concentration observed in Fura-2 loaded retinas is a few tens of nanomolar within about 10 seconds of the onset of this type of illumination. The recovery of the Fura-2 loaded rods shown in Fig. 8*A* does not begin until several seconds after this. Therefore, if the recovery of the photoresponse is delayed by calcium buffering by Fura-2, then the onset of recovery would require that calcium fall to a very low concentration. I examine this possibility again in Chapter 5.

An alternative hypothesis is that Fura-2 interferes more directly with the enzymes that mediate recovery. Chiancone *et al.* (1986) demonstrated that BAPTA, a relative of Fura-2, binds to calcium-binding proteins, including calmodulin. Fura-2 may therefore have a direct effect on protein activity. I examined the possible effects of Fura-2 on the enzymes of phototransduction by comparing the activation kinetics of photoresponses recorded from loaded and unloaded rods. The data shown in Fig. 8*B* is an expanded view of the data shown in Fig. 8*A* around the time of the onset of illumination. This is the rising phase of the response. Lamb and Pugh (1992) have shown that the kinetics of the rising phase are consistent with the expected activation scheme of the cyclic GMP cascade composed of rhodopsin, transducin and phosphodiesterase (but see also Chapters 4 and 5). Torre *et al.* (1986) demonstrated that the rising phase is unaffected by calcium buffering. In general, the rising phase of a typical Fura-2 loaded rod is not very different from that of an unloaded rod. In the particular example shown in Fig. 8*B*, the rising phase of the Fura-2 loaded rod is somewhat slower. In responses observed in other rods, it was somewhat faster. On average, there was no definite effect. These observations suggest that Fura-2 does not inhibit the activation of cyclic GMP hydrolysis.

Responses elicited from loaded and unloaded rods by brief, non-saturating stimuli are also the same. The photocurrents recorded from two rods in response to a 25-millisecond flash that isomerized approximately 30 rhodopsin molecules and was delivered at the time marked zero are shown in Fig. 8*C*. These two cells were among the group of rods that contributed to the data shown in Figures 8*A* and 8*B*. The data from

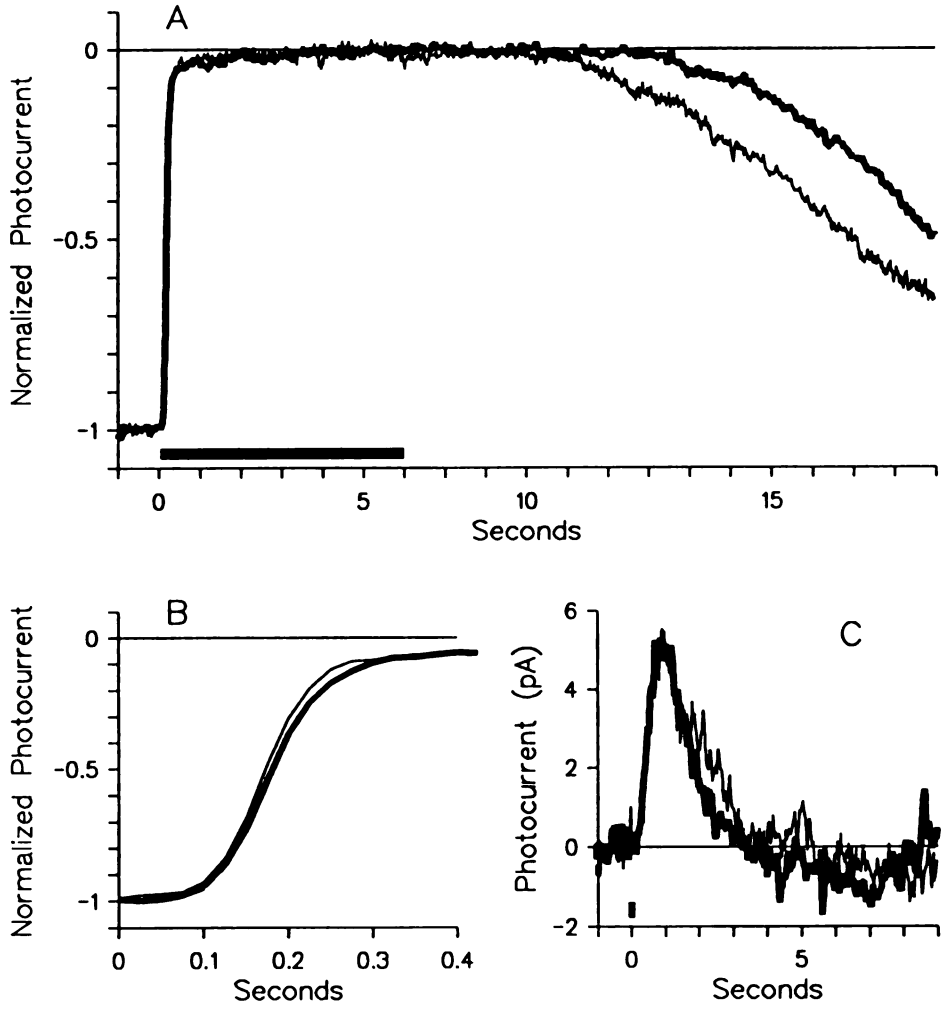

Figure 8. The effect of Fura-2 on the kinetics of photoresponses. *A*, the average normalized photoresponse from four Fura-2 loaded rods, thick trace, and four unloaded rods, thin trace, from the same frog. The delayed recovery of the Fura-2 loaded rods after the standard six-second stimulation are typical. *B*, the rising phase of the data shown in *A*. *C*, the photocurrents recorded from a Fura-2 loaded rod, thick trace, and an unloaded rod, thin trace, when they were stimulated by a 25-millisecond flash that isomerized approximately 30 rhodopsin molecules. The photocurrent for the Fura-2 loaded rod is the average of two records. The photocurrent for the unloaded rod is from a single stimulation. Saturating responses recorded from these same rods contributed to the data shown in *A*.

the rod containing Fura-2 are displayed as a thick trace. The responses are similar and differences can be attributed to experimental noise. These observations suggest again that Fura-2 does not noticeably alter the buffering properties of rods. They also imply that Fura-2 does not interfere significantly with the enzymes that regulate non-saturating responses.

The Exchange Current During Exposure to IBMX

Because the ratio method cannot be used to determine calcium concentrations in rods, I was motivated to estimate it by an alternate assay based on the exchange current observed in isolated rods exposed to the normal/IBMX solution. In Fig. 9, I display the photoresponse elicited by the standard saturating, six-second stimuli one minute after exposure to the normal/IBMX perfusate. That the total light-suppressible current is greater than that observed in rods exposed to the control solution and the exchange component is apparently saturated at early times (1-2 seconds). The increase in light-suppressible current is much less than that reported by Cervetto and McNaughton (1986) and Hodgkin *et al.* (1987) and is probably due to the relative slowness of the solution changes. After several minutes, the exchange component is no longer saturated at any time and the total light-suppressible current is reduced. The decrease in both the exchange current and total current probably results from ionic gradient rundown, the same reason cited earlier for a similar effect observed in the presence of the Ca^{2+}-free solution. The rising phase of the photoresponse lasts approximately one second in the presence of

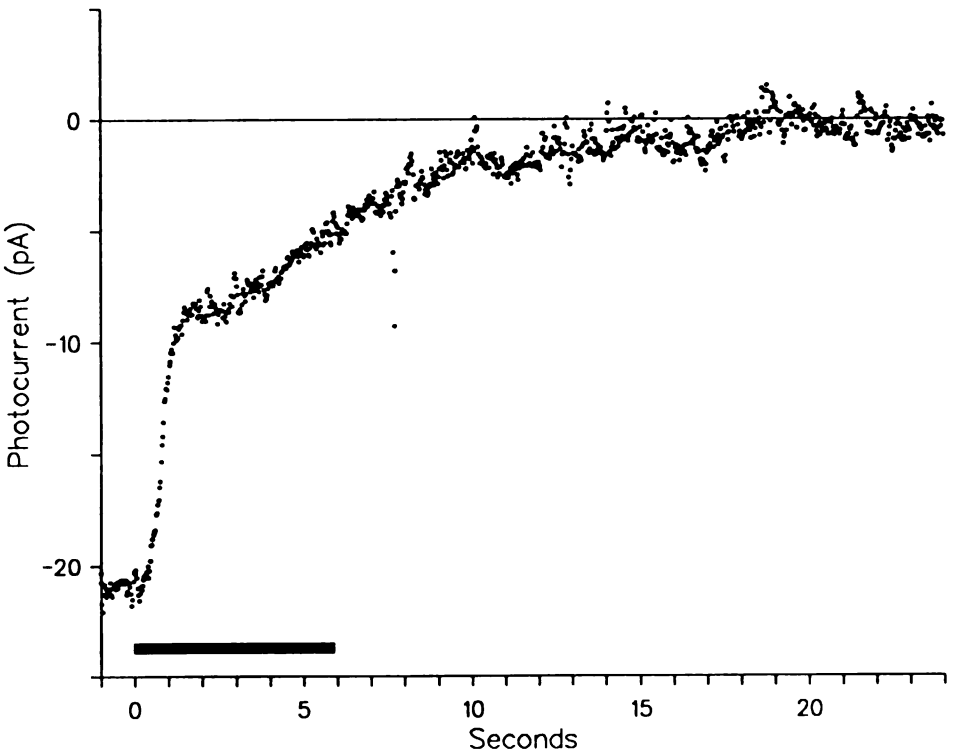

Figure 9. The exchange current recorded shortly after an isolated rod was exposed to the normal/IBMX solution. The data shown are the photoresponse of an unloaded rod approximately one minute after it had been exposed to the normal/IBMX solution. The light-suppressible current of the rod was approximately 15 pA while it was exposed to the control solution. The level portion of the current record, between 2 and 3 seconds after the onset of the stimulus, demonstrates that the exchange mechanism is almost saturated at this time. The timing of the standard six-second stimulus is shown by the bar.

the normal/IBMX solution suggesting that there is a very large number of open cyclic GMP-gated channels.

In Fig. 10*A*, I show the average exchange current recorded after several minutes exposure to the normal/IBMX solution. The function fitted to the data has time constants of two and 10 seconds. The longer time constant is approximately two and one-half times greater than the time constant observed for cells exposed to the control solution. I believe this to be a consequence of the fourth-order sodium dependence of the exchanger. A two and one-half-fold increase in the time constant might be explained by a 25% increase in the intracellular sodium concentration, consistent with the expectation of decreased ionic gradients. The early part of the function fitted to the data is my best intuitive guess. I estimate the initial magnitude of the exchange current after several minutes of exposure to the normal/IBMX solution at approximately 6 pA.

Lagnado *et al.* (1988) showed that the Na^+: Ca^{2+}, K^+ exchange mechanism has a first-order free calcium dependence described by:

$$J_{ex} = J_{sat} \frac{[Ca^{2+}]}{K_{ex} + [Ca^{2+}]} \qquad (4)$$

where J_{ex} is the current generated by the exchanger, J_{sat} is its magnitude when saturated and K_{ex} is its calcium dissociation constant which they found to be 2.3 μM. This equation may be modified to express an estimate of the cytoplasmic free calcium concentration in

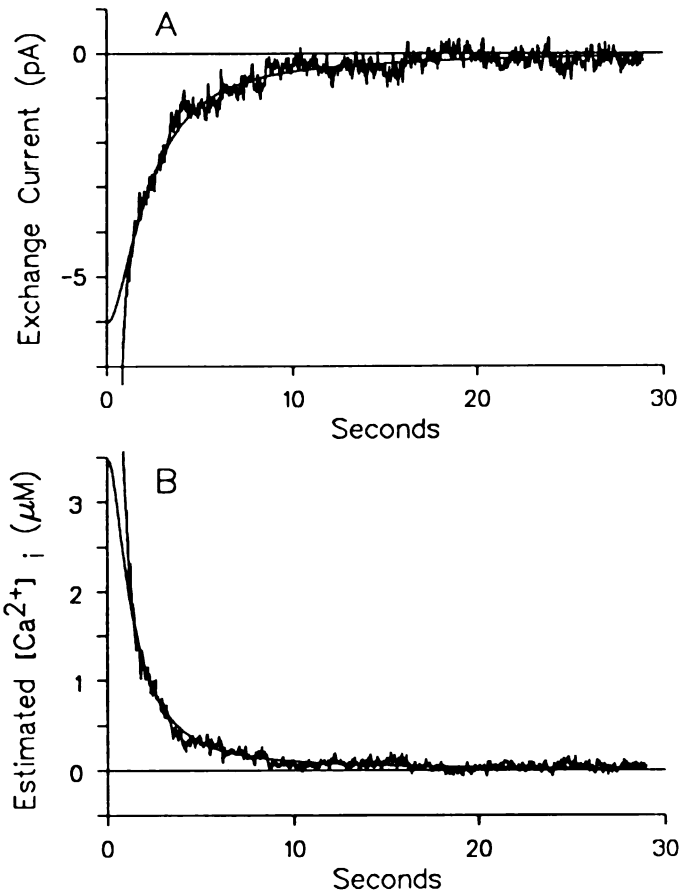

Figure 10. The exchange current and estimated light-induced change in the cytosolic free calcium concentration after several minutes of exposure to the normal/IBMX solution. *A*, the average exchange current from two rods. The data shown in Fig. 9 were recorded from one of these rods. In this case, however, the stimulus was a 30-second step of illumination that isomerized 10,000 rhodopsin molecules per second. Photocurrents recorded in the presence of the normal/IBMX solution were noisier than photocurrents recorded from rods exposed to the control solution. After approximately 15-20 minutes exposure to the normal/IBMX solution, rods lost their shape and became unresponsive. *B*, the cytosolic free calcium concentration derived from the data shown in *A* and eqn (5) and a K_{ex} for the exchanger of 2.3 μM. The curve drawn through the data in *A* was fitted by eye and is $2e^{-t/0.5} - 7e^{-t/2} - e^{-t/10}$ pA. The curve drawn through the data in *B* is the result of evaluating eqn (5) with this same function.

terms of measured exchange current.

$$[Ca^{2+}] = K_{ex} \frac{J_{ex}}{J_{sat} - J_{ex}} \quad (5)$$

The estimate of cytosolic free calcium concentration for rods exposed to the normal/IBMX solution is shown in Fig. 10*B*. I have assumed that the saturated exchange current, J_{sat}, is approximately 10 pA; the value measured when cells were first exposed to the normal/IBMX solution.

Calcium Dependence of Fura-2 Fluorescence

When more than one source of Fura-2 fluorescence is present, the observed fluorescence may still be expressed in a form similar to eqn (1).

$$\phi = \phi_o + \phi_1 \beta_1 + \phi_2 \beta_2 \quad (6)$$

$$\psi = \psi_o + \psi_1 \beta_1 + \psi_2 \beta_2$$

Here, the variables are equivalent to those of eqn (1), but ϕ_β, ψ_β and β have each been split to represent two calcium-sensitive pools of Fura-2. There may be more than two physical pools but only two calcium-sensitive pools can be resolved after eliminating the contribution from unhydrolyzed Fura-2 AM (Fig. 5 and Fig. 6). If there are more than two physical pools, they may still be grouped into two generalized pools. Manipulation of eqn (6) yields the contribution of each pool to the calcium dependent change in fluorescence elicited by 380 nm illumination.

$$\psi_1 \beta_1 = \frac{(\phi - \phi_o) - m_2 (\psi - \psi_o)}{m_1 - m_2} \qquad (7)$$

$$\psi_2 \beta_2 = \frac{(\phi - \phi_o) - m_1 (\psi - \psi_o)}{m_2 - m_1}$$

As in eqn (2), $m_1 = \phi_1/\psi_1$ and $m_2 = \phi_2/\psi_2$, and so the calcium dependent change in fluorescence elicited by 340 nm illumination from each pool is easily obtained. I point out that these relations do not assume any specific type of calcium dependence.

Of the variables on the right side of eqn (7), only m_1 and m_2 are not measured directly. The composite slope in control conditions, m of eqn (1), is directly measured. I strongly suspect that the composite slope represents a pool of Fura-2 that is the same as the species of Fura-2 characterized in the *in vitro* calibrations and described by Grynkiewicz *et al.*, (1985) The agreement between the measured slope and the slope predicted from the *in vitro* calibration results is too great to ignore. In addition, from the dynamics of the quench (Fig. 6) I expect that all other pools contribute very little to the fluorescence elicited by 380 nm illumination from rods exposed to the control solution. This means that I also expect all other pools to contribute very little to the determination of the composite slope in these conditions. Thus, there is only one effective pool in the control conditions. In this case, either m_1 or m_2 may be assigned the value -1.5. I have chosen the index *1* to represent the pool of classic Fura-2 and so set $m_1 = -1.5$.

The other slope, m_2, is estimated by examining the fraction of total fluorescence

contributed by each pool to the fluorescence elicited by 380 nm illumination during the tail end of the data shown in Fig. 4*A*, when the retina was perfused with the IBMX solution. These data were obtained at the end of experiments and so the contribution of unhydrolysed Fura-2 AM is small. I estimate, based on the rate of Fura-2 quenching shown in Fig. 6, that less than 25% of the 380 nm fluorescence can be attributed to pool 2. The method for determining m_2 is described in Appendix A. Essentially, the relative contribution from each pool, which is more measurable than the less intuitive variable, m_2, is used as the free parameter. For a 75% to 100% contribution from the classic Fura-2 pool, I estimate m_2 to be 4.5 to 1.3, respectively. The positive value of this parameter means that the fluorescences elicited from the immobile pool by both stimulus wavelengths increases as the cytosolic free calcium concentration increases. This is unlike the behavior expected from a free form of Fura-2 but is consistent with the observed initial rates of change of each fluorescence displayed in Fig. 4*A*.

In Fig. 11, I show the calcium-dependence of the two pools of Fura-2. The data are the results of the left side of eqn (5), displayed as $-\psi_1\beta_1$ and $\psi_2\beta_2$, when evaluated from the data shown in Fig. 4. Their dependence on calcium is determined from the estimate of the cytosolic free calcium, eqn (7), which is derived from the function fitted to the exchange current shown in Fig. 10*A*. I have set $\psi_1 = \alpha\psi_o(1\text{-}F)/F$, for reasons set forth in the Appendix, and $\psi_2 = (\psi_m - \psi_o) - \psi_1$, where ψ_o is the fluorescence elicited by 380 nm illumination at the tail end of the data shown in Fig. 4*A*, α is the fraction of

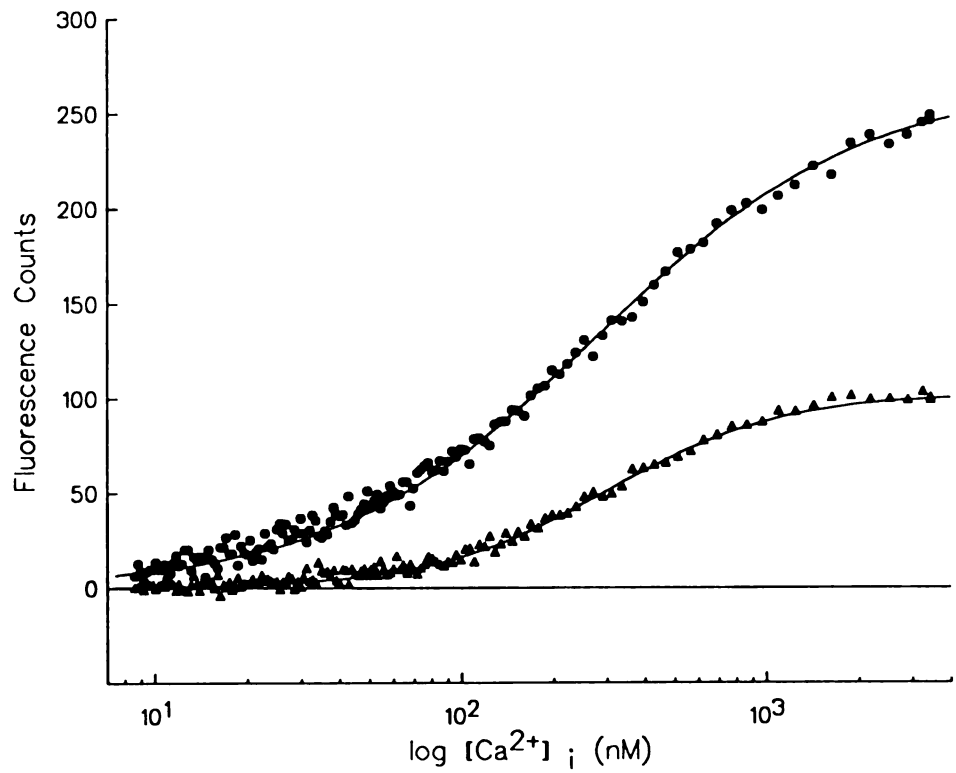

Figure 11. The calcium dependence of each pool of Fura-2. The data shown are the same as the data shown in Fig. 4 but evaluated using eqn (8) with $m_1 = -1.5$ and $m_2 = 3.4$ ($\alpha = 0.8$). The data representing the light-induced change in fluorescence from the pool of classic Fura-2 (circles) are shown inverted, i.e. $-\psi_1\beta_1$. The position of each data point along the abscissa was determined from the time course of the data shown in Fig. 4 and the time course of the curve drawn through the data shown in Fig. 10*B*. Therefore, the calcium dependence of each pool of Fura-2 is derived from the fluorescence measured from retinas exposed to the normal/IBMX solution and the exchange current recorded from isolated rods exposed to the same solution. The curve drawn through the data representing the pool of classic Fura-2 was fitted by eye and is a standard first-order titration curve with a dissociation constant of 280 nM. The curve drawn though the data representing the light-induced change in fluorescence elicited from the immobile pool (triangles) is a cooperative titration curve with a Hill coefficient of 1.5 and a half-maximum change at 300 mM.

this fluorescence that is contributed by the classic Fura-2 pool, and ψ_m is the 380 nm fluorescence measured at the beginning of the same data. The results displayed in Fig. 11 were obtained with $\alpha = 0.8$ ($m_2 = 3.4$). What is important, however, is that the calcium-dependence of the immobile pool does not depend on α, while the calcium-dependence of the classic Fura-2 pool changes only slightly for α greater than 0.7.

The results for the classic Fura-2 pool are fitted well by a standard first-order titration curve and a dissociation constant of 280 nM. The results for the other pool are fitted by a titration curve with a Hill coefficient of 1.5-1.7 and a half-maximum value at 300 nM. I point out that at no time have I imposed a calcium dependence on the results. The term, classic Fura-2, for the pool of Fura-2 that underlies the light-induced change in fluorescence elicited from cells exposed to the control solution was based on the agreement between expected and measured slopes. The excellent agreement between the calcium-dependence expected for the Fura-2 described by Grynkiewicz *et al.* (1985) and the results shown in Fig. 11 simply support my terminology.

Cytosolic Free Calcium Concentration in Rods

The well defined calcium dependence of the classic Fura-2 pool allows me to estimate calcium concentrations in rods exposed to the control solution. I cannot, however, rely on the ratio method. Instead, with the knowledge that $\beta_1 = [Ca^{2+}]_i / (K_d + [Ca^{2+}]_i)$, the cytosolic free calcium concentration may be written as:

$$[Ca^{2+}]_i = K_d \frac{(\phi - \phi_o) - m_2 (\psi - \psi_o)}{(m_1 - m_2)\,\psi_1 - (\phi - \phi_o) + m_2 (\psi - \psi_o)} \qquad (8)$$

The numerator can be written as $(m_1-m_2)(\psi-\psi_0)$ for data recorded from rods exposed to the control solution. Therefore, continuing the evaluation of ψ_1 as $\alpha\psi_0(1-F)/F$, we write:

$$[Ca^{2+}]_i = K_d \frac{\langle\Delta\psi\rangle F}{\alpha\psi_o(1-F) - \langle\Delta\psi\rangle F} \qquad (9)$$

where I take advantage of the fact that the fluorescence elicited by each of the two stimulus wavelengths are measured by substituting $\langle\Delta\psi\rangle = [(\phi-\phi_0)+m_1(\psi-\psi_0)]/2m_1$ for $(\psi - \psi_0)$.

The change in cytoplasmic free calcium concentration in response to a six-second step of illumination that isomerized 10,000 rhodopsin molecules per rod per second is shown in Fig. 12 for three values of α. These results are derived from eqn (9) and the data shown in Fig. 1. The kinetics of the change in calcium concentration depend weakly on the value of α. However, the resting cytoplasmic free calcium concentration in dark-adapted rods ranges between 125 nM and 200 nM for α between 1 and 0.75, respectively. My estimate of the concentration of cytoplasmic free calcium in a frog rod in darkness is no less than 125 nM, no more than 200 nM and probably less than 150 nM. These results assume a calcium dissociation constant of 280 nM from K_{ex} = 2.3 μM for the exchanger.

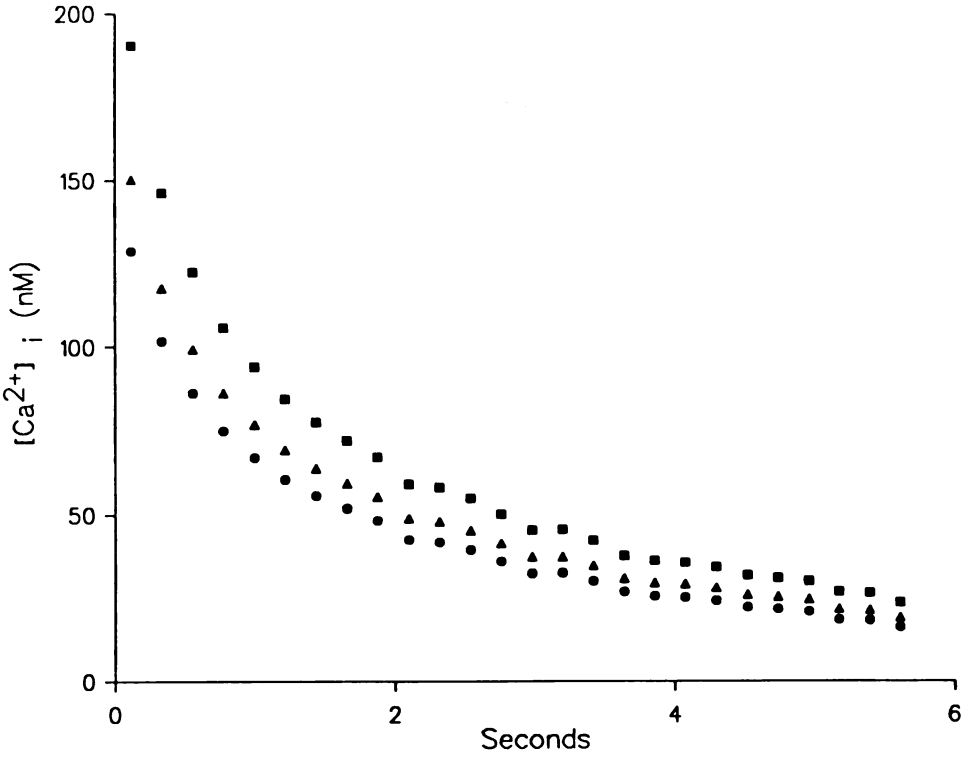

Figure 12. The light-induced change in the cytosolic free calcium concentration in dark-adapted rods. The data shown are derived from the data shown in Fig. 1 and eqn (10) for three different values of α: 1 (circles); 0.875 (triangles); 0.75 (squares). The absolute calcium concentrations are based on a calcium dissociation constant for the classic pool of Fura-2 of 280 nM (Fig. 11).

DISCUSSION

Perhaps the most important finding, in terms of light adaptation in vertebrate photoreceptors, is that the cytosolic free calcium concentration in the outer segments of the rod is reduced to a few nanomolar during bright illumination (see also Younger, 1991). This conclusion does not depend on the analysis of the properties of Fura-2 loaded into rods. Rather, it is derived from the fact that the fluorescence ratio measured during bright illumination is the same as the fluorescence ratio measured when rods are exposed to the Ca^{2+}-free perfusate and the conviction that the concentration of free calcium in the cytosol of rods exposed for an extended period to the Ca^{2+}-free perfusate is negligible. It is also supported by the conclusion that only the light-induced change in the cytosolic free calcium concentration in the rod outer segments is responsible for the light-induced change in measured fluorescence. The fact that the cytoplasmic free calcium concentration is reduced to such a low level suggests that calcium-dependent light adaptation processes are modulated over their full range.

I am confident of the range of calcium concentrations I report for dark-adapted rods. My calculations make use of the observation that the light-induced change in fluorescence measured from retinas bathed in the control solution appears to originate from a single pool of Fura-2. They also depend on the fraction of the total fluorescence that can be attributed to this pool which is estimated from the rate at which fluorescence is quenched in the presence of manganese. The largest source of error is in my estimate

of the calcium dissociation constant of the pool of Fura-2 that is responsible for the light-induced change in fluorescence. The dissociation constant I have used, 280 nM, was determined from the calcium dependence of the pool of classic Fura-2 which was derived from the exchange current recorded from rods exposed to the normal/IBMX solution and K_{ex} of 2.3 μM. I assumed that the cytosolic free calcium concentration was uniform across the rod outer segment during illumination. Other studies I have performed, (see Chapter 4), suggest that this may not be entirely true. The practical result of an inhomogeneous cytosolic free calcium concentration, according to the worst-case analysis, is that the estimate of the apparent calcium dissociation constant of the pool of classic Fura-2 may be too low by as much as a factor of two. Negulescu and Machen (1990) however, measured the calcium dissociation constant of Fura-2 in parietal cells and reported a value of 350 nM. In addition Groden *et al.* (1991), measured an *in vitro* Fura-2 dissociation constant of 236 nM in a solution with an ionic strength of 150 mM and Uto *et al.*, (1991), measured a dissociation constant under similar conditions of 266 nM when the ionic strength was 170 mM. These values are similar to my estimate. Therefore, although I recognize that there are potential inaccuracies when the exchange current recorded from cells exposed to the normal/IBMX solution is used as an assay for cytosolic free calcium, I believe that the absolute magnitude of the cytosolic free calcium concentrations I report are approximately correct.

I have shown that the high apparent calcium concentrations reported by Ratto *et al.* (1988) are probably the result of the unexpected properties of Fura-2 in rods. I

believe that the values reported by Korenbrot and Miller (1989) who used Quin-2, a close relative of Fura-2, might also be explained in the same way.

The source of the Fura-2 fluorescence that accounts for the unrealistically high fluorescence ratio measured during bright illumination has been identified as an immobile pool of Fura-2 that fluoresces more brightly during 340 nm illumination than during 380 nm illumination. An hypothesis that suggests itself almost immediately is that some Fura-2 may be trapped within the disks of the outer segment that senses a high calcium concentration there (Szuts and Cone, 1977, Schröder and Fain, 1984, Somlyo and Walz, 1985). Several observations lead me to believe that this is unlikely. First, the immobile pool appears to be calcium-insensitive in both the control solution and the Ca^{2+}-free solution but is quenched by extracellular application of manganese. It seems improbable that the interior of disks would not be influenced by changes in the cytosolic free calcium concentration but would be accessible to manganese, another divalent cation. Second, the fluorescence imaging experiments demonstrated that the inner segment is brighter than the outer segment. If a significant amount of Fura-2 was immersed in a high calcium concentration within disks, I would expect the opposite to be true. Third, based on the *in vitro* calibration parameters, at least 30% of the total fluorescent Fura-2 in rod outer segments must be contained inside the disks in order to account for an *in situ* value of R_o of 2.0. Ratto *et al.* (1988) reported that only 13% of the total Fura-2 in rod outer segments could be inside or bound to disks however. Finally, the second, "immobile" pool is not calcium-insensitive when rods are exposed to the normal/IBMX solution. It

could be argued that IBMX has some affect on intradiskal calcium concentrations, but the light-induced change in fluorescence is not compatible with the calcium-sensitive properties of the classic form of Fura-2. These observations do not argue that the calcium concentration inside of disks is not high. Rather, they imply that, if it is high, there is insufficient Fura-2 present within them to entirely account for the *in situ* values of R_o.

It seems more likely that the "immobile" pool is composed of Fura-2 that is tightly bound to intracellular proteins. Konishi *et al.* (1988) and Bancel *et al.* (1992) have shown that this occurs with *in vitro* preparations. Konishi *et al.* (1988) went further and demonstrated that up to 85% of the total Fura-2 loaded into myocytes is bound to protein. This phenomenon may partly explain why a pronounced undershoot in the photoresponses is nor recorded from Fura-2 loaded rods but that Torre *et al.* (1986) reported one for rods dialyzed with a solution containing 10 mM of BAPTA and which Korenbrot and Miller (1989) demonstrated with rods containing approximately 270 μM of Quin-2. It may also explain why Fura-2 has so little effect on the exchange current recorded from Fura-2 loaded rods exposed to the control solution. If most of the Fura-2 in the outer segment is bound to protein it will add little to the rod's buffering capacity; thus I would expect to see little difference between loaded and unloaded rods.

As I have discussed, I do not believe that the principal influence of Fura-2 on the photoresponse of Fura-2 loaded rods is mediated by significant alteration of their buffering capacity. A more intriguing hypothesis is that Fura-2 binds directly to some

of the enzymes that are involved in the regulation of circulating current and light adaptation. I have shown that Fura-2 does not normally affect the activation of cyclic GMP hydrolysis. The delayed recovery of Fura-2 loaded rods following bright illumination, however, suggests that guanylate cyclase or some other enzyme may be affected. Chiancone *et al.* (1986) reported that BAPTA, the parent compound of Fura-2 can bind to several calcium-binding proteins, including calmodulin. My data does not, however, allow me to make any definite statements regarding Fura-2 interactions with rod proteins.

Although I am not able to say with certainty what the physical basis of the second pool of Fura-2 might be, I am confident that the fluorescence I measure in the control solution reflects changes in cytosolic free calcium. I am also confident that the time course and relative changes in the cytosolic free calcium concentration in response to illumination can be determined. Calcium regulation in the rod outer segment and the role it plays in light adaptation can now be examined.

CHAPTER FOUR: CALCIUM BUFFERING AND REGULATION IN ROD OUTER SEGMENTS OF THE BULLFROG

INTRODUCTION

I have demonstrated that bright illumination results in a decrease in the free calcium concentration in the outer-segment cytosol. But what happens to the cytosolic free calcium concentration when illumination does not completely close all of the cyclic GMP-gated channels? Central to the query is the desire to know how the free calcium concentration in a rod outer segment is regulated. How are calcium influx and efflux balanced? What are the calcium buffering characteristics of rod outer segments? How rapidly does the free calcium concentration respond to a change in illumination? In short, do changes in the cytosolic free calcium concentration go hand-in-hand with light adaptation?

Other studies have already investigated some of these questions. It appears that calcium ions can cross the outer-segment plasma membrane only via the cyclic GMP-gated channel and the exchanger, the latter having a first-order dependence on cytosolic free calcium concentrations in cells exposed to IBMX (Cervetto *et al.*, 1987, Lagnado *et al.*, 1992). It has been estimated that approximately 10-15% of the current flowing

through the cyclic GMP-gated channel is carried by calcium ions, (Yau and Nakatani, 1985). Fain and Schröder (1987) have presented data which suggests that there is a light-induced release of calcium from internal stores in the outer segment. Szuts (1980) and, more recently, Lagnado *et al.* (1992) have presented data that disputes this assertion. Lagnado *et al.* (1992) have also investigated calcium buffering and describe two dominant buffering systems; one has a dissociation constant of 0.7 μM, the other has a much lower affinity but much higher capacity. These buffers are reported to be rapidly equilibrating and thus suggest that the free calcium concentration is approximately proportional to the total accessible calcium in outer segments exposed to the control solution. A buffering system of this type is consistent with - and in fact was suggested by - the fact that the exchange current appeared to decline exponentially with a time constant of approximately 400 milliseconds following bright illumination (Yau and Nakatani, 1985, Hodgkin *et al.*, 1987). Miller and Korenbrot (1987) combined most of these concepts of calcium regulation with their own measure of the light-induced extrusion of calcium to model the time-dependent change in cytosolic free calcium. Forti *et al.* (1989) made similar assumptions in an attempt at a complete model of phototransduction, except they also included a slowly equilibrating buffer. Taken together, these observations and analyses appear to offer an easily grasped philosophy of the relationship between cytosolic free calcium and illumination.

In only one of these investigations, however, were cytoplasmic free calcium concentrations actually measured. The exception is the work of Lagnado *et al.* (1992)

who could only measure concentrations above approximately 400 nM with aequorin. In my investigation of light-dependent calcium regulation, I have found that some of the observations and assumptions described above are not completely accurate. I, along with Dr. James Younger, do find that only the Na^+: Ca^{2+}, K^+ exchanger and the cyclic GMP channel regulate calcium flux across the outer-segment plasma membrane. The fraction of the current flowing through the cyclic GMP-gated channels that is carried by calcium, however, is greater than has been previously reported. More significant, I find that neither the cytosolic free calcium concentration determined by measuring the fluorescence elicited from Fura-2 in rod outer segments nor the exchange current is consistent with the relatively simple calcium buffering system that has been reported. I present a parsimonious model inspired by the internal structure of rod outer segments to explain my findings. It correctly predicts the calcium concentrations that are measured with Fura-2 when rods are illuminated with a non-saturating step of illumination and when the rods recover from illumination that had closed all of the cyclic GMP-gated channels.

RESULTS

Only the Cyclic GMP Channel and the Na^+: Ca^{2+}, K^+ Exchanger Set $[Ca^{2+}]_i$

As I mentioned above, it is believed that calcium moves across the outer-segment plasma membrane only through the cyclic GMP-gated channels and the Na^+: Ca^{2+}, K^+ exchanger. A steady illumination which results in a reduction in the mean number of open cyclic GMP-gated channels with respect to the dark is, therefore, expected to result in a similar reduction in the steady-state concentration of cytosolic free calcium. Capovilla *et al.* (1983) and Colamartino *et al.* (1991), however, have presented evidence which implies that the permeability of the cyclic GMP-gated channel to calcium ions depends on the cyclic GMP concentration. Torre *et al.* (1992) have reported that the cyclic GMP channel exists in two distinct varieties in the rod. In addition Hsu and Molday (1993) have recently suggested that calmodulin changes the characteristics of the cyclic GMP-gated channel. As noted before, there have also been reports that light induces a release of calcium from internal stores (Fain and Schröder, 1987). It is not clear, then, what the relationships between illumination, the cytosolic free calcium concentration and the relative permeability of the cyclic GMP channel might be.

In Fig. 1, I show that steady illumination does, in fact, reduce the cytosolic free calcium concentration. As important, steady illumination suppresses the circulating current by the same fraction as it does the cytosolic free calcium concentration. Both are

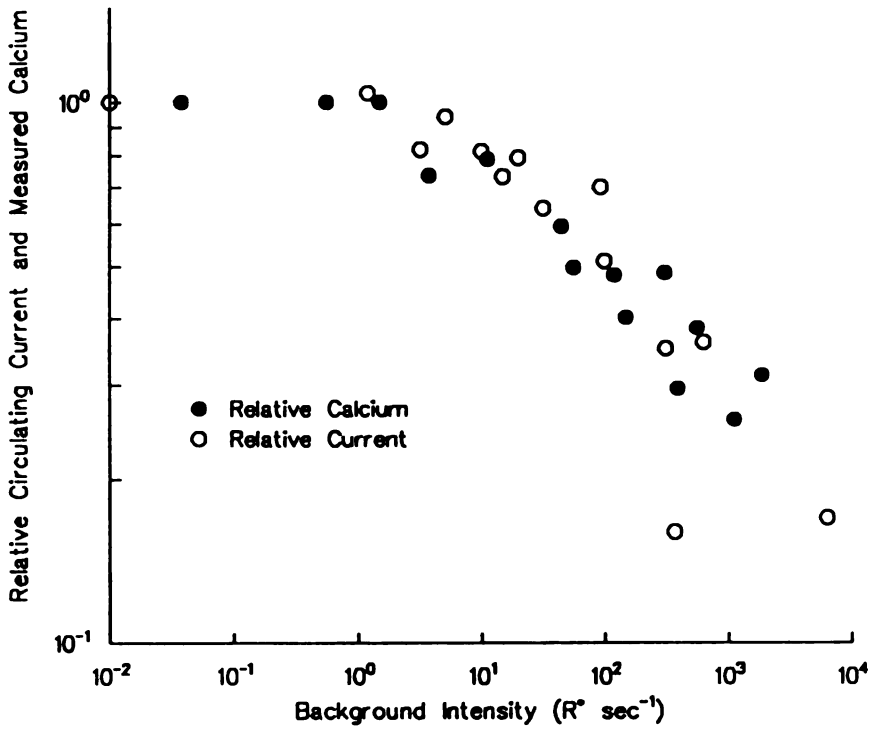

Figure 1. The steady-state dependence on illumination of calcium concentrations measured in Fura-2 loaded retinas and the circulating current recorded from loaded and unloaded rods. Calcium concentrations were determined after 30 seconds of exposure to the adapting intensities indicated. Currents were recorded no less than 15 seconds after the onset of the adapting illumination. There was no difference between the currents recorded from loaded and unloaded rods. (Calcium data were obtained by Dr. James Younger.)

reduced to one-half of their value in the dark when 100-200 rhodopsin molecules are isomerized per rod per second. If only the cyclic GMP channel and the exchanger regulate calcium flux across the plasma membrane and if one also assumes that the exchange current is proportional to the cytosolic free calcium concentration, then these data mean that the relative permeability to calcium of the cyclic GMP-gated channel is not altered significantly by illumination.

Is the exchange current, in fact, linearly dependent on the cytosolic free calcium concentration? In Fig. 2*A*, the responses of a rod to bright stimuli when it was in a dark-adapted state and again when it was in a light-adapted state are compared. In both cases, the bright stimulus was the standard six seconds of illumination that isomerized approximately 10,000 rhodopsin molecules per second. The steady illumination that light-adapted the rod isomerized approximately 300 rhodopsin molecules per second and resulted in suppression of the circulating current by almost 50%, slightly less than usually observed. The slow declines of the photocurrents following the onset of bright illumination are the exchange currents, which are redisplayed for emphasis in Fig. 2*A*. The exchange current is suppressed by approximately the same percentage as the total circulating current. Similar results were obtained for other rods and other states of light adaptation. In combination with the relationship between the steady-state cytosolic free calcium and the steady-state circulating current shown in Fig. 1, this suggests that the relative magnitude of the exchange current is proportional to the relative free calcium concentration in the outer segment within the limits of measurement.

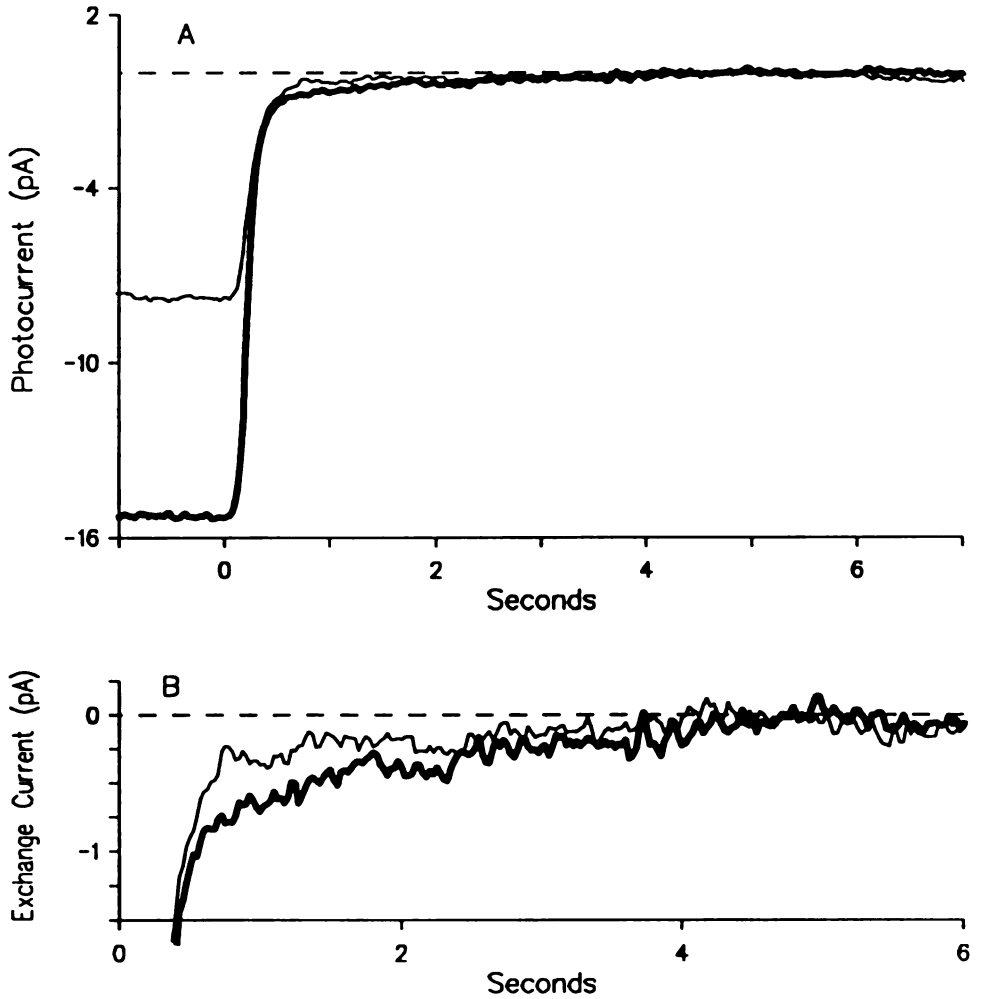

Figure 2. Suppression of the circulating current and exchange current by adapting illumination. These currents were recorded from a single rod. The saturating illumination in each case was the standard six-second stimulus (10,000 R^* sec^{-1}; 5 trials each). The adapting illumination isomerized approximately 300 R^* sec^{-1}. The total current (A) and the slow phase of the exchange current (B) are suppressed by approximately the same amount.

The first-order relationship between the exchanger and the concentration of cytosolic free calcium is also illustrated in Fig. 3. The data are the average exchange currents recorded from seven Fura-2 loaded rods and the cytosolic free calcium concentrations measured for intact, Fura-2 loaded retinas. The data are displayed in logarithmic form, normalized with respect to the initial values, and are the same as those shown in Fig. 7 and Fig. 12 for $\alpha = 0.75$ of the previous chapter. In the case of the exchange current, the initial value was taken to be 2 pA for reasons discussed below. Both data sets were recorded in response to the standard six-second, bright stimulus. It is clear that the exchange current and the cytosolic free calcium concentration decline at the same rate after the first half-second of illumination. This again suggests that the exchange current is related to the cytosolic free calcium concentration in a linear and well defined manner.

The data, thus far, indicate that only the cyclic GMP-gated channel and the exchanger regulate the calcium flux across the outer segment plasma membrane. But what about a light-induced release of calcium from internal stores? As I have mentioned, this concept has been examined by a number of investigators who arrived at dissonant results. Younger (1991) has added his voice to the chorus with a critical piece of evidence. He determined the cytosolic free calcium concentration in intact retinas loaded with Fura-2 when they were perfused with the solution developed by Matthews *et al.* (1988). This technique had been assumed to block calcium efflux through the exchanger but maintain the cytosolic free calcium concentration in the physiological range. Dr.

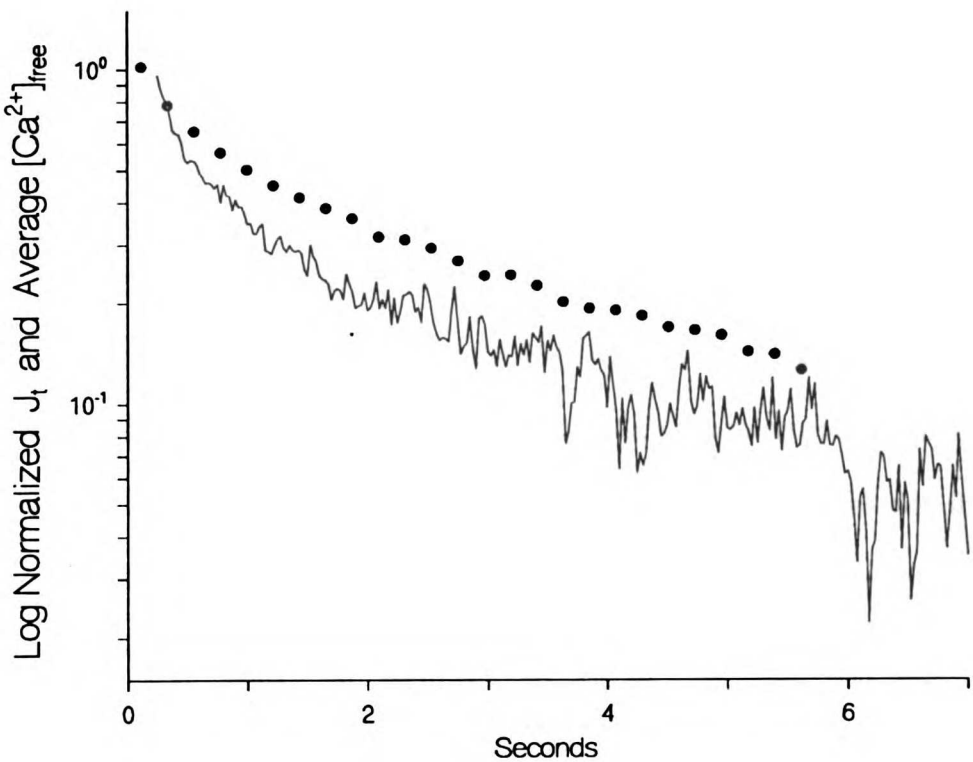

Figure 3. A representation of the similarity between the exchange current measured from seven Fura-2 loaded rods (line) and the average calcium concentration measured from three Fura-2 loaded retinas (circles). The logarithmic ordinate helps to show that the exchange current and calcium have the same kinetics after the first second or so of illumination. These data are the same as were shown in Chapter 3 (Fig. 7 and Fig. 12).

Younger found that this assumption was correct and observed that retinas bathed in this solution continued to respond to illumination but that the free concentration of calcium in the cytoplasm did not change during illumination. This observation means that there is no rapid, light-induced release of calcium from an internal store. It also demonstrates that Na^+: Ca^{2+}, K^+ exchange activity is required to reduce the cytosolic free calcium concentration during illumination.

It is clear that calcium flux across the plasma membrane must be regulated only by the cyclic GMP-gated channels and the Na^+: Ca^{2+}, K^+ exchanger. This conclusion is consistent with those reviewed by McNaughton (1990). A more novel conclusion is that neither the calcium permeability of the cyclic GMP-gated channel nor the intrinsic character of the exchanger is significantly affected by illumination.

20-30% of the Cyclic GMP-gated Current is Carried By Calcium

The results of the previous section are a comforting verification of some of the commonly held concepts of calcium regulation. My results now begin to deviate from widespread expectations.

Yau and Nakatani (1985) estimated that 10-15% of the current flowing through the cyclic GMP-gated channel was carried by calcium ions in toad rods. This estimate was based on the integral of the current flowing through the cyclic GMP-gated channels

of rods bathed in a solution in which lithium was substituted for sodium. This net charge was then compared to the charge transferred by the Na^+: Ca^{2+}, K^+ exchanger when extracellular sodium was restored after the cyclic GMP-gated channels had been closed by bright illumination. Thus the estimate of 10-15% as the percentage of current carried by calcium is explicitly valid when lithium rather than sodium, which is less permeable, is the dominant charge carrier.

I have also made an estimate of the fraction of current carried by calcium ions in frog rods, but it is obtained from the initial magnitude of the total current and the exchange current observed for frog rods perfused with the control solution, in which sodium is the dominant carrier.

My estimate relies on the work of Baylor and Nunn (1986), who showed that the only channel in the outer segment plasma membrane of any consequence is the cyclic GMP-gated channel, and that of Yau and Nakatani (1985), Younger (1991) and Lagnado *et al.* (1992) who showed that the only other electrogenic mechanism in the outer segment plasma membrane is the Na^+: Ca^{2+}, K^+ exchanger. The total current flowing into the outer segment may then be written as:

$$J_t = J_g + J_{ex} \qquad (1)$$

where J_t is the total current, J_g is the current flowing through the cyclic GMP-gated channels and J_{ex} is the current generated by the action of the exchanger.

In order to make the estimate, it must be assumed that either the current flowing through the cyclic GMP-gated channel or the exchange current can be described. One could make the assumption that the exchange current is strictly proportional to the cytosolic free calcium concentration measured using Fura-2. This would be consistent with the common belief. As it should become clear in subsequent sections, however, I have reason to doubt such an assumption. Therefore, I choose to describe the current flowing through the cyclic GMP-gated channels. Because bright illumination rapidly causes the cyclic GMP-gated conductance of the outer segment to become impermeable, only the rising phase of the photoresponse needs to be described at this point. The derivation of the model of the behavior of the cyclic GMP cascade is detailed in Appendix B. Lamb and Pugh (1992) have recently published a similar model. My model was constructed independently but makes many of the same assumptions and I acknowledge their influence on the final analysis. There are, however, two significant differences, which are discussed in the appendix, and so I will continue to use my derivation.

The model predicts that the rising phase of the photoresponse will be approximately described by:

$$J_g(t) \approx J_g(0)\ e^{-k_I I t^n} \qquad (2)$$

where J_g is the current flowing through the cyclic GMP-gated channel, k_I is an activation constant following the terminology of Lamb and Pugh (1992), I is the rate at which rhodopsin molecules are isomerized by the bright step of illumination. The term, η, is

an exponent which is predicted to be between three and five. It is used to approximate the power series described in the appendix. η does not need to be an integer. This allows for the activation of transducin as an independent step in the acceleration of cyclic GMP hydrolysis and to account for possible cooperative interactions between active transducin and phosphodiesterase.

In Fig. 4*A* I show the average current recorded from seven Fura-2 loaded rods. I show the form of the exponential term of Eqn (2), with $k_I = 0.24$ Rh^{-1} sec^{-3}, $I = 10{,}000$ Rh sec^{-1} and $\eta = 4$ in Fig. 4*C*. These parameters were chosen so that the curve may be easily compared to the rising phase of the photoresponse shown in Fig. 4*B*. The curve in Fig. 4*C*, which represents the normalized current flowing through the cyclic GMP channel, approaches zero much more rapidly than does the photocurrent. The difference reflects the exchange current, which can be estimated from these figures to be approximately 2 pA.

A refinement of these estimations appears in Fig. 5*A*. Here, the data from Fig. 4*B* are fitted with the function of Eqn (2) with $J_g(0) = 12.5$ pA, the same k_I and I as in Fig. 4*C*, and $\eta = 4.25$. The fitted function has been displaced along the negative ordinate by 2.1 pA, an estimate of the initial magnitude of the exchange current, in order to demonstrate the fidelity of the fit. In Fig. 5*B*, I show the exchange current, determined by subtracting the function shown in Fig. 5*A* from the photocurrent (Fig. 4*A*).

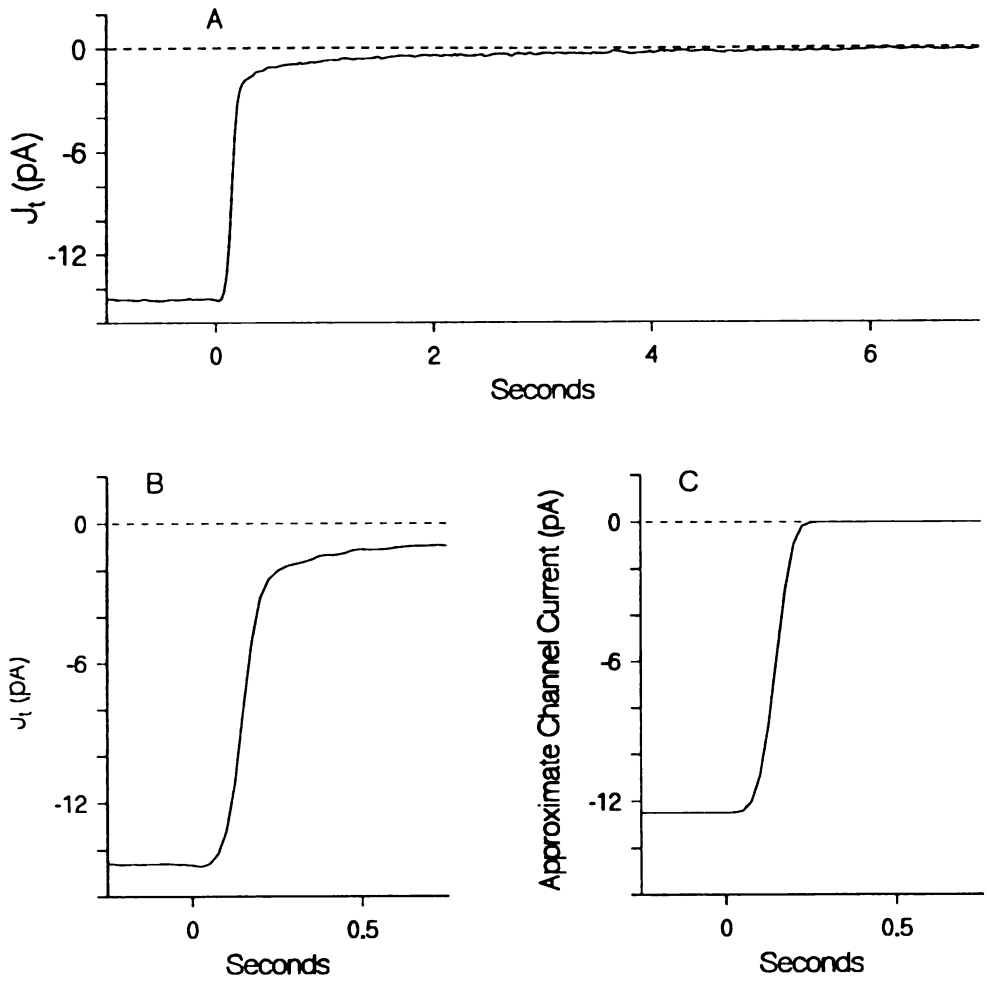

Figure 4. The rising phase of the photoresponse. *A*, the average current recorded from seven rods (shown in Chapter 3 as Fig. 1*D*). *B*, an expanded view of the same current around the time of the onset of illumination. *C*, an approximate prediction of the current flowing through the cyclic GMP-gated channels during the rising phase. The curve is derived from Eqn (2) with $k_I = 0.24\ R^{*-1}\ sec^{-3}$, $I = 10^4\ R^*\ sec^{-1}$ and $\eta = 4$.

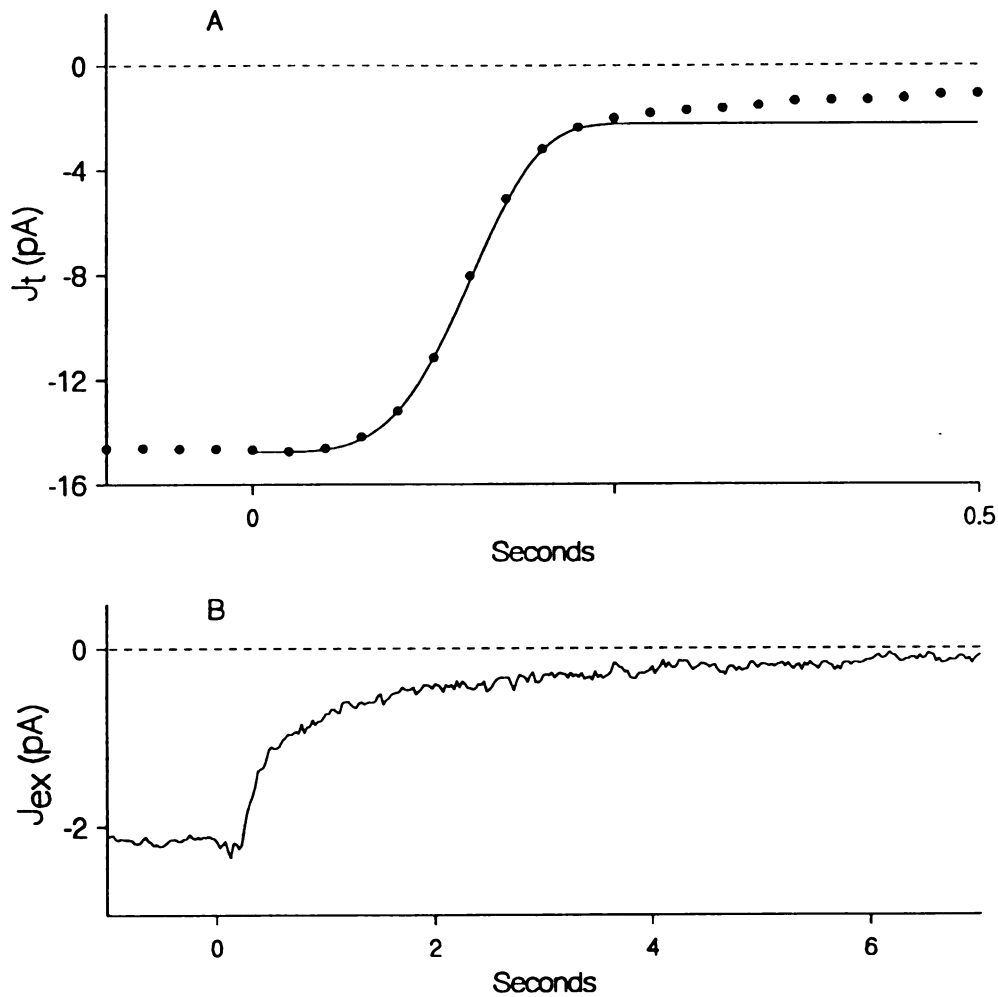

Figure 5. Separation of the exchange current and the current flowing through the cyclic GMP-gated channels. *A*, a portion of the rising phase of the current shown in Fig. 4*B* (circles). The curve passing through the data was obtained from Eqn (2) with $k_I = 0.24$ R^{*-1} sec^{-3}, $I = 10^4$ R^* sec^{-1} and $\eta = 4.25$ but is shifted along the negative ordinate so that it aligns with the data. The total current flowing through the cyclic GMP-gated channels in the dark is approximately 12.5 pA in this instance. *B*, the exchange current obtained by subtracting the curve in *A* from the current shown in Fig. 4*A*. Note the change in the abscissa between *A* and *B*. The initial value of the exchange current is approximately 2.1 pA.

In the midst of this discussion of calcium regulation, I pause to point out that the value of $\eta = 4.25$ is significant. According to the model of Lamb and Pugh (1992) one would expect a value of η of approximately three for a step of illumination. In my model the value of η is predictive of the character of phosphodiesterase activation for any value between three and five, as explained in the appendix. The fact that η is greater than four implies that each activated transducin does not bind independently and with equal influence to the gamma subunits of phosphodiesterase. Rather, I expect significant cooperativity. That is, the first transducin to bind to phosphodiesterase has much less of an impact than the second. On the other hand, the fact that η is near four suggests that phosphodiesterase is rapidly activated by transducin, consistent with the original assumption by Lamb and Pugh (1992). I shall return to an examination of the rising phase and the activation of the cyclic GMP cascade in the next chapter.

The best estimate of the initial magnitude of the exchange current is 2.1 ± 0.1 pA. For every positive charge translated into the outer segment by the exchanger, one calcium ion is extruded (Cervetto *et al.*, 1989). As discussed previously, only the cyclic GMP-gated channels and the exchanger afford routes by which calcium ions may cross the outer-segment plasma membrane. Also shown was the fact that calcium ions carry a constant fraction of the current flowing through the cyclic GMP-gated channels. The calcium influx that balances the efflux via the exchanger would therefore appear to account for 4.2 ± 0.2 pA of this current in the dark. The exchanger is, however, voltage-dependent with an *e*-fold increase in current for a 70 mV hyperpolarization (Lagnado *et*

al., 1988). One therefore expects that 20-30% of the current flowing through the cyclic GMP-gated channels in the dark represents calcium influx - twice the previous best estimate (Yau and Nakatani, 1985).

Less Than One Percent of the Total Exchangeable Calcium is Free

The fact that the calcium flux is restricted to the cyclic GMP-gated channel and the exchanger and the fact that calcium accounts for a constant fraction of the current flowing through the cyclic GMP-gated channel mean that the rate of change of the total calcium concentration in the rod outer segment may be expressed as:

$$\frac{d[Ca^{2+}]_t}{dt} = -\frac{\frac{f}{2} J_g - J_{ex}}{e A_v V} \qquad (3)$$

where $[Ca^{2+}]_t$ is the concentration of total calcium, f is the fraction of the channel current that is carried by calcium ions, e is the quantal charge, A_v is Avogadro's number, and V is the free volume of the outer segment, approximately 1 pl. I use the convention that positive charge flowing into the outer segment is described as a negative current.

The change in the total calcium concentration of the outer segment may be determined by integrating Eqn (3) when J_g and J_{ex} are given by Eqn (2) and recorded photocurrents. The time course of the change in the total calcium concentration, $\Delta[Ca^{2+}]_t$, may be obtained in a similar manner and can be written as:

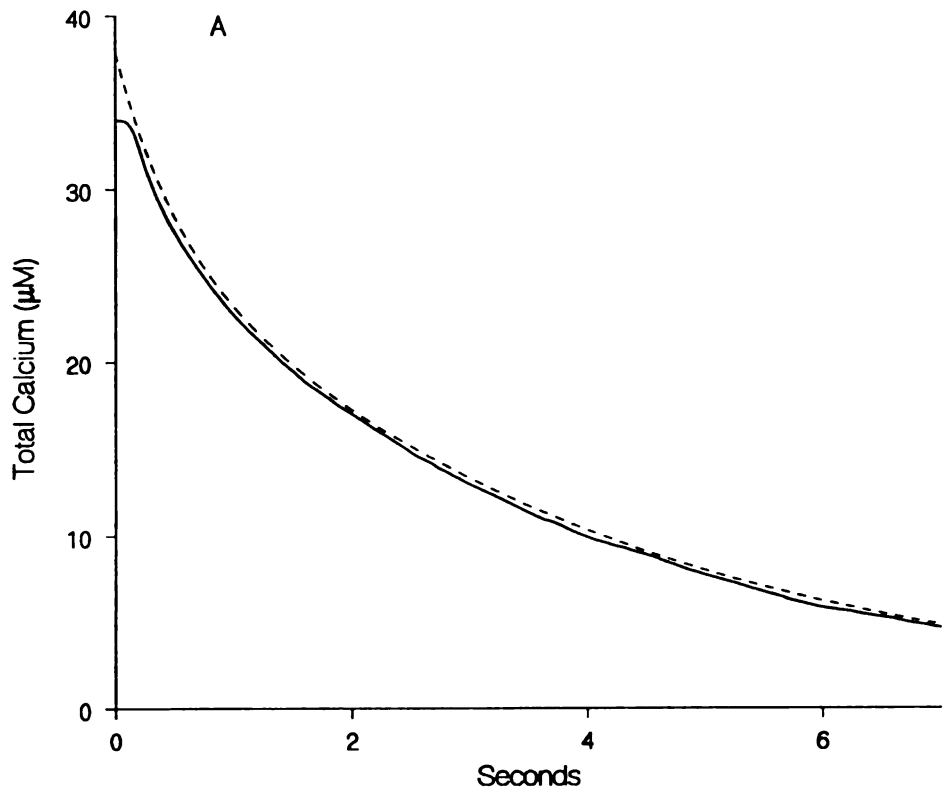

Figure 6. The total calcium that is extruded from a rod during bright illumination. The solid line is obtained from Eqn (4) and the current shown in Fig. 4*A*. The dashed line is the integral of Eqn (6) which approximately describes the exchange current. The apparent total calcium concentration in the dark is approximately 34 μM but this is only 80-90% of the true value because only this much of the circulating current is captured by the suction electrode. The change in the total calcium concentration reflects only that fraction of the total calcium that can be extruded.

$$\Delta[Ca^{2+}]_t = \int_t^{\infty} \frac{\frac{f}{2} J_g - J_{ex}}{e\, A_v\, V}\, dt' \qquad (4)$$

Fig. 6*B* illustrates the result of evaluating the data shown in Fig. 4*A* in accordance with Eqn (4) and $f = 0.34$. The integral of the exchange current yields an apparent initial calcium concentration of 34 μM. The recorded photocurrent is only 80 to 90% of the actual current, however. I therefore estimate that the initial total calcium concentration that is accessible by the exchanger is 38 to 44 μM.

Previous results suggest that the cytosolic free calcium concentration in the outer segment of a dark-adapted rod is between 100 and 200 nM. The estimate of the total accessible calcium concentration under the same conditions implies that only about 1 in 200-300 of the calcium ions that can be extruded from the outer segment is free. This is two to three times fewer free calcium ions per bound calcium ion than estimated by Lagnado *et al.* (1992) in aequorin-loaded rods. They recognized, however, that a significant quantity of their "high-affinity" (K_d = 0.7 μM) calcium buffer was lost during the loading process. My estimate is even more different than one would expect from the single, 400 ms exponential decline of the exchange current reported by Yau and Nakatani (1985) and Hodgkin *et al.* (1987). I believe that the difference is primarily due to the greater resolution in my measurement of exchange currents. The exchange current in frog rods can be described better by the sum of two exponentials, one with a time constant of 400 to 500 milliseconds and the other with time constant of approximately 4 seconds.

The slow phase accounts for approximately 30% or 0.65 pA, of the initial magnitude of the exchange current in frog rods. I believe the exchange current of salamander rods might also have a slow phase which may easily have been mistaken for experimental drift. This is an important difference in terms of determining buffering capacity because a substantial fraction of the total calcium extruded is done so during the slow phase.

The Exchange Current is Not Proportional to the Average Measured $[Ca^{2+}]_i$

Given the previous statements, it is probably clear that I have been hedging about several aspects of calcium regulation. I have been somewhat mysterious about the detailed relationship between the exchange current and the cytosolic free calcium concentration measured with Fura-2. As I have mentioned, the time course of the exchange current cannot be described by a solitary exponential. The same is true of the space-averaged concentration of cytosolic free calcium measured with Fura-2. What is more important, however, is that the exchange current is not proportional to the cytosolic free calcium concentration. I shall demonstrate below that this conclusion is not a result of a systematic error in my experimental techniques nor is it a result of high-affinity buffering. Rather, I believe it is an indication of something more interesting.

In Fig. 7, I show again the cytosolic free calcium concentration measured during a bright step of illumination. These are the same data that were originally shown in Fig. 11 ($\alpha = 0.75$) of the previous chapter. The first measured value is the average free

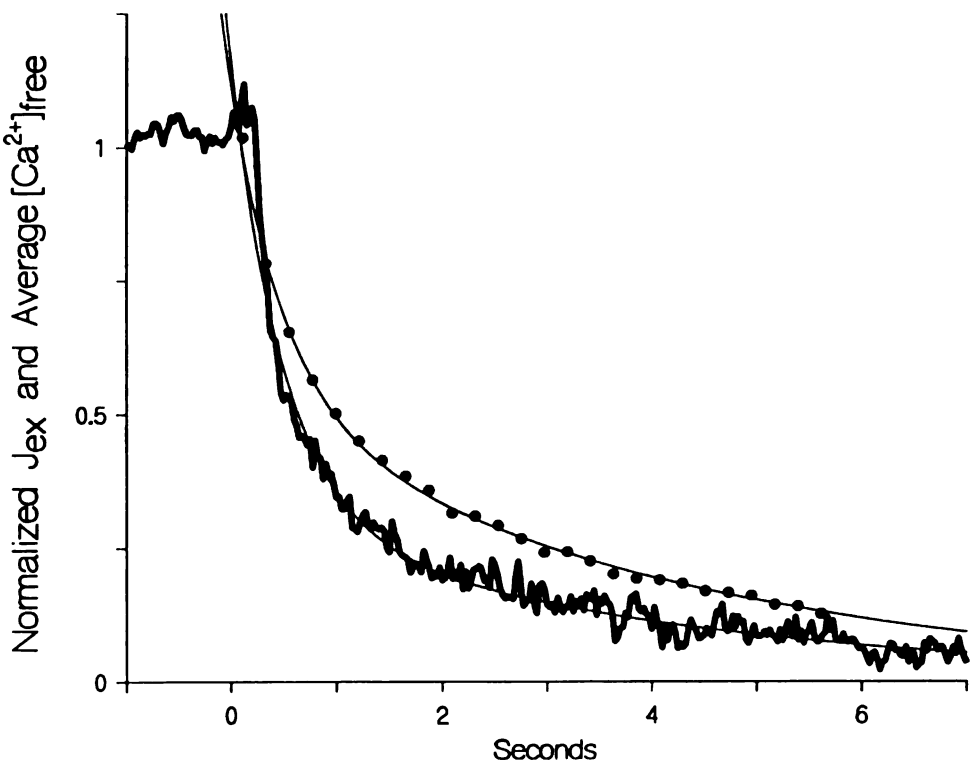

Figure 7. A comparison and description of the exchange current (thick line) and the change in calcium concentration measured from Fura-2 loaded retinas (circles). Eqn (5) and Eqn (6) of the text generated the curves passing through the exchange current and calcium, respectively. Although each is the sum of two exponentials, they are clearly not the same. The curves begin 100 ms after the onset of illumination (t=0). This is the time at which the calcium concentration begins to change.

calcium concentration during the first 220 milliseconds of illumination. Also shown is the corresponding exchange current (Fig. 7). Again, it is derived from the photocurrent displayed in Fig. 1 of the previous chapter. Now, however, I have subtracted the current flowing through the cyclic GMP-gated channels in accordance with Eqns (1) and (2) and in exactly the same manner as was described for Fig. 5. The fact that the exchange current does not decay during the rising phase of the photoresponse, approximately the first 200 milliseconds, is in part a result of my estimate of the current flowing through the cyclic GMP-gated channels, in part due to noise and probably in part due to voltage-dependent behavior. Although the exchange current shown is rather too abrupt, it is generally consistent with the observation that cytosolic free calcium measured with 50 milliseconds resolution does not change significantly for the first 200 milliseconds of bright illumination (Younger, 1991). The first datum of the cytosolic free calcium data, Fig. 7*A*, thus represents a calcium concentration that is very close to the free calcium concentration in the cytosol of a dark-adapted rod. The measured calcium concentration and the exchange current are clearly not proportional although they are similar enough to suggest a common underlying process.

Through each set of data of Fig. 7, I have fitted functions of that are the sum of two exponentials. Slightly better fits can be obtained if three exponentials are allowed. In each case, the functions begin at 100 milliseconds to account for the fact that neither the exchange current or cytosolic free calcium concentration change immediately. The fitted functions are:

$$[Ca^{2+}]_f = 150\ [\ 0.47\ e^{-(t-0.1)/0.5} + 0.53\ e^{-(t-0.1)/4}\ ]\ \text{nM} \quad (5)$$

$$J_{ex} = 2.1\ [\ 0.70\ e^{-(t-0.1)/0.5} + 0.30\ e^{-(t-0.1)/4}\ ]\ \text{pA} \quad (6)$$

where time, t, is expressed in seconds.

The form of these functions is unexpected for two reasons. Lagnado *et al.* (1992) and Cervetto *et al.* (1987) have demonstrated that the exchange rate is proportional to calcium in the presence of IBMX. The exchange current I measure is not, however, proportional to the *average* cytosolic free calcium concentration I measure. In addition, Lagnado *et al.* (1992) presented data that suggests that there are two dominant buffering systems in the salamander rod outer segments. One has a very low affinity. The other has a dissociation constant of approximately 0.7 μM. I would therefore expect that free calcium concentrations of 200 nM and less would constitute roughly constant fractions of the total calcium. This, the fact that calcium is extruded only by the exchanger during bright illumination and the expectation that the exchange rate is proportional to the cytosolic free calcium concentration, dictates that the exchange current should decay as a single exponential, as reported by Yau and Nakatani (1985).

An easy first attempt to resolve this discrepancy is to suppose that the exchange current is actually strictly proportional to the cytosolic free calcium concentration and that I have made an error in our measurements. As demonstrated in Fig. 7 of the previous chapter, the same average magnitude and time course of the exchange current is observed

in Fura-2 loaded rods and unloaded rods. Similar exchange currents were seen in cells that were not included in either average. Thus, the exchange current data shown in Fig. 7 are not unusual. The calcium data are also typical. They are virtually indistinguishable from data obtained by Younger (1991). One could then suppose that the model of the rising phase is incorrect when few cyclic GMP-gated channels are open. In Fig. 8, I show again the same exchange current and calcium data. This time, the calcium data has been assumed to be proportional to the slow phase of the exchange current. The calcium data plotted in this way indicate what would be expected of the exchange current if it were in fact proportional to the measured cytosolic free calcium concentration. There is a clear discrepancy during the early phase. If this difference were due the closure of cyclic GMP-gated channels, the latter portion of the rising phase would need to decay exponentially with a time constant of approximately 500 milliseconds. This seems unlikely. Photocurrents measured by Torre *et al.* (1986) from rods loaded with the calcium chelator, BAPTA, and photocurrents recorded by Matthews *et al.* (1988) when the exchanger was blocked show no such slow decay in the closure of the cyclic GMP-gated conductance. Rather, they appear to be consistent with the model. I believe, therefore, that my description of the exchange current is accurate.

A somewhat more subtle explanation which is possible is that the cytosolic free calcium concentration or buffering capacity varies longitudinally within outer segments. The cytosolic free calcium usually measured is dominated by the distal portion of the

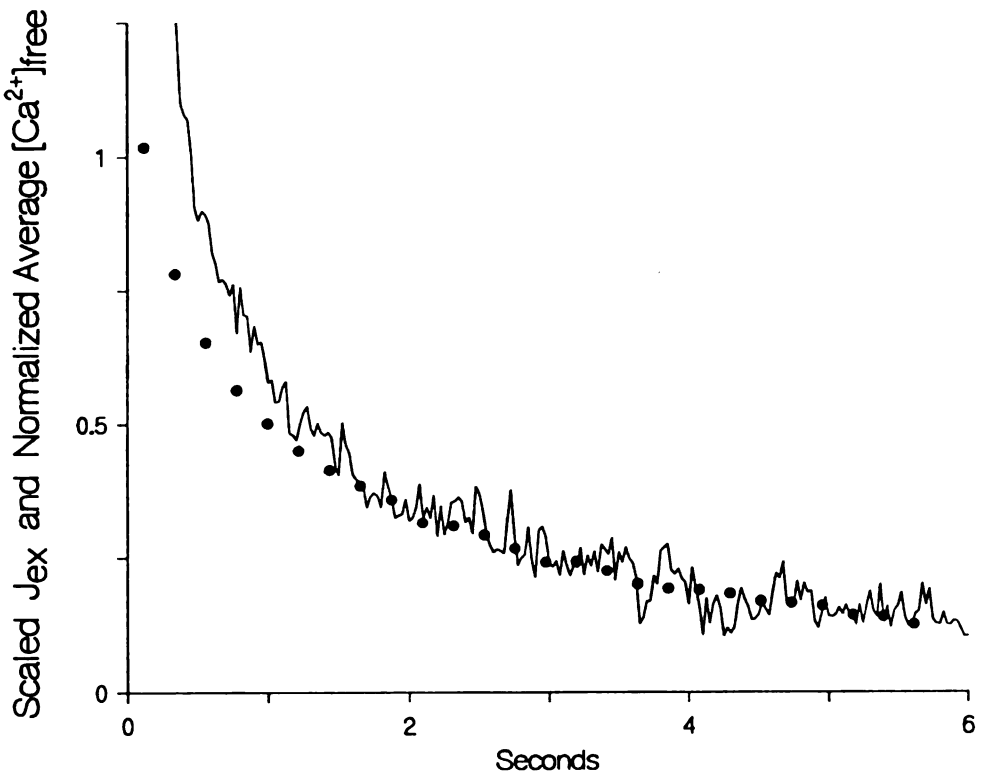

Figure 8. The exchange current and calcium concentration are proportional during the slow phase. The data shown are the same as in Fig. 7. The current has been scaled so that it is coincident with the calcium concentrations. At early times, however, the exchange current decays more rapidly. This behavior cannot be attributed to the closure of cyclic GMP-gated channels.

outer segment because the ultraviolet stimulating illumination and the resulting fluorescence are absorbed significantly by rhodopsin. The exchange current is, however, recorded from the entire outer segment without preference to where it originates. If, for example, calcium were extruded from the distal portion of the outer segment more slowly than from the proximal portion, the measured cytosolic free calcium concentration would not be expected to be proportional the exchange current. The data in Fig. 9 demonstrate, however, that there is no significant longitudinal variation in the rate of calcium extrusion. The data are the cytosolic free calcium concentration measured in a Fura-2 loaded retina when the photoreceptors were nearest the ultraviolet stimulus and the calcium concentration measured when the retina was inverted so that the photoreceptors pointed away from the stimulus. The data are normalized to account for an approximately 30% loss in the magnitude of the light-induced change in fluorescence incurred when the retina was inverted. In the photoreceptor-up configuration the average measured cytosolic free calcium concentration reflects primarily the distal outer segment. In the photoreceptor-down configuration, the data reflect the free calcium concentration in the proximal outer segment. The data from each configuration have the same time course and so I conclude that there is no longitudinal variation in extrusion rates or buffering characteristics.

It is worth mentioning that neither a change in cytosolic sodium concentration nor the hyperpolarization of the rod in response to the closure of the cyclic GMP-gated channels of the outer segment could lead to the second, slower rate of fall. In the first

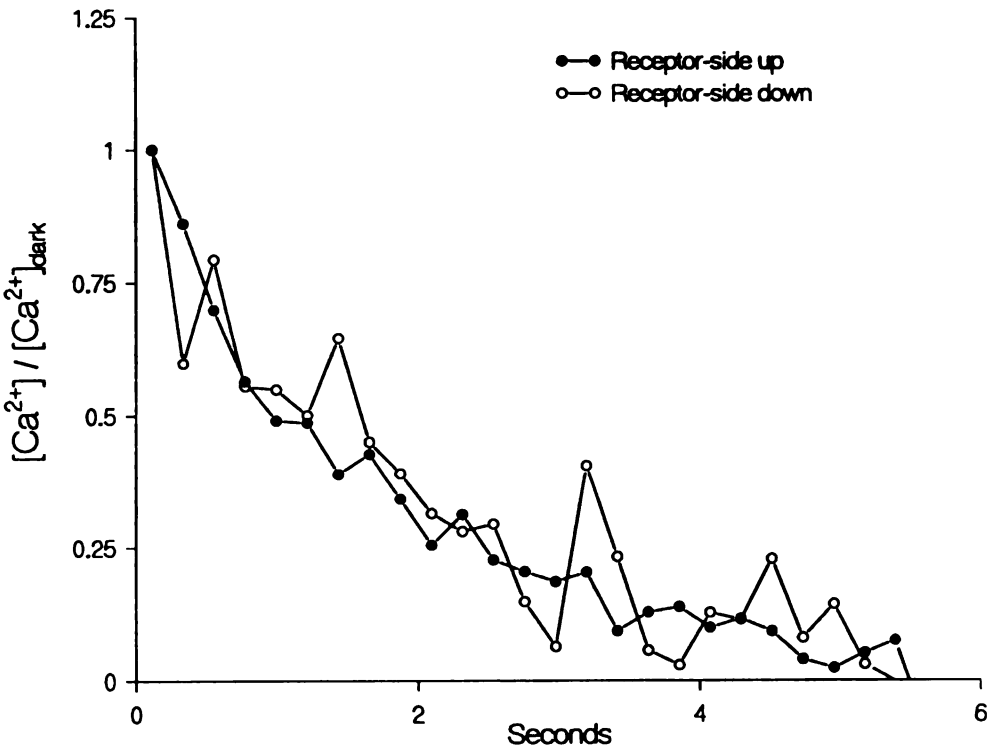

Figure 9. The calcium kinetics are the same near the inner segment and near the tip of the distal portion of the outer segment. The calcium concentrations shown were measured from a Fura-2 loaded retina - first when the photoreceptors pointed towards the actinic stimulus (solid circles) and later when the retina had been flipped so that the photoreceptors pointed downward (open circles). In the receptor-side-up configuration, most of the fluorescence is derived from the distal part of the outer segment: the part that is nearest the stimulus. In the receptor-side-down configuration, the proximal portion of the outer segment near the inner segment dominates. The fact that the kinetics of the change in calcium are the same in each case demonstrates that there is no significant longitudinal variation in the exchange rate.

case, sodium that normally enters the outer segment through the cyclic GMP-gated channels and exchanger is balanced by efflux from the inner segment. When the cyclic GMP-channels are shut by illumination, efflux continues and so one would expect the cytosolic sodium concentration to be reduced. Thus, the driving force on the exchanger would be increased and the calcium concentration would fall more rapidly in the later phase of extrusion, not more slowly, as is observed. In the case of membrane hyperpolarization, Lagnado *et al.* (1988) have shown that the exchanger has a voltage dependence that would result in more rapid efflux of calcium during the later phase. This again is contrary to our findings.

The Kinetics of the Change in $[Ca^{2+}]_i$ are Independent of $[Ca^{2+}]_i$

I could continue to examine ways in which I might have made errors in the measurement of either the exchange current or the cytosolic free calcium concentrations. The fact that both are described by the sum of two exponentials and the fact that the time constants are similar in each case is not so easily dismissed.

My original hypothesis to account for the fact that neither the exchange current nor the cytosolic free calcium concentration could be described by a single exponential, was that the effect stemmed from the influence of a high-affinity calcium buffer. In the dark, the cytosolic free calcium concentration was assumed to be sufficiently high that the high-affinity buffer would be nearly saturated. The fast phase of the exchange current

would then reflect the remaining low-affinity buffering capacity of the outer segment. As the cytosolic free calcium concentration decreased in response to illumination, the high-affinity buffer would begin to unload. The additional buffering capacity when the cytosolic free calcium concentration was near the dissociation constant of the high-affinity buffer would result in a slowing of the rate of change of extrusion. Subsequent experiments demonstrated, however, that this hypothesis was not correct.

In Fig. 10*A*, I show the average cytosolic free calcium concentrations measured from a retina when it was dark-adapted and then again when it had been adapted to 30 seconds of illumination that isomerized approximately 125 rhodopsin molecules per rod per second. In Fig. 10*B*, I show the same data, but the data from the light-adapted case are shifted along the abscissa so that the measured calcium concentrations are aligned during the slow phase. If the kinetics of the change in cytosolic free calcium were due solely to rapid, high-affinity buffering, the data would superimpose. In Fig. 10*C*, the same data are displayed, but normalized with respect to the first point. The fact that the data superimpose very well in this case, but not very well in Fig. 10*B*, is very strong evidence that the change in cytosolic free calcium concentration induced by bright illumination has no strong dependence on free calcium in this range. This property indicates that any high-affinity buffers that are in the outer segment, including Fura-2, do not constitute a significant fraction of the total buffering capacity. The dominant calcium buffering system in frog rod outer segments has, therefore, an effective dissociation constant that is much greater than a few hundred nanomolar.

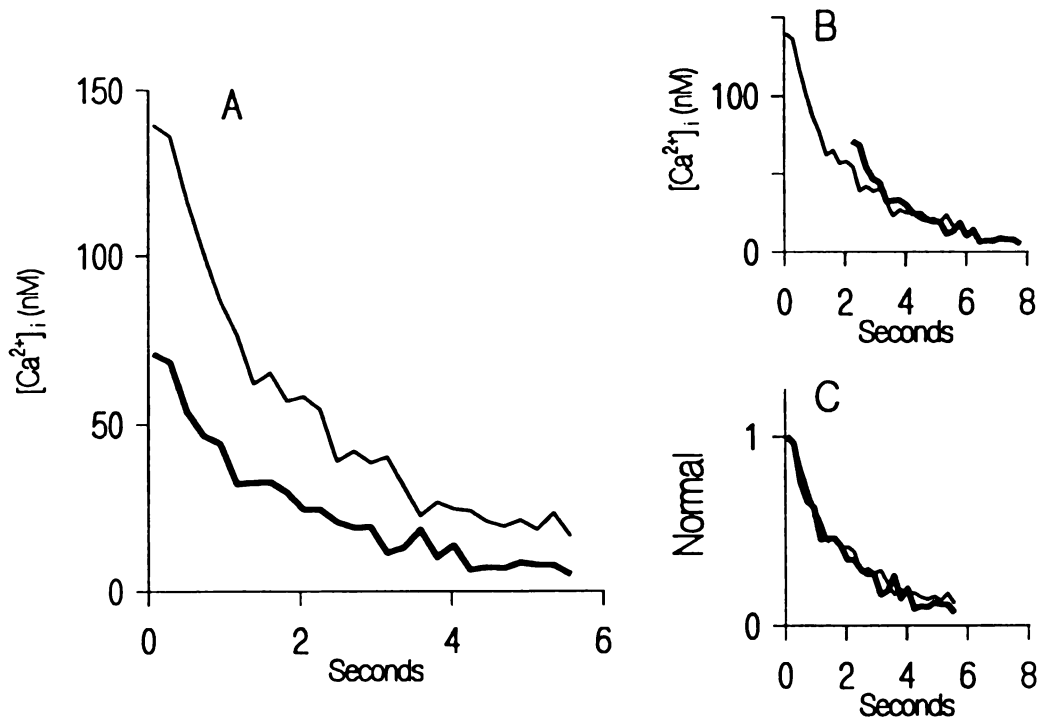

Figure 10. High-affinity buffers do not account for the slow phase of the fall in calcium during bright illumination. *A*, the light-induced fall in calcium concentration recorded from a dark-adapted retina (thick line) and later when an adapting illumination had reduced the steady-state calcium concentration by approximately one-half (thin trace). *B*, the data obtained after light adaptation are shifted in time so that they overlie the data recorded before adaptation. *C*, both sets of data are normalized with respect to their initial value. If high-affinity buffers slowed the rate of change of free calcium, the kinetics should be calcium dependent. *B*, shows that they are not. *C*, shows that the kinetics of the change if calcium depended only on time. An examination of other adapting backgrounds, which suppressed the steady-state calcium concentration by different amounts, led to the same conclusions. These data were obtained by Dr. James Younger.

Calcium is Not Uniformly Distributed Across the Rod Cross-section

The notion that the dominant calcium buffering system in a rod outer segment has a low affinity for calcium is not unprecedented (Hodgkin *et al.*, 1987, Lagnado *et al.*, 1992). The observation that the measured calcium does not fall with a single exponential time course has, however, a more surprising consequence: one should not necessarily expect the exchange current to be proportional to the average cytosolic free calcium concentration. When all of the cyclic GMP-gated channels are closed, the change in total calcium is the integral of the exchange current, as already described. It is untenable that the cytosolic free calcium concentration, whose kinetics are described by at least two exponentials, can be proportional both to the exchange current and its integral.

I believe that the solution is found in the way in which calcium concentrations are measured. Fura-2 measurements reflect the free calcium concentrations averaged over the entire cross-section of the outer segment. On the other hand, the exchange current reflects the calcium concentration only at the plasma membrane. The exchange current shown in Fig. 7 clearly decays more rapidly than the average measured calcium concentration. The conclusion is that the rod outer segment is not a well-stirred compartment: the calcium concentration is not radially uniform. Rather, calcium near the membrane is more readily extruded than calcium in the interior of the rod.

Homogeneous Restrictions on Radial Diffusion Do Not Account for These Observations

This sort of behavior is, of course, what is expected of any diffusion limited process. If calcium mobility is limited, its concentration will be reduced more rapidly near where it is extruded than in the more central regions of the rod. The rate at which calcium could diffuse radially from the rod interior to replace ions that had already been extruded would be hindered by the availability of binding sites along the way. Diffusional restrictions on calcium efflux have, in fact, been considered previously (Lagnado *et al.*, 1992) but discounted as not a limiting factor based on the estimated calcium extrusion rate being an order of magnitude slower than the diffusional time constants they expected. The resolution of the exchange current and free calcium concentration I have shown is, however, clearly better. In addition, the slowness with which the exchange current and calcium concentration decay reflects a buffering capacity which is substantially larger than earlier estimates. A re-examination of calcium mobility seemed prudent.

My first attempt at predicting calcium kinetics assumed that the outer segment contained a single, evenly distributed low-affinity buffer and that there were no significant physical barriers to calcium mobility. The mathematics and boundary conditions that describe this situation are developed in Appendix C. The results are given by:

$$\frac{J_{ex}(t)}{J_{ex}(0)} = \frac{Ca(R,t)}{Ca_o} = \sum_{m}^{\infty} \frac{2\,\varepsilon}{\varepsilon^2 + (R/\lambda_m)^2} e^{-t/\tau_m} \qquad (7a)$$

where

$$\frac{\langle Ca(t)\rangle}{Ca_o} = \sum_{m}^{\infty} \frac{2\,\varepsilon}{\varepsilon^2 + (R/\lambda_m)^2} \frac{2\,\varepsilon}{(R/\lambda_m)^2} e^{-t/\tau_m} \qquad (7b)$$

$$\lambda_m^2 = \frac{D}{\beta}\,\tau_m$$

and

$$\varepsilon = \frac{R^2}{2}\,\frac{\beta}{D}\,\frac{J_{ex}(0)}{e\,A_v\,V\,Ca_t(0)}$$

In these equations, $J_{ex}(t)$ is the exchange current with an initial value of $J_{ex}(0)$, $Ca(R,t)$ is the calcium concentration near the plasma membrane, $\langle Ca(t)\rangle$ is the space-averaged calcium concentration, Ca_o is the initial free calcium concentration and $Ca_t(0)$ is the initial total calcium concentration. The radius of the rod is represented by R. β is the buffering power (the ratio of total calcium to free calcium) and D is the intrinsic diffusion constant for calcium in the cytosol. The variables, λ_m and τ_m, are the cylindrical length constants and time constants, respectively. They are determined by the boundary conditions, represented by the constant, ε, which effectively describes the turnover rate of the exchanger and the buffering capacity of the outer segment. The remaining variables are physical constants: quantal charge (e), Avagadro's Number (A_v) and the free volume of the outer segment (V).

The exchange current and average calcium concentration derived in this way are described by a series summation of exponential terms. This is like the sum of exponentials that were used as empirical descriptions. It would appear, then, that Eqns

(5) and (6) are close to a solution; however, a closer analysis demonstrates that the assumptions I have made in terms of buffer distribution and physical barriers result in a description of calcium kinetics that does not agree with the observations.

In Fig. 11, I show the average free calcium concentration and exchange current I would expect if Eqn (7) were valid. In Fig. 11*A*, the curves are obtained when $\varepsilon = 0.5$ - a value that is within the range of values which could be reasonably expected (0.4-0.6) based on the previous data and an intrinsic diffusion coefficient of 1000 μm^2 sec^{-1} (Handbook of Chemistry and Physics, 1982). In Fig. 11*B*, I show curves obtained when ε is 1.5, a larger value than I would expect. In each case, the average free calcium concentration is overwhelmingly dominated by the first term of the series and declines with a single, slow exponential time constant. On the other hand, the exchange currents do display the influence of multiple terms of the series. This behavior reflects the depletion of calcium from a very thin layer near the plasma membrane. Increasing values of ε accentuate this effect. However, the predicted average calcium concentration and exchange current never agree with the experimental observations for any value of ε.

A Simpler Representation of Diffusional Restrictions

The failure of the above description to predict the free calcium concentration and

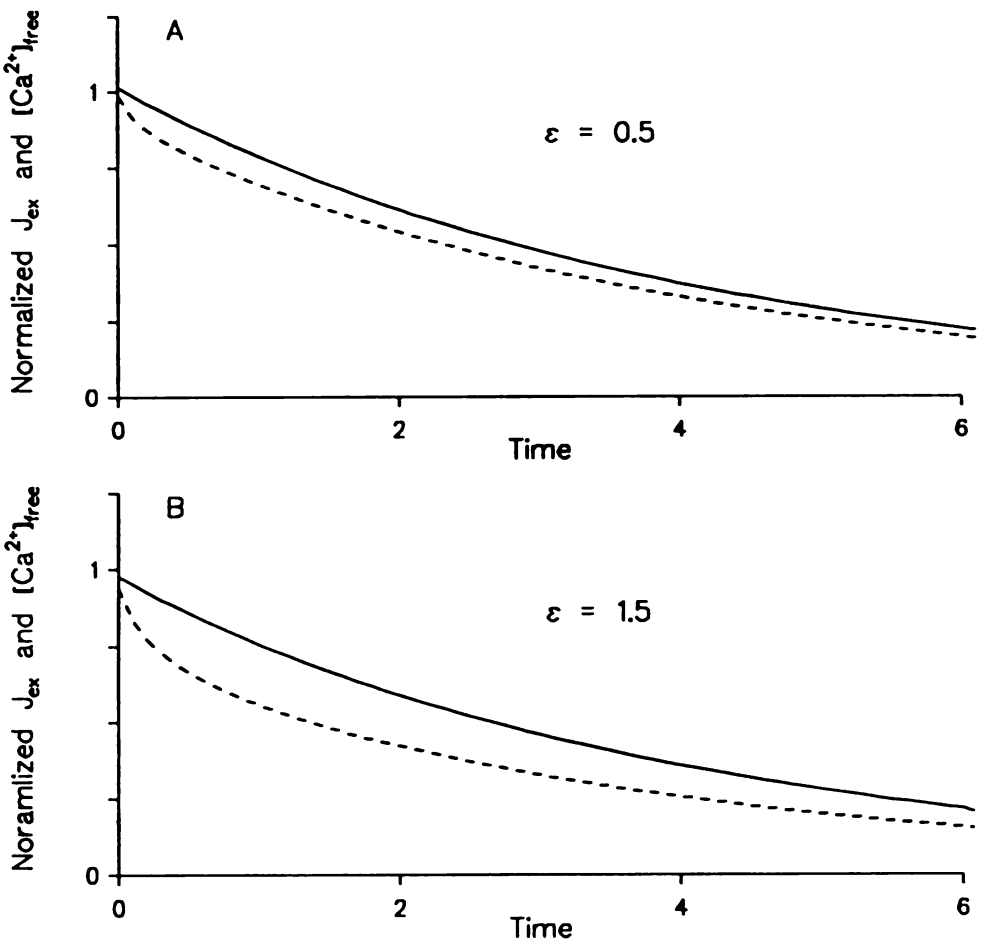

Figure 11. Calcium concentrations (solid lines) and exchange currents (dashed lines) that would be expected to be observed if diffusional restrictions were uniform throughout the outer segment. For both *A* and *B*, the curves were generated by the first five terms of Eqn (7a) and Eqn (7b) for different values of the boundary parameter ε. In each case one would expect to observe the calcium concentration to fall along a curve that could not be distinguished from a single exponential. The rapid decrease in the predicted exchange currents are similar to but not the same as the measured exchange currents. There is no value of ε which accurately predicts what is observed.

exchange current observed does not mean that calcium is uniformly distributed across the outer-segment cross-section. It only means that my original assumptions were invalid. It appears that one must assume either that the low-affinity buffer is also distributed unevenly or that calcium ions have a degree of freedom in some parts of the rod that they do not have in others. In either case, the effective diffusion coefficient cannot be assumed to be the same everywhere within the outer segment. I could attempt to modify the derivation that led to Eqn (7) to include a spatial-variation in the effective diffusion coefficient but the mathematics becomes intractable and I would be imposing an arbitrary condition. Instead, I have adopted a simpler and more successful approach.

I give up the attempt to describe the radial profile of calcium concentration in any detail. In Appendix C I note that the spatial and temporal dependences of the calcium concentration are separable for any well behaved spatial variation in the effective diffusion constant. A series summation of weighted exponentials will, therefore, still be a solution, as it is in Eqn (7). Neither the weighting coefficients nor the time constants can be determined from first principles without a detailed knowledge of the radial dependence of the effective diffusion constant, however. Fortunately, the average calcium concentration and exchange current measured are reasonably well described as a sum of a few exponentials. I therefore assume that only a few terms of the complete solution are dominant. In effect, the radial distribution of calcium is reduced to two domains - the space-average of calcium in the central region of the outer segment and the space-average of calcium in the periphery. This approach is a compartmental model which can be

represented as:

$$\dot{Ca}_1 = -\alpha_{ex}(Ca_1 - Ca_o j_r) + \alpha_1 (Ca_2 - Ca_1) \quad (8)$$

$$\dot{Ca}_2 = -\alpha_2 (Ca_2 - Ca_1)$$

Here, Ca_1 represents calcium in the compartment near the membrane, Ca_2 represents calcium in the inner compartment and Ca_o is the initial cytosolic free calcium concentration. The variable j_r is the total current flowing across the plasma membrane during a light response divided by the current that flows in the dark. The rate constant α_{ex} is related to the rate at which calcium is extruded by the exchanger while the rate constants α_1 and α_2 are related to the rate at which calcium ions flow out of and into the inner compartment, respectively.

A word of caution is perhaps necessary because too strict an interpretation of the physical meaning of the compartment model has created confusion in the past. By adopting a compartment model I do not suggest that there are two discrete and well defined compartments within the rod. Rather, the approach may be considered a mathematical trick or approximation: a simplification that is motivated by my belief that the calcium mobility in the outer segment is not as restricted as would be the case if the effective diffusion coefficient were uniformly low throughout the cross-section of rod. I could have presented a model in which I represented the cross-section as three or more compartments; however, because I have only the average free calcium concentration and the exchange current for data and the fact that each can be reasonably well described by

the sum of two exponentials, I have adopted only two compartments. The compartments should therefore be interpreted to represent space-averages of the interior and periphery of the outer segment and the boundary between the domains should not be considered at all sharp. Even this interpretation is only as good as the model's predictive abilities.

Having cautioned against a discrete interpretation of the compartments, the presence of calcium inside the disks of the outer segment suggests a candidate compartment. I discount this possibility. Both compartments must be sensed by Fura-2 and the calcium they contain must be entirely depletable. I have shown that the total extrudable calcium accounts for approximately 40 μM of the total calcium in a dark-adapted rod. This is, however, less than 7% of the total calcium in the outer segment estimated by Somlyo and Walz (1985) and an even smaller percentage of the total calcium reported by Schröder and Fain (1984) It is difficult to imagine that the remaining calcium is anywhere other than within the disks. I would expect, therefore, that the calcium concentration within the disks is high, much greater than the dissociation constant of Fura-2 for calcium. So, even if some calcium left the disks during bright illumination, Fura-2 would remain saturated and would not contribute to the change in fluorescence observed.

During bright illumination, when j_r rapidly becomes proportional to the exchange current, the compartmental model results in a representation of the exchange current and average measured calcium concentration that can be written as:

$$J_{ex}(t) = J_{ex}(0) \left[A_1 e^{-t/\tau_1} + A_2 e^{-t/\tau_2} \right] \quad (9)$$

$$\langle Ca(t) \rangle = Ca_o \left[B_1 e^{-t/\tau_1} + B_2 e^{-t/\tau_2} \right]$$

where τ_1 and τ_2 are the fast and slow time constants of the observed calcium and exchange current kinetics. A_2 and B_2 are the coefficients of the slow phase determined for the observed exchange current and calcium concentration, respectively. A_1 and B_1 are, appropriately, 1-A_2 and 1-B_2. Again the derivation is detailed in an appendix (Appendix D).

The compartment model does not predict the coefficients or time constants of Eqn (9). These are equated to the parameters of the functions fitted to the data as shown in Fig. 7. Rather, these parameters define the rate constants, α_{ex}, α_1 and α_2, and the contribution of each compartment to the overall average free calcium concentration measured with Fura-2. The relationships are developed more fully in Appendix D and are:

$$\alpha_{ex} = \left[A_1/\tau_1 + A_2/\tau_2 \right] \quad (10)$$

$$\alpha_2 = \frac{1}{\tau_1 \tau_2 \alpha_{ex}}$$

$$\alpha_1 = \frac{1}{\tau_1} + \frac{1}{\tau_2} - \alpha_{ex} - \alpha_2$$

and

$$a_1 = \frac{B_1/\tau_1 + B_2/\tau_2}{A_1/\tau_1 + A_2/\tau_2}$$

such that

$$\langle Ca(t) \rangle = a_1 \, Ca_1 + (1 - a_1) \, Ca_2$$

The variable, a_1, is a weighting factor. Its physical interpretation is that it is an estimate of the fraction of the total rod volume in which calcium can be readily accessed by the exchanger.

The values of the parameters are: $\alpha_{ex} = 1.48$ sec^{-1}, $\alpha_1 = 0.45$ sec^{-1}, $\alpha_2 = 0.34$ sec^{-1}, and $a_1 = 0.74$ when $A_2 = 0.31$, $B_2 = 0.53$ sec and $\tau_1 = 0.5$, $\tau_2 = 4$ sec. The value of α_1 suggests that the central domain, in which calcium mobility is relatively low, constitutes only approximately one-quarter of the of the total volume of the rod.

If this representation of calcium kinetics is approximately correct - I show that it is in the next section - then the mobility of calcium ions in the central domain of the outer segment, relative to the mobility of calcium ions in the periphery can be estimated as:

$$\frac{D_{eff.1}}{D_{eff.2}} = \frac{a_1}{1 - a_1} \frac{\alpha_1}{\alpha_2} \qquad (11)$$

where $D_{eff,1}$ and $D_{eff,2}$ are rough estimates of the effective diffusion coefficient for calcium in the periphery and central domains, respectively (see Appendix D). The value obtained for this ratio is approximately 2. This suggests that calcium ions in the periphery are approximately twice as mobile as calcium ions in the interior: the difference between a brisk walk and a mosey.

Calcium During Recovery and Non-saturating Illumination

The significance of the compartment model is not that it results in a two-exponent description of the exchange current and average free calcium concentration. This is a result that is inherent in the approach - it was, in fact, the reason I adopted the approach. The significance is that once the rate constants and weighting factor are obtained from a portion of observed data, all other phenomena that are governed by the same underlying processes should be predictable. The reason for this is that the compartment model is a linear representation of calcium concentrations and depends explicitly only on time.

The model was tested with data that are important in themselves. These are the cytosolic free calcium concentrations measured during the recovery of the photocurrent following a step of illumination that isomerized approximately 10,000 rhodopsin

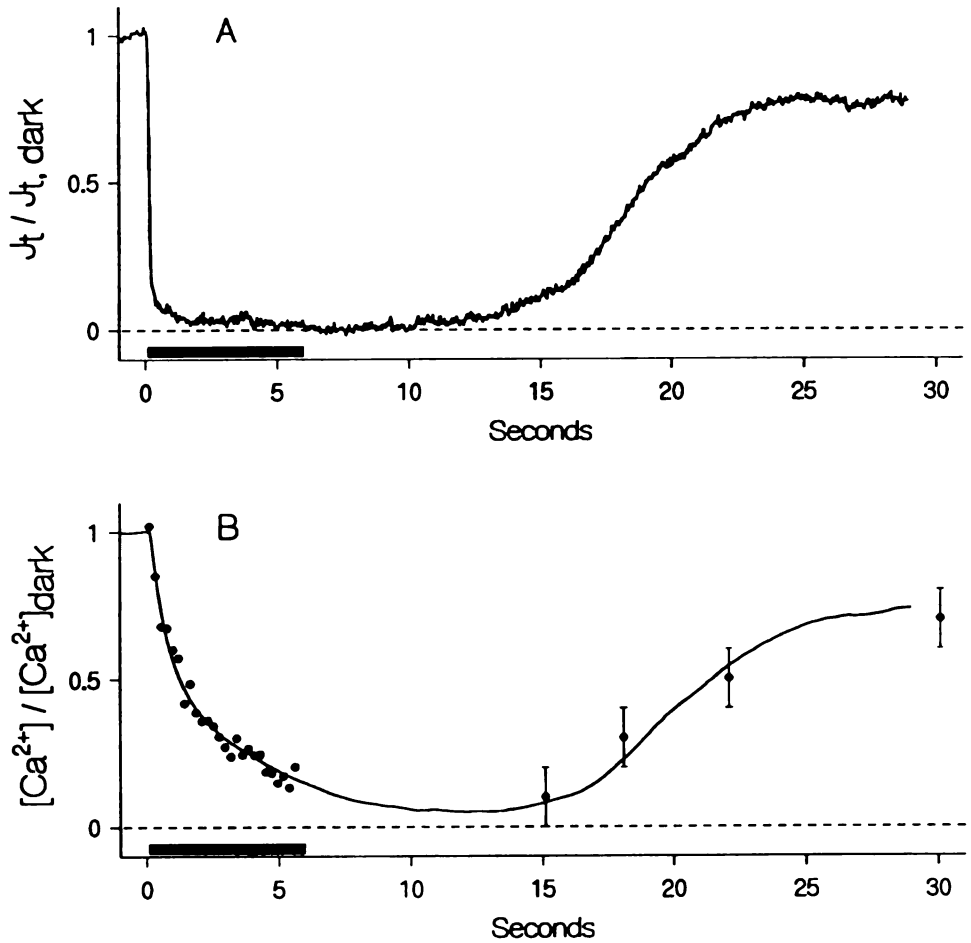

Figure 12. The recovery of calcium after a bright step of illumination. *A*, the average current recorded from a Fura-2 loaded rod when it was illuminated for six seconds (10,000 R^* sec^{-1}; 5 trials). The current is inverted so that it may be more easily compared to the kinetics of the change in calcium concentration measured from a Fura-2 loaded retina, *B* (circles). When the current begins to recover, so does the calcium concentration, but more slowly. The curve in *B* was generated by the compartmental model from the current shown in *A* and the parameters stated in the text. It is a prediction of the space-averaged calcium concentration which would be expected to be measured.

molecules per rod per second. In Fig. 12*A*, I show the photocurrent recorded from a typical, Fura-2 loaded rod. In Fig. 12*B*, the measured free calcium concentration from an isolated, Fura-2 loaded retina is shown. The closely spaced calcium data were recorded during six seconds of actinic illumination. The later data were recorded at the onsets of subsequent stimulations delivered 15, 18, 22 and 30 seconds after the onset of the first stimulus. Neither the photocurrent nor the calcium data have been included in the previous determination of parameters for the compartment model. The curves passing near and through the calcium data in Fig. 12*B* are the predicted space-averaged free calcium concentrations for the entire rod cross-section, $\langle Ca \rangle$. These curves were obtained by evaluating Eqn (8) with the normalized photocurrent, j_r, shown in Fig. 12*A* and the compartment model parameters α_{ex}, α_1, α_2 and a_1. The evaluation was carried out as a temporal iteration. All data and predictions have been normalized with respect to the appropriate values for the dark-adapted situation.

The data show that the average cytosolic free calcium concentration recovers only a little more slowly than the photocurrent. This behavior has significance with respect to the rate at which a rod can adapt to changing illumination. That the compartment model predicts the recovery of free calcium so well is gratifying. It implies that the underlying processes that govern calcium kinetics are well behaved. It also implies that the model will be equally valid for rods that do not contain Fura-2. As shown in the previous chapter, a Fura-2 loaded rod begins to recover from bright illumination a few seconds later than an unloaded rod would. This may, in part, be due to additional

calcium buffering by Fura-2, although the exchange current and dim-flash responses observed do not appear to be significantly affected by Fura-2 (see Chapter 3). In any case, the fact that calcium recovers only a little more slowly than the photocurrent of Fura-2 loaded rods suggests that it will recover at least as rapidly in unloaded rods. The model is not so precise that I can make it better by accounting for this difference.

Younger (1991) has also examined the kinetics of the change in average free calcium during steps of illumination that do not result in a complete closure of the cyclic GMP-gated channels. The compartment model predicts these changes with equal fidelity. In Fig. 13, I show the photocurrent and average cytosolic free calcium concentrations measured during a step of illumination that isomerized approximately 125 rhodopsin molecules per rod per second. The photocurrent was recorded from a rod which had not been loaded with Fura-2. The adapting illumination in the case of the intact, Fura-2 loaded retina was 500 nm light. Calcium concentrations were determined from the fluorescence observed at the onset of the standard, six-second ultraviolet stimulus. The actinic stimuli were delivered at the times indicated after the onset of the visible illumination.

As I will demonstrate in the next chapter, the ability to predict, with reasonable accuracy, the kinetics of the exchange current and average cytosolic free calcium concentration in the outer segment allows me to suggest solutions to many of the prevailing questions regarding the mechanisms of light adaptation.

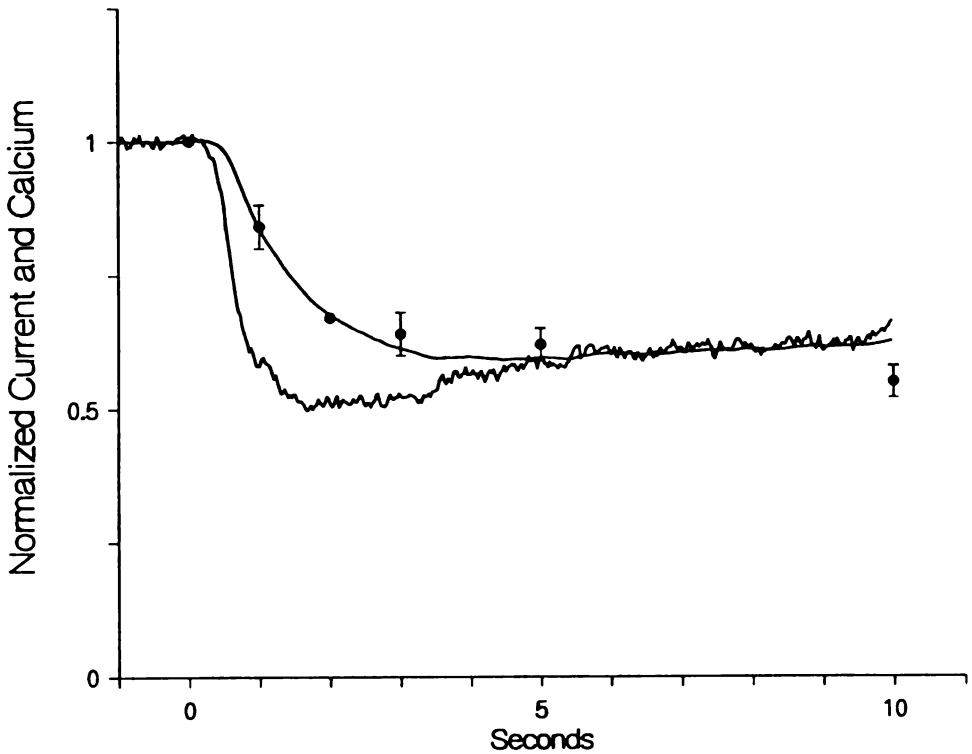

Figure 13. The calcium kinetics during non-saturating illumination. The noisy trace is the current recorded from an unloaded rod exposed to light that isomerized approximately 125 R^* sec^{-1} (5 trials). The calcium concentrations (circles) were measured from a Fura-2 loaded retina at the times indicated after turning on an adapting background that resulted in the same isomerization rate. The smooth curve shows the space-averaged calcium concentration one would expect to measure if the compartmental model were accurate. The agreement with the measured values is good. The calcium data were obtained by Dr. James Younger.

CHAPTER 5: CALCIUM, CYCLIC GMP METABOLISM AND LIGHT ADAPTATION

Light adaptation is commonly believed to be mediated by a regulatory effect on cell enzymes by cytosolic free calcium. Chief among calcium's targets is thought to be guanylate cyclase. Pannbacker (1973), Lolley and Racz (1982), Pepe *et al.* (1986) and Koch and Stryer (1988) have suggested that the very pronounced effect of calcium on cyclic GMP metabolism is on the synthesis pathway. The picture that has been painted is that light causes cyclic GMP-gated channels to close by accelerating the catabolic pathway - the cyclic GMP cascade. The decrease in the cytosolic calcium concentration that results from the channel closure initiates the recovery from illumination by resupplying cyclic GMP through some action on guanylate cyclase (Pugh and Altman, 1988, Stryer, 1991, Chabre and Deterre, 1989). There is also mounting evidence that calcium has a more immediate effect on the cyclic GMP concentration by influencing the cyclic GMP catabolic cascade (Wagner *et al.*, 1989, Robinson *et al.*, 1980, Kawamura and Murakami, 1991, Lagnado and Baylor, personal communication). Nevertheless, there is no complete description of phototransduction or light adaptation.

I have examined the role of calcium in phototransduction and light adaptation. In previous chapters I presented my results concerning calcium regulation, how calcium concentrations are altered by illumination, and the relationship between the current flowing into the outer segment and the dynamics of the changes in the space-averaged calcium concentration and the calcium concentration near the membrane. These findings,

in particular the model for estimating calcium concentrations from the total measured current, have allowed me to ask more precisely what influence calcium might have on cyclic GMP hydrolysis and synthesis.

What I find is that phototransduction and light adaptation are even more complicated than I expected. I cannot confirm that cyclic GMP synthesis is strongly modulated by calcium in intact, isolated frog rods. In fact, my data are more easily explained if cyclic GMP synthesis were not calcium-dependent in the physiological range. I also find an effect, which may reflect a decrease in the lifetime of active phosphodiesterase during sustained illumination, that develops more slowly than the calcium concentration changes and may not depend on calcium at all. There is, however, a very important effect which I believe to be mediated by calcium. This is that the cyclic GMP cascade cannot be efficiently activated when the cytosolic free calcium concentration is low. This last effect could explain the change in the time-to-peak of flash responses that is a hallmark of light adaptation (Baylor *et al.*,1979a). It may also be a large part of why photoresponses are so stereotypical even when only a few photons are absorbed (Baylor *et al.*, 1979b).

Current Relaxes More Slowly Than the Space-averaged Calcium Concentration

In Fig. 1*A*, I show currents that were recorded from an isolated rod when it was illuminated by a succession of non-saturating steps of light. (None of the rods discussed

in this chapter were loaded with Fura-2.) In Fig. 1*B-D* I show the calcium concentration near the plasma membrane, the space-averaged calcium concentration, and the calcium concentration in the "central" compartment, respectively. These calcium concentrations are calculated from the currents in Fig. 1*A* and the compartmental model described in Chapter 4 using the same parameters listed there. The calcium concentrations are of course approximations, but I believe they are good representations of the true physiological values.

The currents shown are typical. For weak illumination, less than approximately 30 R^* sec^{-1}, the currents are suppressed monotonically. For moderate illumination, 30-600 R^* sec^{-1}, the currents overshoot but then relax to a plateau within approximately 10 seconds. Brighter illumination results in the same general behaviour of the current but the relaxation to the plateau is prolonged. Typically the cyclic GMP-gated channels remained closed during illumination which isomerized approximately 13,000 rhodopsin molecules per second.

The calculated calcium concentrations shown change more slowly than the currents. They may be considered progressively low-pass filtered versions of the currents. The calcium concentration in the peripheral domain (Fig. 1*B*), which is the calcium concentration that is proportional to the exchange current, has the form that is most similar to the photocurrent, but with a smaller relaxation from the peak of the undershoot. The space-averaged calcium concentrations (Fig. 1*C*) relax very little.

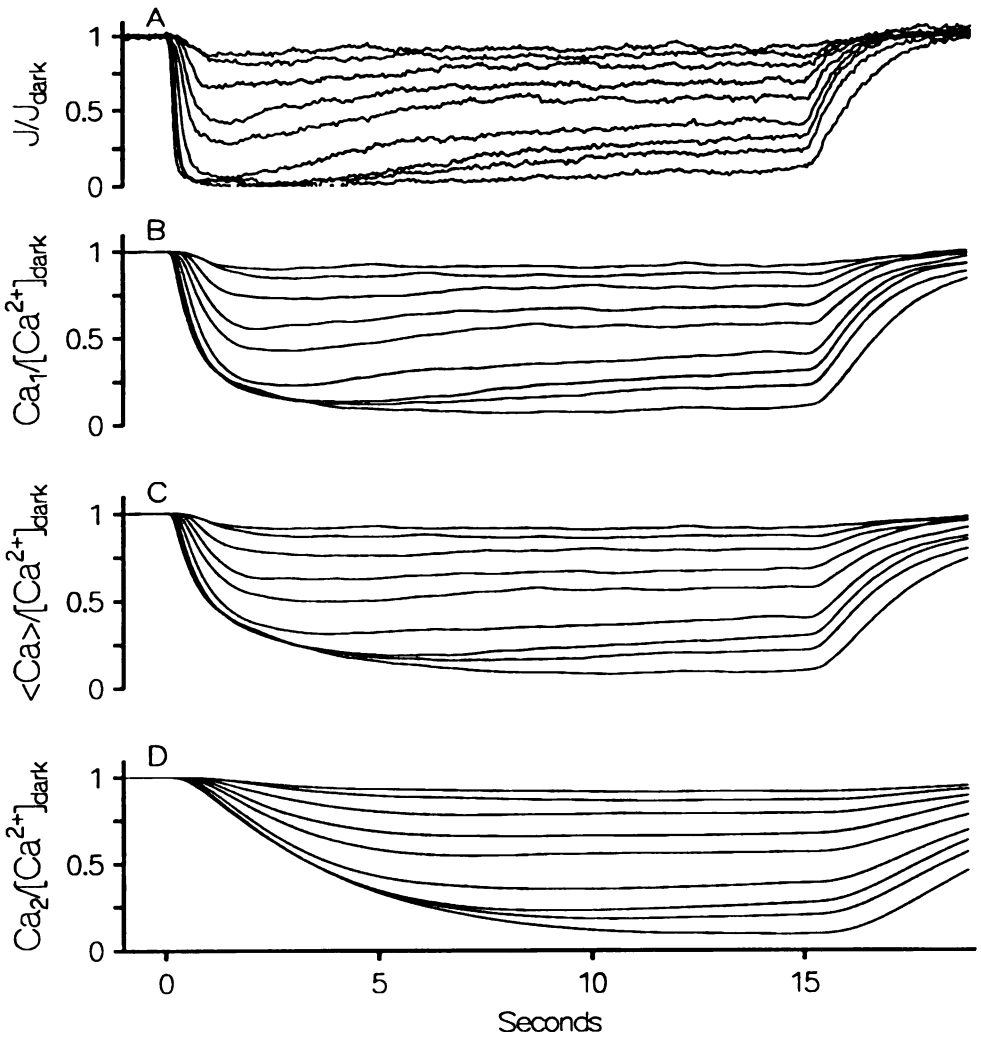

Figure 1. The measured photocurrent along with predicted values of calcium from the compartmental model of Chapter 4 in response to steps of illumination. *A*, nine photocurrents from the same unloaded rod elicited by 15-second steps of illumination which isomerized approximately 14, 24, 60, 140, 240, 600, 1400, 2400 and 6000 $R^* sec^{-1}$ (upper trace to lower trace). The circulating current in the dark for this rod was 18.5 pA. Each trace is a single trial. These currents give rise to the predicted calcium concentrations, relative to dark, shown in *B*, for the periphery of the rod (Ca_1), in *C*, for the space-averaged concentration (<Ca>), and in *D*, for the central domain (Ca_2).

Neither of these estimates of the cytosolic calcium concentration is consistent with a rapid calcium-dependent modulation of cyclic GMP synthesis unless there is also a slow decrease in the rate at which cyclic GMP can be hydrolysed. If calcium rapidly inhibited cyclic GMP synthesis, one would expect that current would increase as the calcium concentration decreased. In both cases, the calcium concentrations increase while the currents recover. The kinetics of the change in calcium concentration in the "central" compartment (Fig. 1*D*) could, be construed to be consistent with a rapid influence of calcium on guanylate cyclase, but results presented in the next section indicate that that is unlikely.

The dynamics of the change in the calcium concentration are much slower than would be predicted if the exchange current could have been described by a single exponential (Yau and Nakatani, 1985, Hodgkin *et al.* 1987). The calcium dynamics are, nevertheless, still too rapid to suggest that calcium has an impact on cyclic GMP synthesis unless that influence requires time to develop or there is also a slow change in the rate at which cyclic GMP can be hydrolyzed.

Cyclic GMP Synthesis May Not Be Modulated By Calcium

It is easier to understand some of my results if cyclic GMP synthesis is not modulated - or, at most, modulated weakly - at calcium concentrations I believe to be physiologically realistic.

In Fig. 2*A* I plot the recovery of the currents which were shown in Fig. 1*A* when illumination was turned off. The majority of the current flowing into the outer segment across the plasma membrane is proportional to the cube of the cyclic GMP concentration within the outer segment (Zimmerman and Baylor, 1986). I believe that the cyclic GMP concentration becomes fairly uniform within the outer segment during sustained illumination. In Fig. 2*B* and 2*C* I illustrate the approximate kinetics of the normalized change in the outer-segment cyclic GMP concentration for each of the currents shown in Fig. 2*A*. The approximate, normalized change in cyclic GMP concentration is written as the left-hand side of:

$$\frac{[cGMP(t)] - [cGMP]_{dark}}{[cGMP(0)] - [cGMP]_{dark}} \approx \frac{(J(t))^{1/3} - (J_{dark})^{1/3}}{(J(0))^{1/3} - (J_{dark})^{1/3}} \qquad (1)$$

where [*cGMP*] and *J* are the cyclic GMP concentration and the transmembrane current, respectively. (The exchange current is not subtracted from the total current to obtain a more accurate estimate of the cyclic GMP concentration because I feel it would add unecessary confusion.) Here, t=0 is the time at which the step of illumination was turned off and the subscript, *dark*, refers to the appropriate value in the dark. All but the cyclic GMP concentrations that correspond to the recovery from the dimmest and brightest steps of illumination are shown in Fig. 2*B*. The cyclic GMP concentrations that correspond to the dimmest, fifth brightest and brightest steps of illumination are shown in Fig. 2*C*.

Except when recovering from dim or very bright illumination, the normalized change in the cyclic GMP concentration can be described by a single exponential after

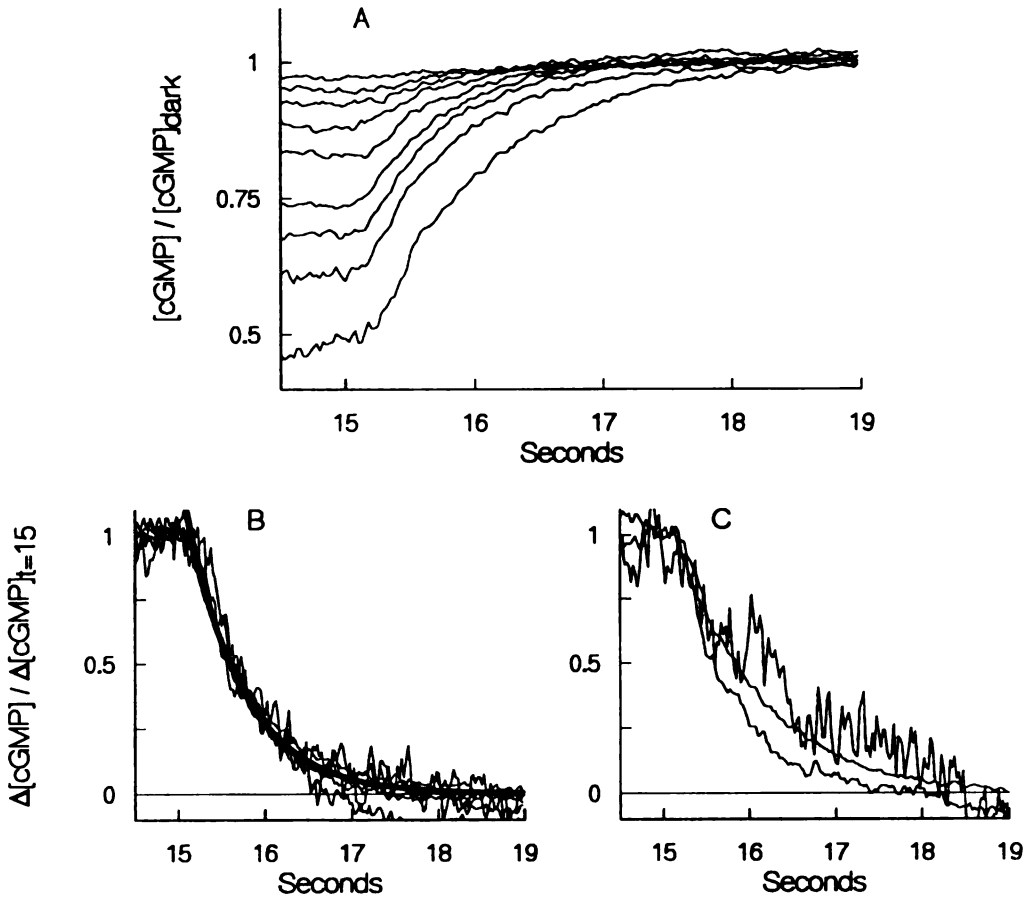

Figure 2. Recovery from steps of illumination of varying intensities. *A*, all nine photocurrents from Fig. 1*A* - beginning shortly before the step of illumination was turned off - reproduced in terms of normalized cyclic GMP concentrations. These were calculated from the relation $[cGMP]/[cGMP]_{dark} = \{J/J_{dark}\}^{1/3}$. *B*, all traces except the dimmest and brightest in *A* shown now in terms of the change in cyclic GMP concentration normalized to the difference between cyclic GMP at end of the step of illumination and its dark value ($[\Delta[cGMP]_{t=15}$), as in Eqn (1). The thick trace which describes the fall is the function $e^{-(t-15.15)/0.65}$. The offset for the time in the exponent is 15 seconds plus a delay of 150 ms. *C*, the fifth brightest (lower trace), brightest and dimmest (noisy trace) reproduced in the same way as in *B*.

a short delay. The curve drawn through the data shown in Fig. 2*B* has a delay of 150 ms and a time constant of 650 ms. There are several ways in which this sort of behavior might be explained.

The space-averaged rate of change of the cyclic GMP concentration can be written as:

$$\frac{d\ [cGMP(t)]}{dt} = -\ k_h(t)\ [cGMP(t)] + V_s(t) \qquad (2)$$

where k_h is the space-averaged cyclic GMP hydrolysis rate constant and V_s is the space-averaged synthesis rate.

Thus, the first and simplest explanation of the single exponential time course of the recovery of cyclic GMP concentration is that both the hydrolysis rate constant and the synthesis rate are constant during the recovery. The time course of the change in the cyclic GMP concentration would therefore be:

$$[cGMP(t)] \approx [cGMP]_{dark} + (\ [cGMP(0)] - [cGMP]_{dark}\ )\ e^{-k_h t} \qquad (3)$$

where

$$[cGMP]_{dark} = \frac{V_s}{k_h}$$

The initial time (t=0) refers to the time at which the cyclic GMP concentration begins to

recover. Eqn (3) supposes that the light-induced increase in the hydrolysis rate constant is rapidly diminished a short time after the illumination is turned off. The residual hydrolysis rate constant would be the same as the basal rate constant of hydrolysis in darkness. It also supposes that the cyclic GMP synthesis rate is constant and therefore does not depend on calcium.

The slower rates of recovery from bright steps of illumination suggests, however, that the hydrolysis rate constant does not return rapidly to its value in the dark. The second potential explanation of the invariance of the normalized change in the cyclic GMP concentrations after moderate illumination is that it reflects a stereotypical decay of the number of active phosphodiesterase molecules. I return to this hypothesis in the next section.

The final possible explanation is that the synthesis rate and hydrolysis rate change synergistically. I cannot determine if this is true from my data. In any explanation, however, it is difficult to understand how cyclic GMP synthesis could be very dependent on the cytosolic free calcium concentration. Both the calculated and measured (Fig. 1 of Chapter 4) calcium concentrations vary over a wide range depending on the intensity of illumination. In addition, the calcium concentrations change more slowly than the currents during the recovery. They are still significantly different from the cytosolic calcium concentration in the dark after the currents have reattained the dark value yet there is no overshoot (Fig. 2). This is the not the behavior one would expect if the cyclic

GMP synthesis rate were high because of the low calcium concentration at this time.

Sather and Detwiler (1987) also suggested that calcium does not influence cyclic GMP synthesis based on the rate at which the current induced by perfusing isolated outer segments with guanine nucleotides decays. The inability to observe an influence of high-affinity calcium buffering on the kinetics of the space-averaged calcium concentrations that were recorded from Fura-2 loaded retinas (Chapter 4) is consistent with this suggestion. Why calcium appears to have a very pronounced effect on guanylate cyclase activity in biochemical studies is, however, somewhat of a mystery (Pannbacker, 1973, Lolley and Racz, 1982, Pepe *et al.* 1986, Koch and Stryer, 1988, Dizhoor *et al.* 1991). A partial solution of this mystery, which I discuss in the final section of this chapter, might be found in the data that I present below.

The Lifetime of Activated Cyclic GMP Hydrolysis Decreases Over Time

In the preceding section, I showed that the normalized rate at which cyclic GMP concentrations recovered was relatively insensitive to moderate illuminating intensities - and hence to calcium concentrations in the physiological range. The rate of recovery depends strongly, however, on the duration of illumination. In Fig. 3, I show the currents that were recorded from a unloaded rod which was stimulated by a step of illumination that isomerized approximately 3000 R^* sec^{-1} followed by a step of illumination that isomerized approximately 250 R^* sec^{-1} for 15 seconds. The experiment was repeated six

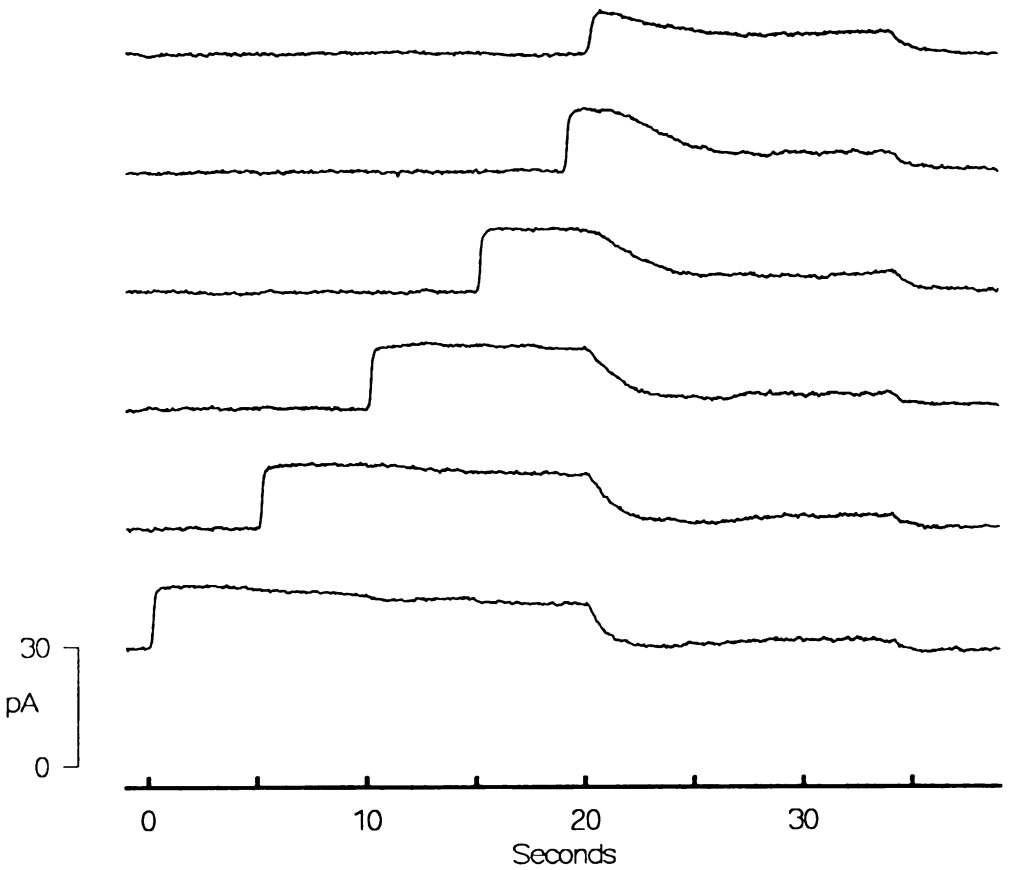

Figure 3. Rod response to a bright step of illumination followed by a much dimmer step. In all traces illumination which isomerized approximately 250 R^* sec^{-1} was turned on at 20 seconds and off at 29 seconds. In the top trace, no bright step preceded this. In other traces, a step of illumination which isomerized approximately 3000 R^* sec^{-1} and which lasted for 1, 5, 10, 15 and 20 seconds (second trace to lowest trace) immediately preceded the dimmer step. All traces are from the same rod whose dark circulating current was 17 pA, and are the results of single trials.

times and each time the initial, bright step of illumination was delivered for a longer duration. A striking feature of these current records is that as the first step of illumination is progressively prolonged, the rate at which the current decays during the second step of illumination is accelerated. A similar effect has been observed in the recovery of the voltage response of frog and toad rods (Coles and Yamane, 1975, Cervetto *et al.* 1984).

The currents recorded during the second step of illumination are displayed again in Fig. 4*A* along with the space-averaged calcium concentrations calculated with the compartment model (Fig. 4*B*). There is no clear correlation between the calcium concentrations and the rate at which the currents changed, but the more rapid recoveries are associated with higher initial calcium concentrations. This again suggests that cyclic GMP synthesis is not stimulated by low calcium concentrations. The data do suggest, however, that the rate at which the currents - and therefore the cyclic GMP concentrations - recover depends on the rate at which light-accelerated hydrolysis is inactivated. This was the second hypothesis discussed in the preceding section. The data demonstrate that there is some process which is not very well correlated with changes in the cytosolic free calcium concentrations that accelerates the inactivation of light-activated hydrolysis as a function of how long the cell had been illuminated.

The same experiment was performed on other cells which gave very similar results even when the first step of illumination isomerized approximately 14,000 R^* sec^{-1} (not

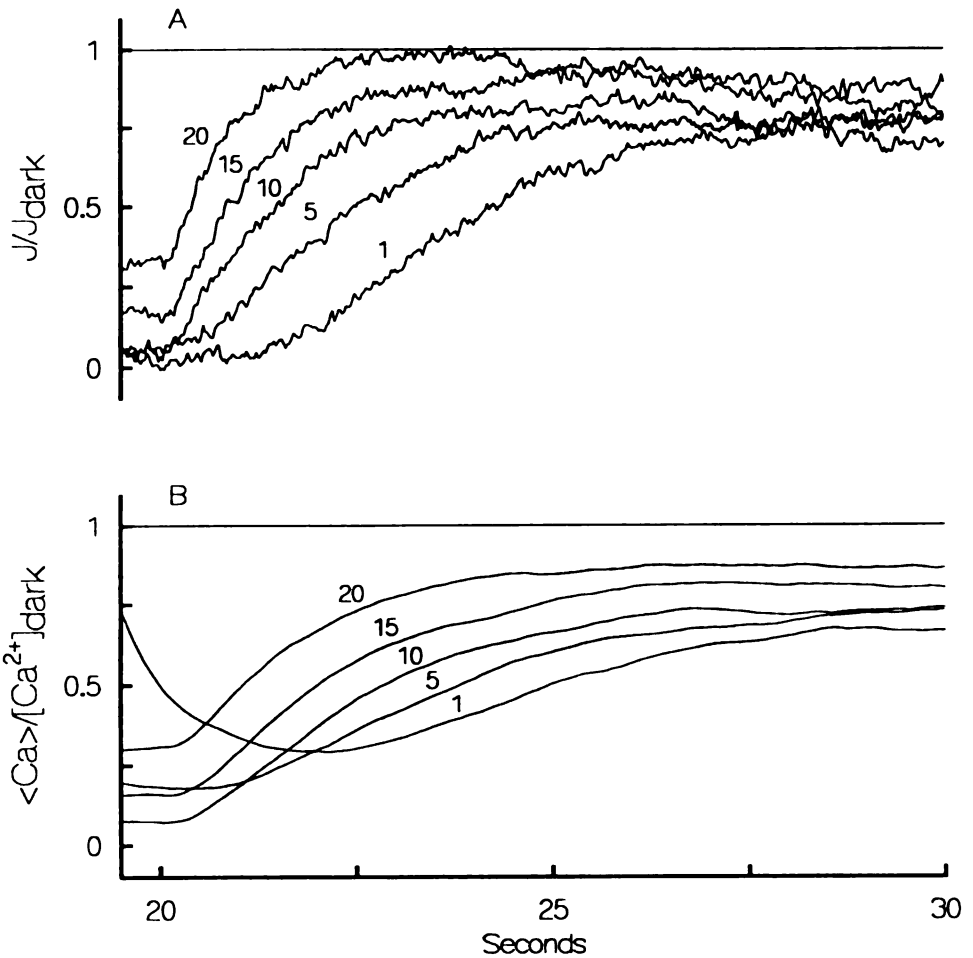

Figure 4. A closer look at the transition from a bright to a dim step of illumination for the currents in Fig. 3. *A*, the currents (shown inverted from their orientation in Fig. 3) normalized with respect to the dark current. At t = 20 seconds the bright step (which had been on for 1, 5, 10, 15 and 20 seconds, shown by the number against each trace) was turned off and dim illumination began. *B*, the predicted space-averaged calcium, relative to its dark value, for each of the traces in *A*. Note that recovery of the current is faster when calcium is higher (compare trace 20 and trace 5 in *A* and *B*, for example) and that there is no correlation before t ≈ 22 seconds between calcium concentration and recovery rate. Other traces not shown here demonstrate that the rate of recovery does not get appreciably faster for exposures to the bright step lasting more than 20 seconds.

shown). The fact that similar behavior was observed when very bright illumination was delivered to the rod suggests that the acceleration of the recovery of the current is not simply because the availability of some enzyme within the cyclic GMP cascade was attenuated although this may be part of the explanation.

The overshoot observed when the current adjusts to the second step of illumination after the first step of illumination had been on for more than 10 seconds is not surprising. Mild overshoots in the recovery of the photocurrent after a flash are a common feature of light-adapted cells (Baylor *et al.*, 1979a). What is surprising, however, is that the current does not overshoot when there is no second step of illumination. In Fig. 5 I show the recovery of currents recorded during two experiments on a rod. In each experiment, the rod was adapted to illumination that isomerized approximately 300 R^* sec^{-1} for at least 30 seconds. A six-second step of illumination that isomerized approximately 10,000 R^* sec^{-1} was then delivered. The currents shown were recorded from the time at which the second, saturating step of illumination was turned off. In one experiment, the adapting illumination was immediately restored and the current first recovered as if there were no adapting illumination, but then reversed itself and adjusted to the adapting illumination. In the other experiment, the rod was allowed to recover in the dark. Why the current should oscillate in one experiment but not the other is unclear. The overshoot is reminiscent of the oscillations observed in BAPTA-loaded rods (Torre *et al.* 1986) and therefore suggests a calcium-mediated process. My data suggests, however, that if it is a calcium-mediated process it does not take effect at the same rate at which the calcium

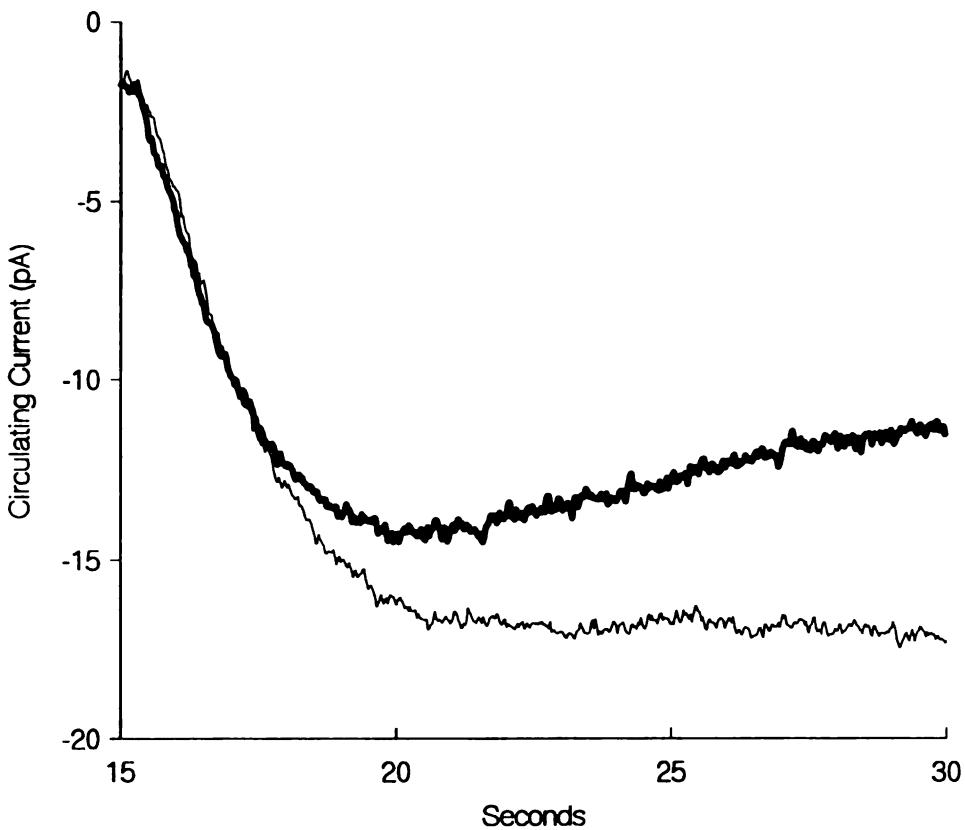

Figure 5. Comparison of recovery from a bright step of illumination to darkness and from a bright step to a dim level of illumination. For both traces, the same rod had been exposed to illumination that isomerized around 300 R^* sec^{-1} for more than 30 seconds, followed immediately by a bright step which isomerized 10,000 R^* sec^{-1} for six seconds. The traces shown here begin at the moment the bright step ended. For the light trace, the rod was left in darkness after the step, and the current shows a monotonic recovery. For the heavy trace, the return to 300 R^* sec^{-1} illumination after the bright step is characterized by an overshoot in the number of open channels.

concentration changes.

It may be that the relaxation of the current to a plateau during sustained illumination, the acceleration of the recovery of the current during prolonged illumination and the overshoot are aspects of the same phenomenon. The favorite candidate for undertaking this task has been calcium-dependent modulation of cyclic GMP synthesis. This seems less likely to me than an alternative. I suggest that the lifetime of light-activated hydrolysis may be decreased during illumination. By the lifetime of light-activated hydrolysis I mean the effective lifetime of activated phosphodiesterase enzymes which in turn depends on the lifetimes of activated transducin and rhodopsin molecules. I return to this possibility later.

PDE Activation is Hindered When $[Ca^{2+}]_{free}$ is Less Than 50% of Its Dark Value

In this chapter, I have not yet been able to ascribe to calcium a definite effect on phototransduction or light adaptation. Now, however, I describe an important effect which I believe to be influenced by cytosolic free calcium.

The currents recorded from a rod in response to non-saturating steps of illumination are shown in Fig. 6. The durations of the steps were increased from 5 seconds to 10 seconds and finally to 15 seconds. When the non-saturating steps of illumination were turned off, I delivered a six-second step of illumination that isomerized

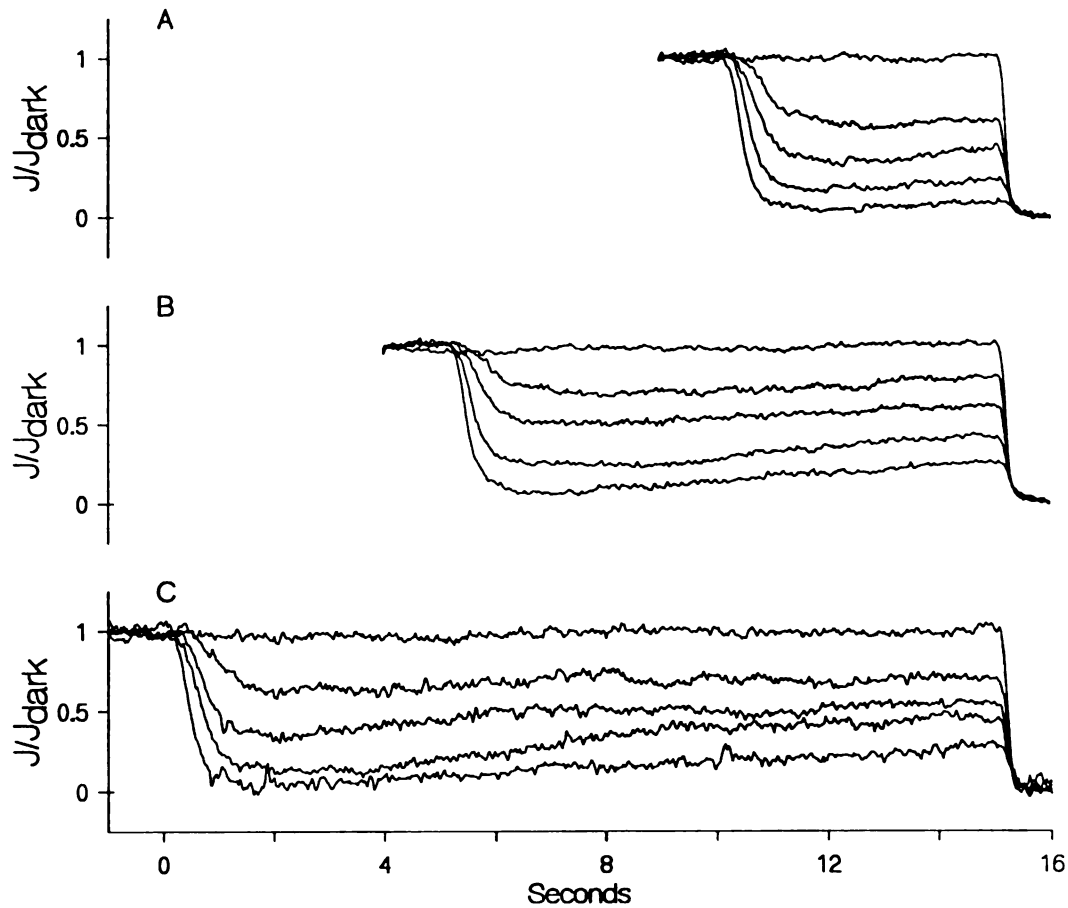

Figure 6. Exposure to non-saturating steps of illumination, followed by a saturating step. The saturating step began at t = 15 seconds for all the traces shown here, and isomerized around 10,000 $R^* sec^{-1}$ for six seconds. *A*, a range of non-saturating steps of illumination were presented to the rod for five seconds immediately prior to the saturating step. *B*, the same intensity steps were presented to the rod for 10 seconds prior to the saturating step. *C*, the same steps were presented to the rod for 15 seconds prior to the saturating step. All traces are single trials on the same rod, whose circulating current in the dark was around 14 pA.

approximately 10,000 R^* sec^{-1} and which abolished the remaining circulating current. In Fig. 7 I show the normalized change in the circulating current when the second, saturating steps of illumination were delivered. These are the normalized rising phases - similar to the rising phase I discussed in Chapter 4 (Figures 4 and 5). They are the currents recorded during the first 750 ms of the saturating step of illumination divided by the magnitude of the circulating current measured just before the saturating step was turned on.

The important feature of these data is the compression of the rising phase that occurs when the non-saturating step of illumination becomes prolonged. After 5 seconds (Fig. 7*A*) the rising phase is progressively delayed for the three brightest steps of non-saturating illumination. By 10 seconds (Fig. 7*B*), only the brightest of the preceding steps delays the rising phase significantly. The data in Fig. 7*D* are the rising phase shown in Fig. 7*A* for the current recorded after the brightest step of non-saturating illumination and the rising phase when there was no preceding illumination.

The solid curve drawn through the data recorded when the rod had not been adapted is from Eqn (2) of chapter 4 with $k_I = 0.055$ and $\eta = 4.25$. (The activation coefficient, k_I, for this cell is approximately four-fold less than reported before (Chapter 4). The activation coefficient varied over a wide range from cell to cell. I do not understand why this occurs but the four-fold decrease in the activation coefficient can be considered as a 50-60 ms delay in the rising phase with respect to the rising phase

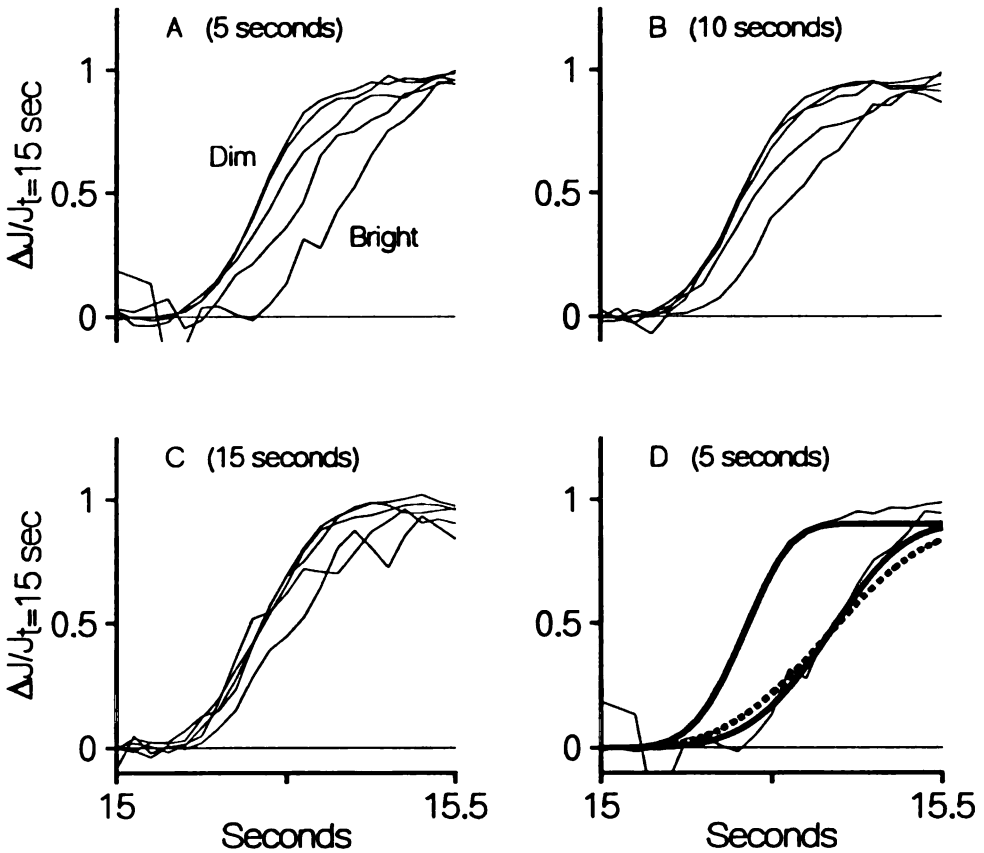

Figure 7. The rising phase of the photocurrent in response to saturating illumination after non-saturating illumination of varying duration and intensity. Data are those from Fig. 6, shown as the fraction of the current circulating immediately before the saturating step that is suppressed by that step. *A*, five seconds of conditioning illumination. *B*, 10 seconds and *C*, 15 seconds of conditioning illumination. In all three figures, the rising phases after the brighter non-saturating steps rise more slowly, although this effect becomes less pronounced for longer conditioning steps. *D*, reproduction of the rising phase after the brightest non-saturating conditioning step from *A* and of the rising phase for the same rod for the same saturating step delivered in darkness. The steeper solid curve fits the latter trace and is derived from Eqn (2), Chapter 4, with exponent $\eta = 4.25$. The former trace is fairly well descibed by a curve with a different activation coefficient, but the same exponent (shallower solid curve). The dashed curve is the best possible fit that can be obtained with $\eta = 3.25$, clearly a worse description of the rising phase.

displayed in Fig. 5 of chapter 4. What is important is that the same activation exponent, $\eta = 4.25$, describes the data for this cell and most other cells). The other solid curve, which is drawn through the data recorded after the rod had been exposed to the brightest step of non-saturating illumination for 5 seconds, is also generated by Eqn (2) of chapter 4. In this case, the activation coefficient is different ($k_I = 0.0075$) but the activation exponent is the same ($\eta = 4.25$). The dashed curve is derived from the same equation but with $k_I = 0.0025$ and $\eta = 3.25$. The greater exponent describes each set of data shown in Fig. 7 better than a lesser exponent. The curve generated with $\eta = 3.25$ is shown because this is the behavior that one would expect if the rate of cyclic GMP hydrolysis during the saturating step of illumination were not much greater than it was immediately before the saturating step. For the same general reasons I gave in the discussion of the influence of the rate of phosphodiesterase activation by activated transducin on the kinetics of the rising phase (Appendix B), the magnitude of the hydrolysis rate prior to the saturating step can be considered a damping factor which would appear as a decrease in the value of the activation exponent. In a similar manner, if the mean lifetime of an active phosphodiesterase enzyme were shorter than the duration of the rising phase the activation exponent would be decreased. The complete analysis of the impact of any form of damping (which I have undertaken but do not show here) is of course more complicated than simply changing the value of the activation exponent. Eqn (2) of Chapter 4 is, however, an approximation which is sufficiently accurate that the activation exponent reflects the combined rates of activation and inactivation, the steady-state hydrolysis rate and the cooperativity of phosphodiesterase activation by transducin.

The fact that the activation exponent does not change suggests that illumination does not dampen the kinetics of the accumulation of activated phosphodiesterase enzymes significantly.

On the other hand, the fact that the value of the activation coefficient is decreased suggests that either each isomerized rhodopsin molecule results in fewer activated phosphodiesterase enzymes or that the catalytic ability of each activated phosphodiesterase molecule is diminished. In either case, a change in the activation coefficient can be considered to be a change in the effectiveness of each rhodopsin isomerization. I point out that this phenomenon is different from damping which would alter the value of the activation exponent as well as the activation coefficient.

In Fig. 8*A* I plot the product of the activation coefficient and the intensity (10,000 $R^* sec^{-1}$) of each trace in Fig. 7 against the corresponding current recorded just before the saturating step of illumination. The currents are normalized with respect to the current recorded when the rod was not illuminated. The curve drawn through the data has a Hill coefficient of 4 and is half-maximal when the normalized current has a value of 0.3. The correlation between the normalized current and the activation coefficient is intriguing. It suggests that the effective increase in the hydrolysis rate per isomerized rhodopsin molecule is modulated as rapidly as the photocurrent. In other words, the value of the activation constant depends on how much the circulating current had been suppressed rather than how long the rod had been illuminated. It could be that the activation

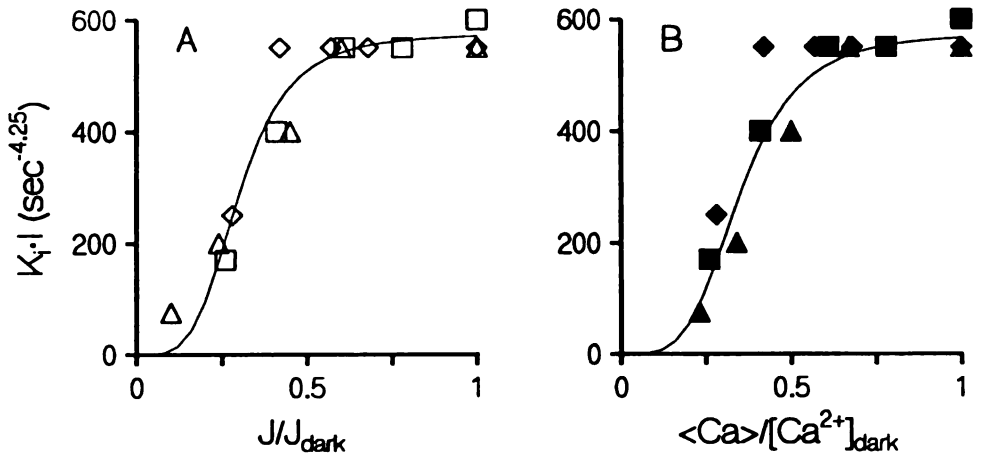

Figure 8. The dependence of the ability of rhodopsin to influence cyclic GMP metabolism on cytosolic free calcium. The activation coefficient from Eqn (2) of Chapter 4 after fitting all of the rising phases of the traces from Fig. 6 is multiplied by the intensity of the saturating step and plotted against the size of the circulating current before the saturating step relative to the dark circulating current (*A*). *B*, the same ordinate plotted against the space-averaged calcium immediately before the saturating step expressed as a fraction of steady calcium in the dark. The curve in *A* has a Hill coefficient of 4 and is half-maximal when the normalized current is 0.3. The curve in *B* has a Hill coefficient of 4 and is half-maximal when the space-averaged calcium is 0.35 of its dark concentration. The durations of the adapting illumination were 5 sec (triangles), 10 sec (diamonds) and 15 sec (square). Note that the activation coefficients intermingle which suggests that they do not depend explicitly on the intensity of the preceding adapting illumination.

coefficient is diminished when the cyclic GMP concentration is low, which would imply a 12th-order dependence with respect to the cyclic GMP concentration. I believe a more likely modulator of the activation coefficient is cytosolic calcium. The space-averaged calcium concentration, relative to the cytosolic calcium concentration in the dark, is almost the same as the normalized current flowing across the plasma membrane within 5 seconds of the onset of a non-saturating step of illumination. By 10 seconds, they are the same. In Fig. 8*B*, I show the correlation between the activation coefficient and the space-averaged calcium concentration, determined with the compartment model. The curve drawn there has a Hill coefficient of 4 and is half-maximal when the space-averaged calcium concentration is 0.35 of the cytosolic calcium concentration in the dark.

One reason to believe that calcium rather than cyclic GMP modulates the activation coefficient comes from the work of Torre *et al.* (1986) and Matthews *et al.* (1988). In these experiments the rate at which the cytosolic calcium concentration within the outer segment could change was hindered by the inclusion of a calcium chelator or by minimizing the flux of calcium across the plasma membrane. If the activation coefficient - which reflects the impact of each rhodopsin isomerization on the rate at which cyclic GMP can be hydrolyzed - depended only on the cyclic GMP concentration, then one would expect that non-saturating steps of illumination would produce the same change in the circulating current in normal cells and in cells in which calcium could not change rapidly, at least for several seconds after the onset of illumination. This is not what has been observed however. In the latter type of cells, the circulating current is

completely suppressed by what I consider to be moderate illumination. This suggests that calcium limits the suppression of the circulating current in normal cells. The highly cooperative calcium dependence of the activation coefficient would be capable of mediating this modulation. Such behavior would be consistent with the effects of calcium on the cyclic GMP cascade observed by Wagner *et al.* (1989), Kawamura and Murakami (1991) and Lagnado and Baylor (personal communication).

Recovery Begins when [Ca^{2+}] Falls Below a Critical Concentration

The possibility that calcium regulates the activation of the cyclic GMP cascade rather than the rate of cyclic GMP synthesis prompted me to examine the relationship between calcium and the responses of light-adapted rods to flashes of light.

In Fig. 9*A* I show the responses of a rod to 50 ms flashes of light which isomerized approximately 500 rhodopsin molecules. Before each flash, the rod was illuminated for 15 seconds with various intensities of light. The corresponding calcium concentrations near the membrane, the space-averaged calcium concentrations and the calcium concentrations in the "central" domain are shown in Fig. 9*B-D*, respectively. As usual, these calcium concentrations were determined from the currents and the compartment model.

The rates at which the currents recover after each flash appear to fall into two

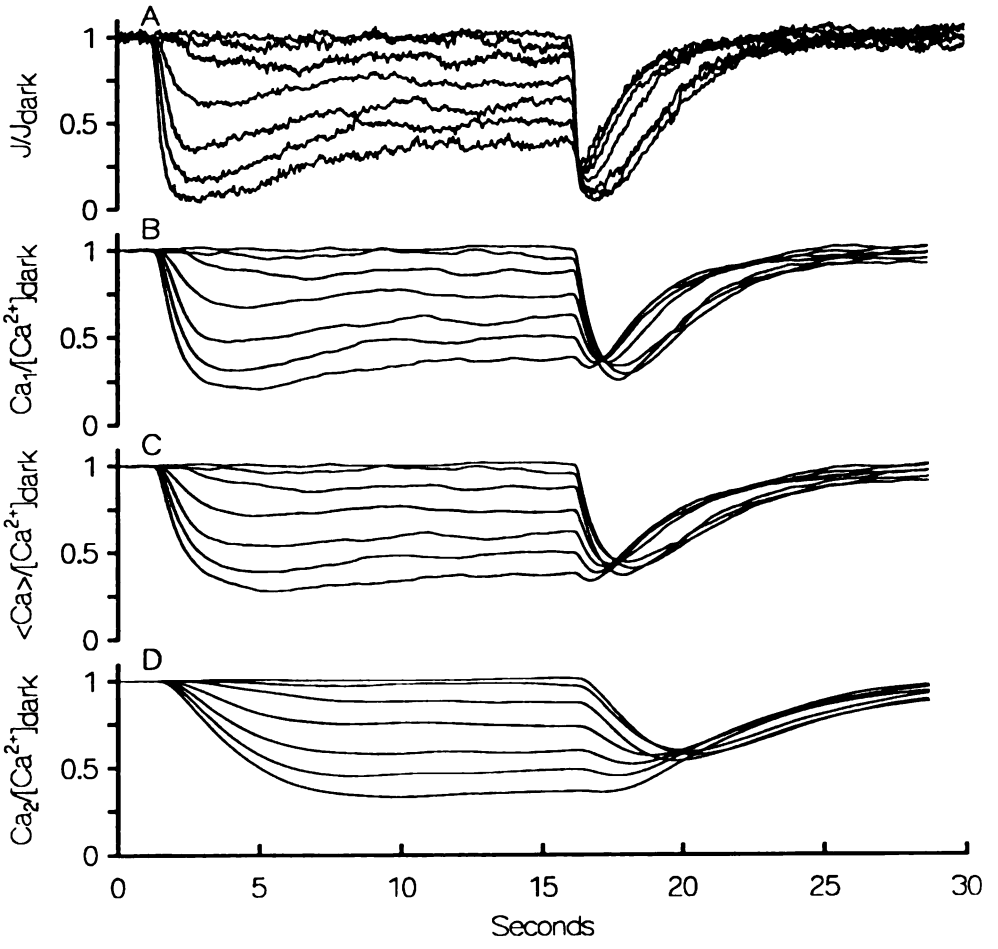

Figure 9. The currents and calcium concentrations when a rod was illuminated with non-saturating steps of light followed by a moderately bright flash. Each step of adapting illumination was delivered to the rod for 15 seconds. In one instance, there was no adapting illumination. The other steps isomerized approximately 3, 6, 25, 64, 150, and 300 R^* sec^{-1}. The subsequent flashes were all the same - 50 ms in duration which isomerized approximately 500 rhodopsin molecules. Each current trace represents a single trial. *B-D* are the corresponding calcium concentration in the peripheral domain, the space-averaged calcium concentration, and the calcium concentration in the "central" domain (predicted from the currents and the compartment model described in Chapter 4).

groups. When a step of illumination suppressed less than approximately 20% of the circulating current, the currents recovered slowly but with similar rates. The recovery was more rapid when the preceding steps of illumination were brighter. This behavior is similar to the slower recovery rate of weakly adapted rods shown in Fig. 2. The fact that the rod seems to remember the intensity of a step of illumination even after a moderately bright flash is consistent with a slowly developing process - similar to the process illustrated in Fig. 4.

But this slow process does not entirely account for the decrease in sensitivity with light adaptation that is evident in the currents recorded immediately after the flashes. As the intensity of the step of illumination preceding the flash is increased, the flash has less of an impact on the circulating current and the time until the current begins to recover is shortened. This behavior is in many ways the definition of light adaptation although dimmer flashes are more customary.

An examination of the calcium concentrations and the results of the preceding section suggest a mechanism by which the time at which the currents begin to recover can be dictated by calcium. The calcium concentrations near the membrane and the space-averaged calcium concentrations fall to approximately 40%-50% of the calcium concentration in the dark before the currents begin to recover (Fig. 9). In Fig. 10, I display in more detail the calculated, space-averaged calcium concentrations when the currents are at their lowest point (peak of the photoresponse). The space-averaged calcium

concentrations at the peak of the photoresponse do not depend strongly on the intensity of the preceding step of illumination (the calcium concentrations near the membrane are similar but are not as insensitive to illumination and are more scattered). When the steady-state, space-averaged calcium concentration is less than approximately 50% of the calcium concentration in the dark, however, the recovery of the photocurrent cannot begin earlier than approximately 450-500 msec. The curve drawn through the data is not important in detail but is meant to suggest that the time at which the current begins to recover may depend on how rapidly the space-averaged calcium concentration in the outer segment can fall to approximately 50% of the calcium concentration in the dark and that there is a lower limit on how rapidly the recovery can begin. I suggest that phosphodiesterase enzymes are activated inefficiently when the cytosolic calcium concentration is less than a critical value. In other words, the cyclic GMP cascade is turned off and the phosphodiesterase enzymes which had already been activated begin to inactivate. The critical calcium concentration is 60-100 nM based on a cytosolic calcium concentration in the dark of 125-200 nM (Chapter 3). Such a mechanism would explain the decrease in the time-to-peak of the flash response in the presence of steady illumination. It would also explain the decrease in the value of the activation coefficient described in the preceding section. In fact, the two observations are probably different measures of the same phenomenon.

I tested this hypothesis in the experiments illustrated in Fig. 11. In these experiments I compared the response of a rod to pairs of flashes with and without a

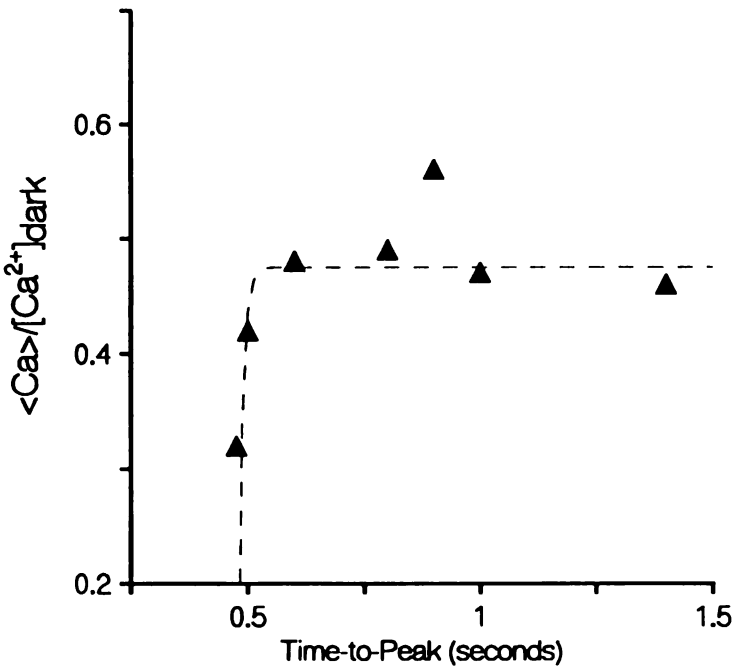

Figure 10. The relationship between the times at which the currents shown in Fig. 9 begin to recover after the flashes and the corresponding space-averaged calcium concentrations at those times. The space-averaged calcium concentration at the onset of recovery is about 0.45-.5 of the calcium concentration in the dark (the drawn curve has a value of 0.475 for times greater than 0.5 seconds). The calcium concentrations are independent of the preceding adapting illumination except for when it suppressed more than 50% of the circulating current. In these cases, the current could not begin to recover earlier than approximately 450-500 ms after the flash was delivered. The curve drawn through the data represents my idealized notion of this behavior.

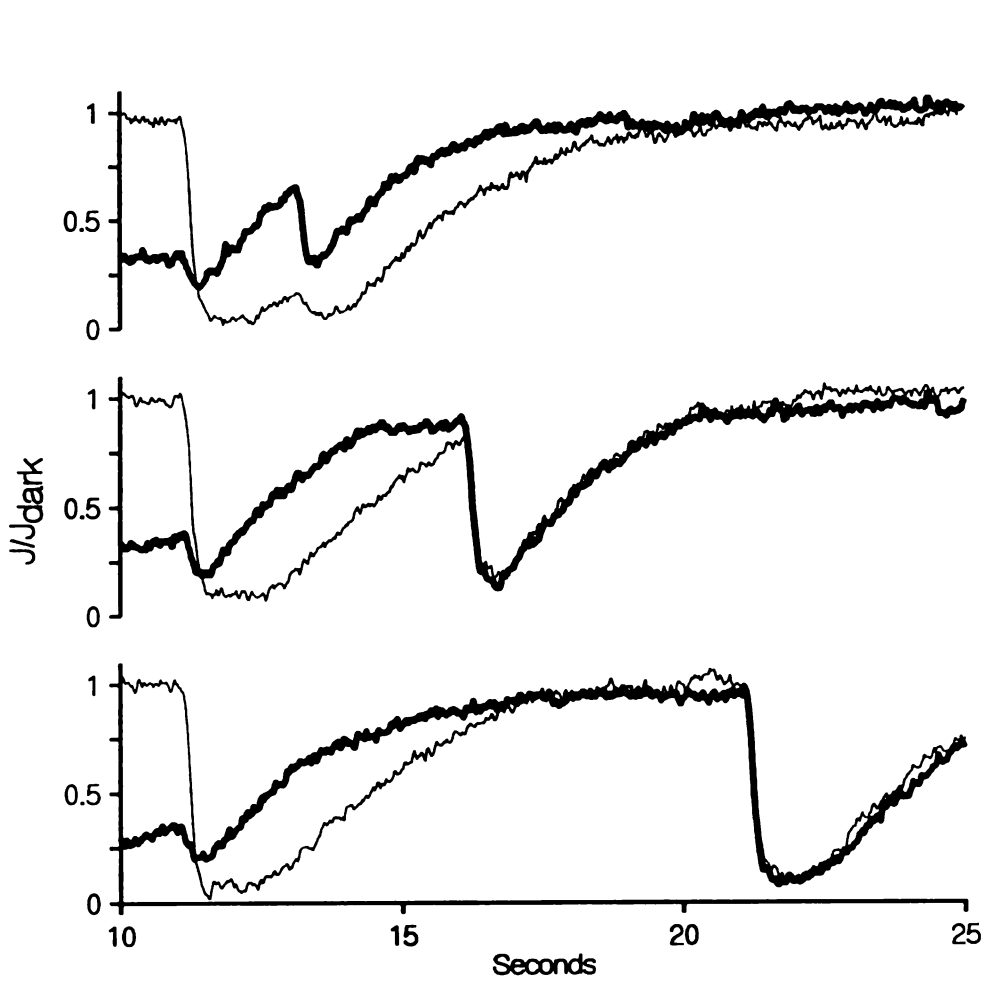

Figure 11. Currents recorded from a rod which was stimulated with pairs of flashes with and without a preceding step of adapting illumination. The adapting illumination was presented for 10 seconds and isomerized approximately 300 R^* sec^{-1}. (The onset of the adapting illumination would correspond to a time of t = 1 second). The flashes were 50 ms in duration and isomerized approximately 500 rhodopsin molecules each. The first flash of each trial was delivered at the time marked as 11 seconds. The second flash was delivered two seconds later (top panel), five seconds later (middle panel) or 10 seconds later (bottom panel). Each trace represents a single trial. The thick lines correspond to the currents that were recorded when the rod was light adapted. The thin lines are for the dark-adapted situations.

preceding step of adapting illumination. Each flash was 50 ms in duration and isomerized approximately 500 rhodopsin molecules. It is clear that the response of the rod to the first flash is attenuated and recovers more rapidly when the rod has been adapted. What is more interesting is that the response to the second flash is independent of the preceding step of illumination when they are presented five seconds apart but not two seconds apart. In Fig. 12, I show the space-averaged calcium concentrations predicted by the compartment model from the currents shown in Fig. 11. In almost every instance, the relative space-averaged calcium concentration is approximately 0.5 when the current begins to recover. Immediately after the adapting step of illumination however, the space-averaged calcium concentration falls to approximately 0.3 before the current begins to recover. The time-to-peak in these instances is 450 ms - the same as the apparent lower limit of the onset of recovery that was observed for the data shown in Fig. 10. Both of these results are consistent with a calcium-dependent mechanism that interrupts the cyclic GMP cascade when the cytosolic calcium concentration is less than a critical value.

The space-averaged calcium concentration that corresponds to the onset of recovery of the response to the flash that was delivered to the dark-adapted rod two seconds after the first flash (Figures 12*A* and 13*A*) is problematic however. In this case the current does not begin to recover for approximately 750 ms after the second flash. The relative space-averaged calcium concentration at this point is approximately 0.3, below the critical calcium concentration. I suspect that the slow process which accelerates the rate of recovery of the circulating current (shown in Figures 4 and 5) has

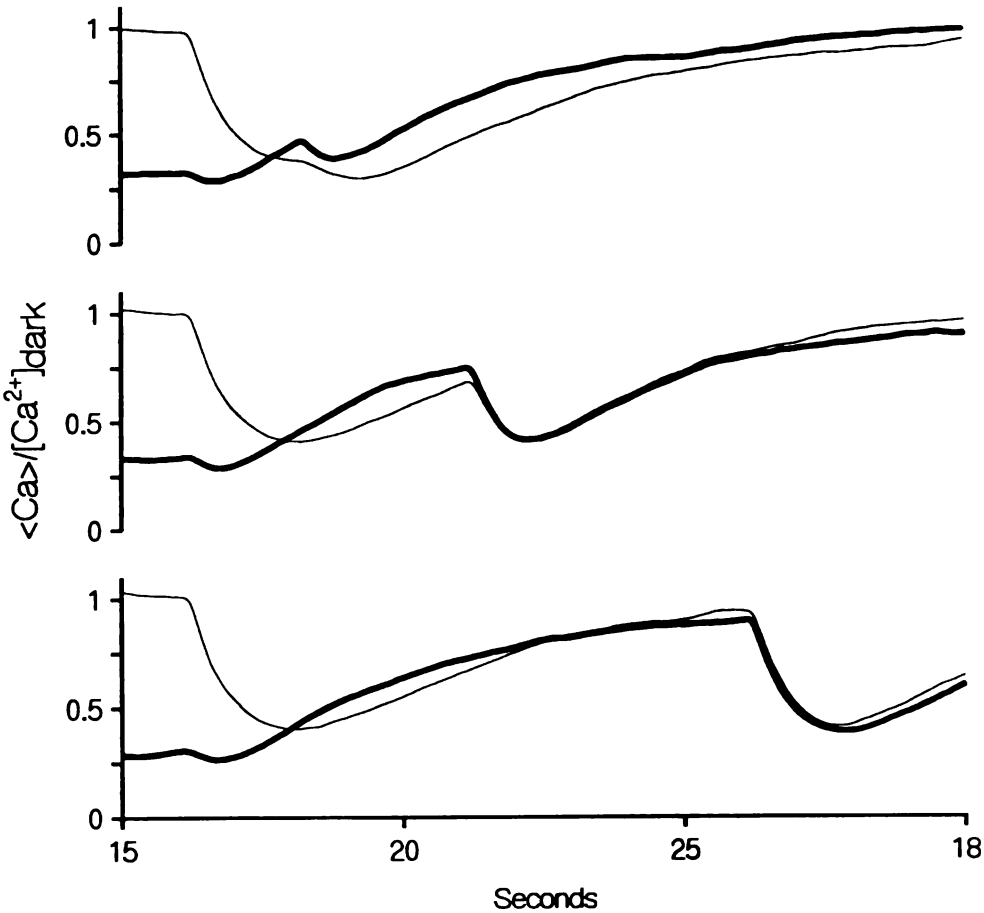

Figure 12. The space-averaged calcium concentrations that correspond to the currents shown in Fig. 11.

not yet had time to develop and thus masks the turn-off of the cyclic GMP cascade by low calcium. The same slowly developing process appears to influence the kinetics of the other flash responses. The responses to the flashes that were delivered to the rod when it was dark adapted are the slowest to recover. The responses to the flashes delivered at the time marked as 21 seconds recover slightly faster even though the currents and space-averaged calcium concentrations are very close to their dark-adapted values. The rate of recovery of the responses to the flashes which were delivered at the time marked 16 seconds are even faster, similar to the rate at which the responses to the flashes which were delivered immediately after the adapting step recover. As before, what appears to be a slowly developing change in the mean lifetime of activated phosphodiesterase molecules is not very well correlated with calcium concentrations.

The "Calcium Latch" Can Explain the Dim-flash Response of Light-adapted Rods

It is difficult to separate the effect of calcium on the ability of isomerized rhodopsin molecules to activate phosphodiesterase enzymes (an effect I refer to as the "calcium latch") from what appears to be a slowly developing decrease in the lifetime of activated phosphodiesterase enzymes during illumination. Although I cannot even be sure that they are separate phenomena, a close examination of the data supports this idea.

Baylor *et al.* (1979b) showed that photocurrents elicited by the isomerization of only a few rhodopsin molecules are semi-quantal. Each isomerization resulted in a small

but measurable suppression of the circulating current with kinetics that were very predictable. The kinetics were interpreted to be consistent with several sequential and independent gain stages such as would result from an enzymatic cascade. The cyclic GMP cascade is at least partially adequate to fit that description. A problem is generated, however, because the first stage of the cascade, the isomerization and then inactivation of a rhodopsin molecule, is stochastic. When many rhodopsin molecules are isomerized the average behavior dominates but when only a few are isomerized, the duration of the flash response should be at least as long as rhodopsin is active. There should therefore be a stochastic variation in the duration of dim-flash responses. Rhodopsin is thought to be inactivated via multiple phosphorylations by rhodopsin kinase and eventually a capping by arrestin (Wilden *et al.*, 1986). This would still be a stochastic process. The only way to minimize the variation in an observable phenomenon that depends on a randomly inactivated process is to impose negative feedback. I have considered two ways in which the negative feedback could operate. Both required that I first examine the restrictions on longitudinal diffusion of cyclic GMP and calcium within the outer segment.

Lamb *et al.* (1981) demonstrated that rhodopsin isomerizations result in localized changes in the membrane permeability of the outer segment. They also showed that thin slits of transverse illumination light-adapt the outer segment over a limited range but that the light adaptation is similar in many respects to that which results from diffuse illumination. These experiments demonstrated that diffusional restrictions which are imposed for the most part by the disks of the outer segment are an important aspect of

phototransduction. Cameron and Pugh (1990) have measured the rate at which small molecules including the non-hydrolyzable cyclic GMP analog, 8-bromo cyclic GMP, can diffuse within the outer segment. The picture that emerges from these studies is that each photoisomerization results in the closure of a significant number, if not most, of the cyclic GMP-gated channels in the region near the isomerization and that diffusional time constants influence the kinetics of dim-flash responses. (See however Lamb and Pugh (1992) for an examination of cyclic GMP diffusion with slighlty different conclusions.)

Diffusional restrictions might also provide some of the negative feedback that is required to minimize the variation of dim-flash responses. Like cyclic GMP molecules, calcium ions are subject to diffusional restrictions. I considered what effect calcium diffusion might have on cyclic GMP metabolism in regions of the outer segment adjacent to the site of a rhodopsin isomerization. At the time, I believed that calcium's dominant role was to modulate cyclic GMP synthesis. Accordingly, I imagined that as an isomerized rhodopsin molecule accelerated the cyclic GMP hydrolysis rate at a point in the outer segment leading to a local reduction in the circulating current, the calcium concentration at that point and in adjacent areas would be reduced. One would therefore expect the rate of cyclic GMP synthesis to increase in those regions. The rate constant of cyclic GMP hydrolysis would, however, be unchanged except at the point of photon capture. Thus, in the regions adjacent to the point at which a rhodopsin molecule was isomerized, cyclic GMP metabolism would be weighted in favor of synthesis which would limit the spread of cyclic GMP depletion.

I now believe that cyclic GMP synthesis may not depend on calcium in the physiological range. However, cyclic GMP hydrolysis could and the same hypothetical result would ensue. A light-induced increase in cyclic GMP hydrolysis at one point along the outer segment would be partially compensated for by a calcium-dependent increase in the ability of the adjacent regions to resupply cyclic GMP. On further examination it became clear, however, that this sort of negative feedback could only limit the variation in the magnitude of the photoresponse and not its duration. In effect, the calcium-dependent imbalance in cyclic GMP metabolism in the regions adjacent the point of isomerization alters the effective diffusional length constant but does not change the duration of accelerated cyclic GMP hydrolysis at the isomerization point.

It would appear, therefore, that the necessary negative feedback must operate at least in part on the cyclic GMP cascade itself before diffusional steady-state is achieved. Once again, the work of Torre *et al.* (1986) with BAPTA-loaded cells supports this assertion. They showed that the kinetics of the rising phase of dim-flash responses were not altered by the inclusion of the calcium chelator. Only the time at which the current began to recover changed, being much delayed in BAPTA-loaded rods. This result strongly suggests that diffusional steady-state is not reached before the dim-flash response of an unloaded cell begins to recover. The variation in the total kinetics cannot therefore be minimized by calcium-dependent feedback in the regions surrounding a rhodopsin isomerization alone.

I suggest that each rhodopsin isomerization leads to a nearly complete closure of the cyclic GMP-gated channels in the immediate vicinity (Lamb *et al.*, 1981). In Fig. 13, I show the currents recorded from a rod when it was illuminated with a series of progressively brighter 25 ms flashes. The brightest flash isomerized 400-450 rhodopsin molecules and just closed all of the cyclic GMP-gated channels in the plasma membrane. Typically, 500 rhodopsin isomerizations closed all of the cyclic GMP-gated channels of a dark-adapted rod for at least 0.5 seconds. This is fewer than one isomerization per disk. The channels also close more rapidly than diffusional steady-state could be achieved based on the behavior of dim-flash responses. Thus, each isomerization must result in a very large increase in the rate at which cyclic GMP can be hydrolyzed. In a dark-adapted rod, therefore, I would expect that each isomerization should result in a closure of most of the cyclic GMP-gated channels in its neighborhood even when only a few rhodopsin molecules are isomerized. The rate at which the current flowing across the plasma membrane in that region is suppressed should be similar to the rate at which the total current flowing across the entire outer segment is suppressed by the brightest flash shown in Fig. 13.

If, as I suggested in the previous section, the cyclic GMP cascade is interupted when calcium falls below a critical concentration and if each isomerization results in an almost total suppression of the calcium influx in the region of the isomerization, then I would expect that the time at which the current begins to recover after a flash should be independent of the number of rhodopsin molecules that were isomerized. The data shown

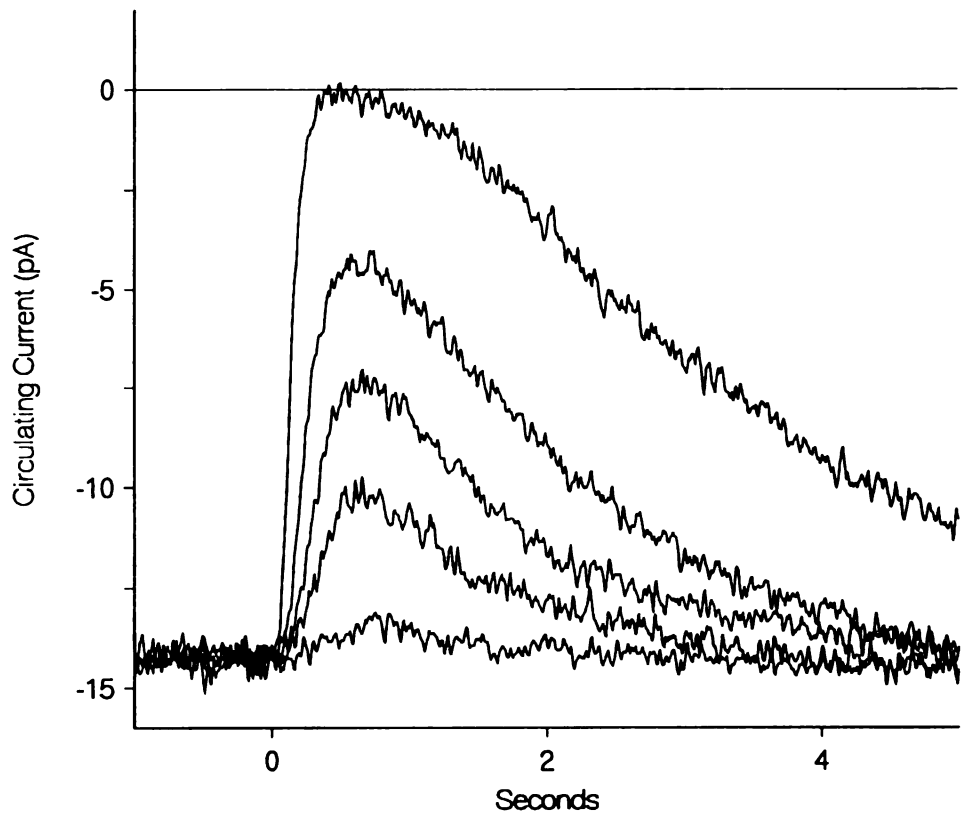

Figure 13. The currents elicited by a series of progressively more intense flashes delivered to a dark-adapted rod. The flashes were 25 ms long and isomerized 4, 22, 45, 100 and 400 rhodopsin molecules, respectively. The time at which the currents begin to recover are the same in each case - suggesting that the whatever process governs the onset of the recovery of bright-flash responses also governs the onset of the recovery of dim-flash responses. The same independence of the time-to-peak from the flash intensity is observed in light-adapted rods.

in Fig. 13 demonstrate that this is the case for a dark-adapted rod. It is also true when a rod has been light-adapted. In the latter case, the currents begin to recover earlier. This too is consistent with my hypothesis. The time it would take for the cytosolic calcium to fall below a critical concentration would depend on the initial calcium concentration. I have shown in Chapter 4 that the steady-state, space-averaged calcium concentration is reduced by steady illumination. Thus, steady illumination should be expected to shorten the duration of a flash response - a classic trait of light adaptation.

In Fig. 14 I show a series of flash responses that were recorded from a rod that was adapted to a series of illuminating intensities. I have normalized the peak magnitude of each current to 1. The actual change in the circulating current that each represents varied between 0.5 and 2 pA. They are therefore dim-flash responses that are all in the linear range.

In Fig. 15*B* I show predicted times at which the flash response should begin to recover and compare them to the times measured for the responses shown in Fig 14. The times-to-peak were predicted using Eqn (5) of Chapter 4. This equation describes the time course of the space-averaged calcium concentration measure when a Fura-2 loaded rod is illuminated with a bright step of illumination. I expect the equation for calcium to be slightly inaccurate when applied to dim flashes. Part of the inaccuracy will arise because calcium will diffuse from neighboring regions and therefore slow the rate of change of cytosolic free calcium concentration near the point at which a rhodopsin was

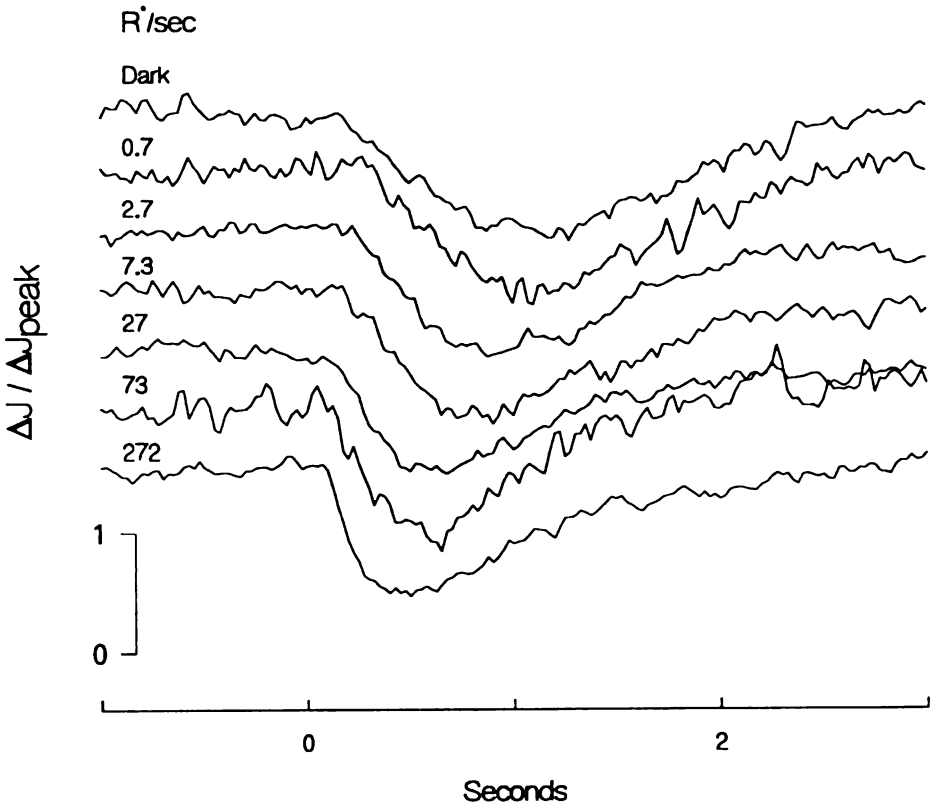

Figure 14. The kinetics of dim-flash responses recorded from a rod which was adapted to various illuminating intensities. Each adapting illumination was continuously delivered to the rod. The isomerization rate that each produced is shown in the figure. The actual peak photocurrents recorded ranged from 0.5 to 2.5 pA, but the data shown has been normalized so that all responses have a peak amplitude of 1. The separation of the responses along the ordinate is for clarity; it does not represent circulating current. Each response is the average of 5 trials from the same rod. The dark-adapted sensitivity of this rod was 0.45 pA per isomerized rhodopsin molecule.

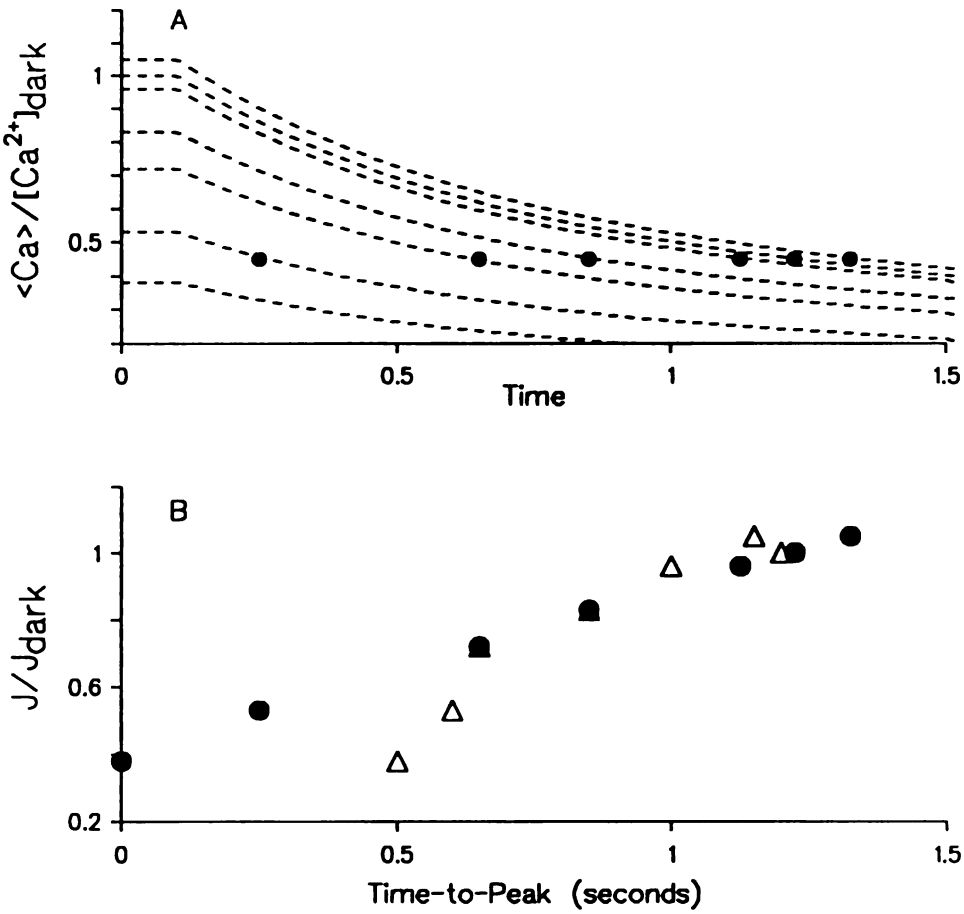

Figure 15. A prediction of the times at which dim-flash responses should begin to recover based on the "calcium latch" hypothesis. *A*, a rough estimate of the kinetics of the fall in calcium concentration near the point of an isomerization. It is based on Eqn (5) of Chapter 4 which is more accurate when it describes the rate at which the space-average of the calcium concentration falls during saturating illumination. The initial relative calcium concentrations of each curve in *A* are the same as the circulating currents, relative to the circulating current in the dark that were measured for the responses shown in Fig. 14. The "calcium latch" hypothesis supposes that currents begin to recover after an isomerization when calcium falls below a critical concentration. In *A* I have taken this critical concentration to be 0.45 (filled circles). The times associated with the filled circles in *A* are therefore the predicted times-to-peak. They are displayed again, with respect to the light-adapted circulating current, in *B*. The open triangles in *B* are the actual times-to-peak that measured from data shown in Fig. 14. The agreement is as close as is needed in a game of horseshoes, which is what I expected. The divergence of the actual data from the predicted data around a time-to-peak of 0.5 seconds reflects the lower limit on how early currents can recover (see also Fig. 10).

isomerized. As reported previously, however, the calcium buffering capacity is very large in the outer segment. I therefore expect that the calcium influx through the cyclic GMP-gated channels and efflux through the exchanger will still dominate for dim flashes. A larger source of inaccuracy arises because cyclic GMP will also diffuse from areas adjacent to the point of isomerization and thus slow the rate at which channels would be closed.

My prediction method is illustrated in Fig. 15*A*. I determine - without excessive scruple - the time at which calcium is expected to have fallen to 40-50% of the calcium concentration in the dark. This is the time at which I would expect the current to begin to recover. The initial calcium concentrations are equal to the relative, steady-state circulating currents measured just before the corresponding flashs shown in Fig. 14.

The predictions underestimate the time at which the current begins to recover when more than approximately 50% of the circulating current was suppressed by the adapting illumination. This is consistent with the observation made in the preceding section. There is a lower limit to the time at which the current can begin to recover. For this rod it is approximately 500 ms, very close to the lower limit reported earlier. For dimmer adapting illuminations, the agreement between the predicted and measured times at which the current begins to recover is good. This supports the hypothesis that the negative feedback mediated by calcium is on the cyclic GMP cascade. It provides a satisfactory explanation for the stereotypical behavior of dim-flash responses and a fair

portion of the classic traits of light adaptation - the attenuation of the magnitude of the flash response and the more rapid kinetics.

I believe that other aspects of light adaptation follow from a more detailed examination of the light-induced change in the average rate at which cyclic GMP can be hydrolyzed that occurs during illumination and its impact on the mean free path length of cyclic GMP molecules. This introduces another level of complexity which I have not completely worked out at this point. Perhaps more important, the deadline for this thesis approaches rapidly. Further models of phototransduction and light adaptation will have to be left for another day.

Discussion

I have presented three important concepts in this chapter: that cyclic GMP synthesis is not strongly influenced by cytosolic free calcium at physiological concentrations, that the lifetime of activated phosphodiesterase is slowly decreased during illumination and slowly recovers when the illumination is dimmed, and that the ability of isomerized rhodopsin molecules to alter the rate at which cyclic GMP can be hydrolyzed is inhibited when the cytosolic free calcium concentration is low.

The first of these is perhaps the most controversial. The prevailing view of calcium's influence on cyclic GMP metabolism is through its regulation of guanylate

cyclase. This notion comes in part from biochemical work on rod homogenates (Pannbacker, 1973, Lolley and Racz, 1982, Pepe *et al.*, 1986, Koch and Stryer, 1988, and Dizhoor *et al.*, 1991). These experiments demonstrated that cyclic GMP accumulated when the calcium concentration was less than approximately 100 nM, although there are inconsistencies between the studies. Koch and Stryer (1988) suggested that calcium acted on guanylate cyclase through a membrane-associated protein. Dizhoor *et al.* 1991 identified this protein as a 23 kD molecule that they termed recoverin. They have recently retracted this assertion however (Hurley *et al.*, 1993) Recoverin has now been identified as a visinin-like protein which does not influence guanylate cyclase but does appear to effect the lifetime of activated phosphodiesterase (Kawamura and Murakami, 1991, Gray-Keller *et al.* 1993). The guanylate cyclase story is therefore not as firm as it was.

Nevertheless, the influence of calcium on cyclic GMP metabolism in rod homogenates is clear. Cyclic GMP accumulation depends very strongly on the calcium concentration. I believe that there may have been residual calcium-dependent hydrolysis in the rod homogenates that were studied. IBMX, the phosphodiesterase inhibitor, was present in these experiments; but IBMX only inhibits cyclic GMP hydrolysis in rods - it does not abolish it (see for example Chapter 3). The accumulation of cyclic GMP could therefore represent an inhibition of cyclic GMP hydrolysis as well as it could reflect an increase in cyclic GMP synthesis. I suspect that the calcium dependence of the inhibition of cyclic GMP hydrolysis was via recoverin, a name that is curiously appropriate. I

believe that recoverin either blocks the activation of phosphodiesterase or attenuates the hydrolytic ability of active phosphodiesterase enzymes when the calcium concentration is less than 60-100 nM (effective K_M = 40-70 nM). This inhibition of rhodopsin's influence on the hydrolytic capacity of the cyclic GMP cascade should have a calcium dependence that can be approximately described by a Hill coefficient of 4. I suggest these parameters based on the data shown in Fig. 8*B*. That figure and the parameters that describe the calcium dependence of the hypothesized influence of recoverin on the cyclic GMP cascade are reminiscent of the data and parameters that were reported by Koch and Stryer (1988) (K_M = 90 nM, Hill coefficient of 3.9) for the calcium-dependent regulation of cyclic GMP synthesis.

The idea that recoverin blocks the activation of phosphodiesterase or impairs its catalytic ability can also explain the "calcium latch". The calcium dependence of the activation coefficient (Fig. 8*B*) is the average behavior. By convention, I have described it with a cooperative titration curve, but this is clearly not very precise. I suspect that individual recoverin molecules are more sharply regulated by calcium than the titration curve suggests. Thus, when the cytosolic calcium concentration falls to some critical concentration, I would expect that recoverin would begin to exert its influence on the cyclic GMP cascade. This is like the behavior ascribed to the "calcium latch". When the calcium concentration is sufficiently low, recoverin may block the continued activation of phosphodiesterase enzymes.

The most significant argument that cyclic GMP synthesis is regulated by calcium can be based on the experiments which have been so valuable to me. These are the experiments with BAPTA-loaded cells by Torre *et al.* (1986) and with Quin-loaded cells by Korenbrot and Miller (1989). Currents recorded from these cells do not recover monotonically when illumination is turned off. Rather they overshoot the dark value of circulating current and then relax through a damped oscillation. This is the behavior of an underdamped system. It suggests that calcium mediates a negative feedback. If, as I suggest, cyclic GMP synthesis is not strongly regulated by calcium then the basal rate of cyclic GMP hydrolysis must be. This is an apparent twist on the "calcium latch" hypothesis. It suggests that calcium can diminish the hydrolytic capability of even unactivated phosphodiesterase enzymes. There are however, two important concepts to keep in mind. First, the current is approximately proportional to the cube of the cyclic GMP concentration. I estimate therefore that the basal rate constant of hydrolysis in the dark needs to be suppressed by only 10-15% to account for the pronounced overshoot observed in Quin-loaded rods (Korenbrot and Miller, 1989). The second, is that at least part of the basal rate of hydrolysis is afforded by spontaneous activation of transducin and phosphodiesterase enzymes. Thus, if the "calcium latch" acts at one of these later stages of the cyclic GMP cascade, it might influence the rate of hydrolysis even in the dark when the calcium kinetics are slowed by the presence of BAPTA or Quin. The increase in circulating current observed by Hodgkin *et al.* (1984) for rods exposed to a calcium-free solution might be explained in the same way.

The preceding hypotheses are of course just that. I am not a biochemist and must deduce the relationship between calcium and cyclic GMP metabolism based on my knowledge of dynamic systems and the currents and the calcium concentrations that I measure (or predict). The "calcium latch" hypothesis seems more likely to me than a pronounced influence of calcium on cyclic GMP synthesis in the physiological range. Furthermore, this hypothesis is the same as that suggested by Wagner *et al.* (1989). In light-scattering experiments they tracked transducin activation. They observed that the number of transducin enzymes that were activated per isomerized rhodopsin molecule was reduced in low calcium concentrations. The hypothesis is also supported by the work of Kawamura and Murakami (1991) who found that S-modulin, which appears to be the same molecule as recoverin, regulates phosphodiesterase activity in a calcium-dependent manner. Such a phenomenon would also be consistent with the "calcium latch".

Our other major concept is that the lifetime of activated hydrolysis appears to decrease during illumination at a rate that is not clearly correlated with changes in the cytosolic calcium concentration. This hypothesis is prompted by the rate at which currents recover from illumination and is similar to the acceleration of the voltage response of toad rods that was observed by Coles and Yamane (1975) and Cervetto *et al.* (1984).

Dr. Vadim Arshavsky has suggested to me a mechanism that could account for the acceleration of the rate of recovery of the current without invoking calcium. Continuing

from published work (Arshavsky and Bownds, 1992) he finds what appears to be a cyclic GMP-dependent inactivation of activated phosphodiesterase enzymes. The cyclic GMP-dependence is most likely to be via the two non-catalytic cyclic GMP binding sites on the phosphodiesterase holoenzyme. The absence of cyclic GMP from these sites is suggested to alter the affinity of the GTP-transducin-bound gamma subunits of PDE for the alpha and beta subunits. When the gamma subunits dissociate from the remainder of phosphodiesterase, GTP-ase activity may be accelerated. What is most interesting about this process is that it seems to be modulated by cyclic GMP concentrations in the physiological range. Such a scheme might very well be responsible for the acceleration of phosphodiesterase inactivation observed.

Another possibility is that there is a light-dependent phosphorylation-dephosphorylation process at work, perhaps of the gamma-subunits of phosphodiesterase (Hermolin *et al.*, 1982). I cannot, however, determine from my data the true biochemical mechanisms that underlie any of the behavior I observe. What is clear, however, is that there are still apparently simple aspects of phototransduction and light adaptation that I don't understand.

CHAPTER SIX: SUMMARY AND DISCUSSION

This thesis has turned out to be much longer than I had expected; but it covers a lot of ground. I believe that it significantly clarifies the light-induced dynamics of cytosolic free calcium in rod outer segments of the frog and the role of calcium in phototransduction and light adaptation.

Much of the work depends on how accurately calcium concentrations in the outer segment can be measured. Although I have reported a range of calcium concentrations which I believe includes the true cytosolic calcium concentration in the dark, relative calcium concentrations are usually more important to me. In both cases, the ability to measure the calcium concentration in the outer segment is limited by how well of the properties of Fura-2 in rods are understood. An aggravatingly large portion of my time was been spent in trying to understand what Fura-2 was doing. Fortunately, the effort has paid off.

Fura-2 exists in at least two calcium-sensitive forms in the outer segment. One of them, which has the characteristics of the Fura-2 described by Grynkiewicz *et al.* (1985), is the dominant contributor to the light-induced change in fluorescence measured in rods exposed to the control solution. This fluorescence represents the light-induced change in the cytosolic free calcium concentration. The other species of Fura-2 contributes a smaller fraction of the total fluorescence. Although, I am not certain of the

nature of this species of Fura-2, many of its characteristics are consistent with a protein-bound form of Fura-2. Some of its other charateristics remain confusing. Despite this, the calcium-sensitive properties of the total fluorescence elicited from rods have allowed for the determination of cytosolic free calcium concentrations.

I am now certain that bright illumination reduces the cytosolic free calcium concentration in the outer segment to a few nanomolar within approximately 15 seconds. As important, steady illumination reduces the circulating current and cytosolic free calcium concentration by the same fraction of their values in the dark. Only the cyclic GMP-gated channels and the Na^+; Ca^{2+}, K^+ exchanger regulate the flux of calcium ions across the plasma membrane; no significant light-induced release of calcium from internal stores is detected.

The kinetics of the light-induced changes in the cytosolic free calcium concentration are more complicated than expected. The space-average of the cytosolic free calcium concentration falls during bright illumination but with a timecourse that is described by two exponentials rather than the expected single exponential. The exchange current, which is proportional to the cytosolic free calcium concentration near the plasma membrane, has a similar timecourse, but is not proportional to the space-average of the free calcium concentration at early times. The complexity stems in part from the large fraction of the current flowing through the cyclic GMP-gated channels that is carried by calcium. In part it is a result of the unexpectedly large calcium buffering capacity of the

outer segment. These factors alone cannot account for the kinetics observed, even when obvious limitations on calcium diffusion are considered. Instead, I have developed a compartment model which accurately describes the space-averaged calcium concentrations and exchange currents I measure.

The compartment model is a phenomenological model that contains two domains. At least one of these is cytosolic and the calcium concentration within it is proportional to the exchange current. The other domain is also likely to be cytosolic and would then represent the interior portion of the outer segment. Enough uncertainty exists regarding Fura-2 and the sequestration of calcium within the outer segment, however, that the nature "inner" compartment cannot be stated unequivocally. The importance of the compartment model is that it accurately predicts the kinetics of the calcium concentrations in each domain and the space-averaged calcium concentration from the total measured current even when all of the cyclic GMP-gated channels are not closed.

I have also examined the activation kinetics of the cyclic GMP cascade. Although I did not separate the discussion of the activation kinetics from the study of calcium, except in Appendix B, I believe the model is important. It is similar in most respects to the work of Lamb and Pugh (1992) and the final analysis was influenced by that work, but it was derived independently and differs in some important aspects. My model predicts that each of the two transducin molecules that are required to activate fully a phosphodiesterase enzyme have a different impact on the rate at which phosphodiesterase

can hydrolyze cyclic GMP.

The model of the activation of the cyclic GMP cascade and the compartment model for estimating calcium concentrations have also been important in the examination of the role of calcium in phototransduction and light adaptation. My conclusions are at odds with one of the most widely held theories on calcium's influence on cyclic GMP metabolism.

I find that the dynamics of the light-induced change in cytosolic free calcium do not support the concept that cyclic GMP synthesis is strongly regulated by calcium at physiological concentrations. Instead, I find that calcium appears to regulate the ability of isomerized rhodopsin molecules to influence the rate at which cyclic GMP can be hydrolyzed. I propose a mechanism, which I refer to as a "calcium latch", to be the basis of this phenomenon. I suggest that recoverin, which was previously thought to be a calcium-dependent regulator of guanylate cyclase (Dizhoor *et al.* 1991), inhibits the cyclic GMP cascade either by blocking the activation of transducin or phosphodiesterase or by decreasing the rate at which activated phosphodiesterase enzymes can hydrolyze cyclic GMP.

I have also found evidence for what appears to be a light-induced change in the lifetime of activated phosphodiesterase enzymes that is independent of the effects of calcium on the cyclic GMP cascade. This phenomenon develops much more slowly than

the cytosolic free calcium concentration changes which, therefore, suggests that it is not mediated by calcium. In fact, the phenomenon continues to develop even as the cytosolic calcium concentration ceases to fall and begins to increase. I do not know what mediates this process, although cyclic GMP itself is a candidate (Arshavsky and Bownds, 1992, Arshavsky, personal communication).

There are experiments which I can perform to refine my conclusions. I also continue to develop models of phototransduction and light adaptation that have not been presented here. What I have presented are the results of my experiments on calcium regulation within frog rod outer segments, the effect of calcium on the frog rod's response to illumination, and the conclusions that I could make from them. I believe that these results and conclusions substantially advance the understanding of phototransduction and light adaptation. Unfortunately, the biochemical expertise that I expect will be required to completely describe the phenomena I have reported is not within my repertoire, but I eagerly await the results obtained by other researchers. I hope that this work will be of use in understanding the responses of the rods and cones of other animals and, perhaps, in the understanding of intracellular signalling within other cell types.

BIBLIOGRAPHY

Abramowitz, M. and Stegun, A. (1965). *Handbook of Mathematical Functions*. Dover Publications, Inc.: New York.

Arshavsky, V.Y. and Bownds, M.D. (1992). Regulation of deactivation of photoreceptor G protein by its target enzyme and cGMP. *Nature (London)*. **357**:416-417.

Arslon, P., Di Virglio, F., Beltrame, M., Tsien, R.Y. and Pozzan, T. (1985). Cytosolic Ca^{2+} homeostasis in Erlich and Yoshida carcinomas. A new, membrane permeant chelator of heavy metals reveals that these ascites tumor cell lines have normal cytosolic free calcium. *J. Biol. Chem.* **260**:2719-2727.

Bader, C.R., Bertrand, D. and Schwartz, E.A. (1982). Voltage-activated and calcium-activated currents studied in solitary rod inner segments from the salamander retina. *J. Physiol. (London)*. **331**:253-284.

Bancel, F., Salmon, J.-M., Vigo, J., Vo-Dinh, T. and Viallet, P. (1992). Investigation of noncalcium interactions of Fura-2 by classical and synchronous fluorescence spectroscopy. *Anal. Biochem.* **204**:231-238.

Barkdoll, A.E., Pugh, E.N. Jr. and Sitaramayya, A. (1989). Calcium dependence of the activation and inactivation kinetics of the light-activated phosphodiesterase of retinal rods. *J. Gen. Physiol.* **93**:1091-1108.

Baylor, D.A., Lamb, T.D. and Yau, K.-W. (1979a). The membrane current of single rod outer segments. *J. Physiol. (London)*. **288**:589-611.

Baylor, D.A., Lamb, T.D. and Yau, K.-W. (1979b). Responses of retinal rods to single photons. *J. Physiol. (London)*. **288**:613-634.

Baylor, D.A. and Nunn, B.J. (1986) Electrical properties of the light-sensitive conductance of rods of the salamander *Ambystoma tigrinum*. *J. Physiol. (London)*. **371**:115-145.

Bennett, N. and Clerc, A. (1989). Activation of cGMP phosphodiesterase in retinal rods: mechanism of interaction with the GTP binding protein (transducin). *Biochemistry*. **28**:7418-7424.

Cameron, D.A. and Pugh, E.N. (1990). The magnitude, time course and spatial distribution of current induced in salamander rods by cyclic guanine nucleotides. *J. Physiol. (London)*. **430**:419-439.

Capovilla, M., Cervetto, L. and Torre, V. (1983). The effect of phosphodiesterase inhibitors on the electrical activity of toad rods. *J. Physiol. (London)*. **343**:277-294.

Cervetto, L., Lagnado, L. and McNaughton, P.A. (1987). Activation of the Na:Ca exchange in salamander rods by intracellular Ca. *J. Physiol. (London).* **382**:135P.

Cervetto, L., Lagnado, L., Perry, R.J., Robinson, D.W. and McNaughton, P.A. (1989). Extrusion of calcium from rod outer segments is driven by both sodium and potassium gradients. *Nature (London).* **337**:740-743.

Cervetto, L. and McNaughton, P.A. (1986). The effects of phosphodiesterase inhibitors and lanthanum ions on the light-sensitive current of toad retinal rods. *J. Physiol. (London).* **370**:91-109.

Cervetto, L., Torre, V., Pasino, E., Marroni, P. and Capovilla, M. (1984). Recovery from light-desensitization in toad rods. In Borsellino, A. and Cervetto, L. (Eds.), *Photoreceptors* (pp. 159-175). NATO ASI Series, Series A: Life Sciences Vol. 75. Plenum Press: New York.

Chabre, M. and Deterre, P. (1989). Molecular mechanism of visual transduction. *J. Biochem.* **179**:255-266.

Chiancone, E., Thulin, E., Boffi, A., Forsén, S. and Brunori, M. (1986). Evidence for the interaction between the calcium indicator 1,2-bis(*o*-aminophenoxy)ethane-*N,N,N',N'*-tetraacetic acid and calcium-binding proteins. *J. Biol. Chem.* **261**:16306-16308.

Cobbold, R.S.C. (1974). *Transducuers for Biomedical Applications: Principles and Applications.* John Wiley & Sons: New York.

Colamartino, G., Menini, A. and Torre. V. (1991). Blockage and permeation of divalent cations through the cyclic GMP-activated channel from tiger salamander retinal rods. *J. Physiol. (London).* **440**:189-206.

Coles, J.A. and Yamane, S. (1975). Effects of adapting lights on the time course of the receptor potential of the anuran retinal rod. *J. Physiol. (London).* **247**:189-207.

Corless, J.M., Fetter, R.D., Zampighi, O.B., Costello, M.J. and Wall-Buford, D.L. (1987). Structural features of the terminal loop region of frog retinal rod outer segment disk membranes: II. Organization of the terminal loop complex. *J. Comp. Neurology.* **257**:9-23.

Dizhoor, A.M., Ray, S., Kumar, S., Niemi, G., Spencer, M., Brolley, D., Walsh, K.A., Philipov, P.P., Hurley, J.B. and Stryer, L. (1991). Recoverin: A calcium sensitive activator of retinal rod guanylate cyclase. *Science.* **251**:915-918.

Fain G.L. and Schröder, W.H. (1987). Calcium in dark-adapted toad rods: evidence for pooling and cyclic-guanosine-3'-5'-monophosphate-dependent release. *J. Physiol. (London).* **389**:361-384.

Forti, S., Menini, A., Rispoli, G. and Torre, V. (1989). Kinetics of phototransduction in retinal rods of the newt *Triturus cristatus*. *J. Physiol. (London).* **419**:265-295.

Furakawa, T. and Hanawa, I. (1955). Effects of some common cations on electroretinogram of the toad. *Jap. J. Physiol.* **5**:289-300.

Gray-Keller, M.P., Polans, A.S., Palczewksi, K. and Detwiler, P.B. (1993). The effect of recoverin-like calcium-binding proteins on the photoresponse of retinal rods. *Neuron.* **10**:523-531.

Groden, D.L., Guan, Z. and Stokes, B.T. (1991). Determination of Fura-2 dissociation constants following adjustment of the apparent Ca-EGTA association constant for temperature and ionic strength. *Cell Calcium.* **12**:279-87

Grynkiewicz, G., Poenie, M. and Tsien, R.Y. (1985). A new generation of Ca^{2+} indicators with greatly improved fluorescence properties. *J. Biol. Chem.* **260**:3440-3450.

Hamm, H.E. and Bownds, M.D. (1986). Protein complement of rod outer segments of frog retina. *Biochemistry.* **25**:4512-4523.

Handbook of Chemistry and Physics (1982). 63rd Ed. R.C. Weast (Ed.) CRC Press, Inc.: Boca Raton, Florida.

Hermolin, J., Karell, M.A., Hamm, H.E. and Bownds, M.D. (1982). Calcium and cyclic GMP regulation of light-sensitive protein phosphorylation in frog photoreceptor membranes. *J. Gen. Physiol.* **79**:633-655.

Hodgkin, A.L., McNaughton, P.A. and Nunn, B.J. (1985). The ionic selectivity and calcium dependence of the light-sensitive pathway in toad rods. *J. Physiol. (London).* **358**:447-468.

Hodgkin, A.L., McNaughton, P.A. and Nunn, B.J. (1987). Measurement of sodium-calcium exchange in salamander rods. *J. Physiol. (London).* **391**:347-370.

Hodgkin, A.L., McNaughton, P.A., Nunn, B.J. and Yau, K.-W. (1984). Effect of ions on retinal rods from *Bufo marinus*. *J. Physiol. (London).* **350**:649-680.

Hsu, Y.-T. and Molday, R.S. (1993) Modulation of the cGMP-gated channel of rod photoreceptor cells by calmodulin. *Nature (London).* **361**:76-79

Hurley, J.B. and Stryer, L. (1982). Purification and characterization of the γ regulatory subunit of the cyclic GMP phosphodiesterase from retinal rod outer segments. *J. Biol. Chem.* **257**:11094-11099.

Hurley, J.B., Dizhoor, A.M., Ray, S. and Stryer, L. (1993). Recoverin's role: Conclusion withdrawn. Letter to *Science*. **260**, 7 May.

Jackson, J.D. (1975). *Classical Electrodynamics*. 2nd Ed. John Wiley & Sons: New York.

Kahlert, M. and Hofmann, K.P. (1991). Reaction rate and collisional efficiency of the rhodopsin-transducin system in intact retinal rods. *Biophys. J.* **59**:375-386.

Kawamura, S. and Murakami, M. (1991) Calcium-dependent regulation of cyclic GMP phosphodiesterase by a protein from frog retinal rods. *Nature (London).* **349**:420-423.

Koch, K.-W., Stryer, L. (1988). Highly cooperative feedback control of retinal rod guanylate cyclase by calcium ions. *Nature (London).* **334**:64-66.

Konishi, M., Olson, A., Hollingworth, S. and Baylor, S.M. (1988) Myoplasmic binding of Fura-2 investigated by steady-state fluorescence and absorbance measurements. *Biophys. J.* **54**:1089-1104.

Korenbrot, J.I. and Miller, D.L. (1989). Cytoplasmic free calcium concentration in dark-adapted retinal rod outer segments. *Vision. Res.* **29**:939-948.

Lagnado. L., Cervetto, L. and McNaughton. P.A. (1988). Ion transport by the Na-Ca exchange in isolated rod outer segments. *Proc. Natl. Acad. Sci. (U.S.A.).* **85**:4548-4552.

Lagnado, L., Cervetto, L. and McNaughton, P.A. (1992). Calcium homeostasis in the outer segments of retinal rods from the tiger salamander. *J. Physiol. (London).* **455**:111-142.

Lamb, T.D and Pugh, E.N. Jr. (1992). A quantitative account of the activation steps involved in phototransduction in amphibian photoreceptors. *J. Physiol. (London).* **449**:719-758.

Lamb, T.D., McNaughton, P.A. and Yau, K.-W. (1981). Spatial spread of activation and background desensitization in toad rod outer segments. *J. Physiol. (London).* **319**:463-496.

Liebman, P.A. and Entine, G. (1968). Visual pigments of frog and tadpole. *Vision Res.* **8**:761-775.

Lolley, R.N. and Racz, E. (1982). Calcium modulation of cyclic GMP synthesis in rat visual cells. *Vision Res.* **22**:1481-1486.

Martell, A.E. and Smith R.M. (1974). *Critical Stability Constants*, Vol. 1. New York: Plenum Press.

Matthews, H.R., Murphy, R.L.W., Fain, G.L. and Lamb, T.D. (1988). Photoreceptor light adaptation is mediated by cytoplasmic calcium concentration. *Nature (London).* **334**:67-69.

McNaughton, P.A. (1990). Light response of vertebrate photoreceptors. *Physiological Reviews.* **70**:847-883.

McNaughton, P.A., Cervetto, L. and Nunn, B.J. (1986). Measurement of the intracellular free calcium concentration in salamander rods. *Nature (London).* **322**:261-263.

Miller, D.L. and Korenbrot, J.I. (1987). Kinetics of light-dependent Ca fluxes across the plasma membrane of rod outer segments. *J. Gen. Physiol.* **90**:397-425.

Negulescu, P.A. and Machen, T.E. (1990). Intracellular ion activities and membrane transport in parietal cells measured with fluorescent dyes. *Methods in Enzymology.* **192**:38-81

Pannbacker, R.G. (1973). Control of guanylate cyclase activity in the rod outer segment. *Science.* **182**:1138-1140.

Pepe, I.M., Boero, A. Vergani, L., Panfoli, I. and Cugnoli, C. (1986). Effect of light and calcium on cyclic GMP synthesis in rod outer segments of toad retina. *Biochim. Biophys. Acta.* **889**:271-276.

Poenie, M. (1990). Alteration of intracellular Fura-2 fluorescence by viscosity: A simple correction. *Cell Calcium.* **11**:85-91

Poo, M.-M. and Cone, R.A. (1974). Lateral diffusion of rhodopsin in the photoreceptor membrane. *Nature (London).* **247**:438-441.

Pugh, E.N. Jr. and Altman, J. (1988). A role for calcium in adaptation. News and Views, *Nature (London).* **334**:16-17.

Pugh, E.N. Jr. and Lamb, T.D. (1990). Cyclic GMP and calcium: The internal messengers of excitation and adaptation in vertebrate photoreceptors. *Vision Res.* **12**:1923-1948.

Pugh, E.N. Jr. and Lamb, T.D. (1993). Amplification and kinetics of the activation steps in phototransduction. *Biochim. Biophys. Acta.* **1141**:111-149.

Ratto, G.M., Payne, R., Owen, W.G. and Tsien, R.Y. (1988). The concentration of cytosolic free calcium in vertebrate rod outer segments measured with Fura-2. *J. Neurosci.* **8**:3240-3246.

Robinson, P.R., Kawamura, S., Abramson, B. and Bownds, M.D. (1980). Control of the cyclic GMP phosphodiesterase of frog photoreceptor membranes. *J. Gen. Physiol.* **76**:631-

645.

Robinson, P.R., Radeke, M.J., Cote, R.H. and Bownds, M.D. (1986). cGMP influences guanine nucleotide binding to frog photoreceptor G-protein. *J. Biol. Chem.* **261**:313-318.

Roe, M.W., LeMasters, J.J. and Herman, B. (1990). Assessment of Fura-2 for measurements of cytosolic free calcium. *Cell Calcium* **11**:63-73.

Sather, W.A. and Detwiler, P.B. (1987). Intracellular biochemical manipulation of phototransduction in detached rod outer segments. *Proc. Natl. Acad. Sci. (U.S.A.).* **84**:9290-9294.

Schröder, W.H. and Fain G.L. (1984). Light-dependent calcium release from photoreceptors measured by laser micro-mass analysis. *Nature (London).* **309**:268-270.

Somlyo A.P. and Walz, B. (1985). Elemental distribution in *Rana pipiens* retinal rods: Quantitative electron probe analysis. *J. Physiol. (London).* **358**:183-195.

Stryer, L. (1991). Visual excitation and recovery. *J. Biol. Chem.* **266**:10711-10714.

Szuts, E.Z. (1980). Calcium flux across disk membranes. *J. Gen. Physiol.* **76**:253-286.

Szuts, E.Z. and Cone, R.A. (1977). Calcium content of frog rod outer segments and discs. *Biochim. Biophys. Acta.* **486**:194-208.

Torre, V., Matthews, H.R. and Lamb, T.D. (1986). Role of calcium in regulating the cyclic GMP cascade of phototransduction in retinal rods. *Proc. Natl. Acad. Sci. (U.S.A.).* **83**:7109-7113.

Torre, V., Straforini, M., Sesti, F. and Lamb, T.D. (1992) Different channel-gating properties of two classes of cyclic GMP-activated channel in vertebrate photoreceptors. *Proc. R. Soc. Lond.* B. **250**:209-215.

Tsien, R.Y. and Harootunian, A.T. (1990). Practical design criteria for a dynamic ratio imaging system. *Cell Calcium.* **11**:93-109.

Uto, A., Arai, H. and Ogawa, Y. (1991) Reassessment of Fura-2 and the ratio method for determination of intracellular Ca^{2+} concentrations. *Cell Calcium.* **12**:29-37.

Vuong, T.M., Chabre, M. and Stryer, L. (1984). Millisecond activation of transducin in the cyclic nucleotide cascade of vision. *Nature (London).* **311**:659-661.

Wagner, R., Ryba, N.J.P. and Uhl, R. (1987). The amplified P-signal, an extremely photosensitive light scattering signal from rod outer segments, which is not affected by

pre-activation of phosphodiesterase with Gα-GTP-γ-S. *FEBS Lett.* **221**:253-259.

Wagner, R., Ryba, N.J.P. and Uhl, R. (1989). Calcium regulates the rate of rhodopsin disactivation and the primary amplification step in visual transduction. *FEBS Lett.* **242**:249-254.

Whalen, M.M., Bitensky, M.W. and Takemoto, D.J. (1990). The effect of the gamma-subunit of the cyclic GMP phosphodiesterase of bovine and frog (*Rana catesbeiana*) retinal rod outer segments on the kinetic parameters of the enzyme. *Biochem. J.* **265**:655-658.

Wilden, U., Hall, S.W. and Kuhn, H. (1986). Phosphodiesterase activation by photoexcited rhodopsin is quenched when rhodopsin is phosphorylated and binds the intrinsic 48-kDa protein of rod outer segments. *Proc. Natl. Acad. Sci. (U.S.A.).* **83**:1174-1178.

Yau, K.-W. and Nakatani, K. (1984). Electrogenic Na-Ca exchange in retinal rod outer segment. *Nature (London).* **311**:661-663.

Yau, K.-W. and Nakatani, K. (1985). Light-induced reduction of cytoplasmic free calcium in retinal rod outer segment. *Nature (London).* **313**:579-582.

Yau, K.-W. and Nakatani, K. (1988). Sodium-dependent calcium efflux at the outer segment of the retinal cone. *Biophys. J.* **54**:473a

Yoshikami, S. and Hagins, W.A. (1973). Control of the dark current in vertebrate rods and cones. In Langer, H. (Ed.), *Biochemistry and Physiology of Visual Pigments* (pp. 245-255). Springer Verlag: Berlin.

Younger, J.P. (1991). *Calcium Regulation of the Light Response of Vertebrate Photoreceptors*. Ph.D. Thesis. University of California, Berkeley.

Zimmerman, A.L. and Baylor, D.A. (1986). Cyclic GMP-sensitive conductance of retinal rods consists of aqueous pores. *Nature (London).* **321**:70-72.

APPENDIX A: TWO POOLS OF FURA-2

My analysis has made use of the fluorescence elicited by 380 nm illumination at the tail end of stimulation, ψ_o, when the cytosolic free calcium concentration in rod outer segments is a few nanomolar. I have also relied on the contribution by each pool to the light-induced change in fluorescence elicited by 380 nm illumination, ψ_1 and ψ_2. These variables may be described by:

$$\psi_o = \psi_{f,1} + \psi_{f,2} \qquad \psi_1 = \psi_{b,1} - \psi_{f,1} \tag{A1}$$

with a similar description for ψ_2. The letter subscripts denote the fluorescence of the calcium-free form, *f*, and calcium-bound form, *b*, of each of the two pools, denoted by the subscripts 1 and 2. Because F is $\psi_{f,1}/\psi_{b,1}$, we may also write $\psi_1 = \psi_{f,1}(1\text{-}F)/F$. The other *in vitro* parameters may be written as $R_o = \phi_{f,1}/\psi_{f,1}$ and $R_m = \phi_{b,1}/\psi_{b,1}$.

Determination of the slope parameter, m_2, for the immobile pool of Fura-2 is quite straightforward, although it looks somewhat complicated. I redefine ψ_o in terms of what fraction of the total fluorescence elicited by 380 nm illumination is contributed by the pool of classic Fura-2 and represent this fraction with the free variable α. The fluorescence elicited from the pool of classic Fura-2, $\psi_{f,1}$, in the absence of cytosolic free calcium can then be written as the upper left-side relation in eqn (A 2). The remaining relations of eqn (A 2) follow from the calibrations parameters measured *in vitro* and the fluorescences measured for each stimulus wavelength when cytosolic calcium is high, ϕ_m and ψ_m, and when it is low, ϕ_o and ψ_o.

$$\Psi_{f,1} = \alpha\Psi_o \qquad \Psi_{f,2} = \Psi_o - \Psi_{f,1} \tag{A 2}$$

$$\Psi_{b,1} = F^{-1}\,\Psi_{f,1} \qquad \Psi_{b,2} = \Psi_m - \Psi_{b,1}$$

$$\phi_{f,1} = R_o\Psi_{f,1} \qquad \phi_{f,2} = \phi_o - \phi_{f,1}$$

$$\phi_{b,1} = R_m\phi_{f,1} \qquad \phi_{b,2} = \phi_m - \phi_{b,1}$$

The slope parameter for the immobile pool is then described by eqn (A 3). I have performed algebra to express m_2 in terms of the directly measured *in vitro* and *in situ* calibration parameters; R_o, R_m and F, and R'_o, R'_m and F', respectively.

$$m_2 = \frac{\phi_2}{\Psi_2} = \frac{\phi_{b,2} - \phi_{f,2}}{\Psi_{b,2} - \Psi_{f,2}} = \frac{\dfrac{R'_m - R'_o\,F'}{F'} - \alpha\,\dfrac{R_m - R_o\,F}{F}}{\dfrac{1 - F'}{F'} - \alpha\,\dfrac{1 - F}{F}} \tag{A 3}$$

The only free variable in this formulation is α which can be estimated fairly well from the rate at which Fura-2 is quenched.

APPENDIX B: THE RISING PHASE OF THE PHOTOCURRENT DURING A STEP OF ILLUMINATION

In the text, I present equations that describe the rising phase of the photoresponse of a rod illuminated with a bright step of light. The derivations of these equations below. The derivation is similar to that of Lamb and Pugh (1992) but was derived independently several years ago and differs from theirs in several important aspects. Both approaches make use of the characteristics of the cyclic GMP cascade and the cyclic GMP-gated channel which have been thoroughly reviewed by Chabre and Deterre (1989), Pugh and Lamb (1990) and Stryer (1990). Many of the specific numerical estimations are adopted from the comprehensive review and analysis of Pugh and Lamb (1993).

Briefly, the cyclic GMP cascade is composed of rhodopsin, transducin (a G-protein) and a cyclic GMP phosphodiesterase (PDE), all of which are bound to or span the disk membrane. A photon activates a rhodopsin molecule by isomerizing its 11-*cis*-retinal chromophore to all-*trans*-retinal. The isomerized rhodopsin catalyzes a GTP-for-GDP exchange on the alpha subunits of a number of transducin holoenzymes. The GTP-bound alpha subunit dissociates from the beta-gamma subunits but remains attached to the disk surface (Wagner *et al.*, 1987). Each GTP-bound alpha subunit of transducin can bind to one of the two gamma subunits of a phosphodiesterase. It is not clear if this binding is cooperative or if each phosphodiesterase gamma subunit feels the presence of

a GTP-bound alpha subunit of transducin independently - each alpha subunit being responsible for realizing approximately one-half of the catalytic potential of a phosphodiesterase molecule in frogs (Whalen *et al.*, 1990). It is also not clear if the gamma subunits remain bound to the alpha and beta subunits of phosphodiesterase or if the GTP-bound alpha subunit of transducin initiates a dissociation. The interaction of the GTP-bound subunit of transducin with the gamma subunit(s) of phosphodiesterase creates, however, an enzyme that can hydrolyse cytosolic cyclic GMP at a high rate (Hurley and Stryer, 1982)

Less is known about the inactivation of the enzymes of the cyclic GMP cascade. *In vitro* biochemical evidence suggests that rhodopsin remains active until it is subjected to multiple phosphorylations of its carboxyl-terminus tail (Liebman and Pugh, 1974) and is then capped by the cytosolic enzyme, Arrestin (Wilden *et al.*, 1986). Active phosphodiesterase molecules appear to be inactivated only when the GTP bound to the alpha subunit of transducin is converted to GDP by an inherent GTPase activity of the active complex. More recent evidence suggests, however, that S-modulin may regulate the lifetime of activated cyclic GMP hydrolysis in response to a reduction in the cytosolic free calcium concentration (Kawamra and Murakami, 1991).

Although all of the details of the activation and inactivation are not entirely clear, I believe that an approximate relationship for the rate at which each participant enzyme is activated can be written as:

$$\dot{R}^* = I(t) - k_R^\circ R^* \tag{B1}$$

$$\dot{G}^* = k_G^* G R^* - k_P^* P G^*$$

$$\dot{P}^* = k_P^* P G^* - k_P^\circ P^*$$

In this equation, R represents rhodopsin, G represents transducin and P represents phosphodiesterase. Variables denoted by an asterisk reflect activation. Variables denoted by a naught refer to inactivation. Undecorated variables represent the quantity of each enzyme that may be activated. The function, $I(t)$, represents the rate at which rhodopsin molecules are isomerized by illumination. The time-dependence of all other variables, except the rate constants, k's, are implied. The most significant assumption explicit in this representation of the cyclic GMP cascade is that each active alpha subunit of transducin affects phosphodiesterase independently and with equal effectiveness. I am not confident that this is true and partially allay the impact of this assumption below.

Like Lamb and Pugh, (1992), I assume that neither active rhodopsin nor active phosphodiesterase is inactivated during the time that elapses while cyclic GMP-gated channels close in response to bright illumination. I differ from them, however, in the treatment of activated transducin. They have assumed that activated transducin combines immediately with phosphodiesterase. The result, in their treatment, is that the rate of accumulation of active transducin is proportional to the rate of accumulation of active phosphodiesterase. Their analysis also includes a delay factor which I do not believe is

necessary.

I believe that there is not enough information to assume that the rate of formation of activated transducin is proportional to the rate of formation of activated phosphodiesterase. My recalcitrance is motivated by several factors. Poo and Cone (1974) measured the rate of diffusion of rhodopsin on the disk surface and estimated a two-dimensional diffusion constant of 4×10^{-9} cm^2 sec^{-1}. The rapid diffusion of rhodopsin has been attributed to the composition of the disk membrane, which is one of the most fluid of known phospholipid membranes, rather than any unique properties of rhodopsin. I would expect, therefore, that transducin and phosphodiesterase would enjoy similarly unhindered lateral mobility and suffer roughly the same number of collisions per second as do rhodopsin molecules. Differences in protein size and position within the membrane will influence the collision rate, but not drastically. Hamm and Bownds (1986) state that there are approximately 15 times as many transducin molecules on the disk surface as there are phosphodiesterase enzymes. If collisions between active transducin and unactivated phosphodiesterase are approximately as effective as collisions between active rhodopsin and uncatalysed transducin, then, within the time one would expect an active transducin molecule to combine with a phosphodiesterase, approximately 15 additional active transducins would be created within the same neighborhood. It would appear, therefore, that phosphodiesterase would stand little chance of escaping activation. This appears to be the logic behind the assumption of Lamb and Pugh (1992). It implicitly posits, however, that transducin and phosphodiesterase are as mobile as rhodopsin and

that phosphodiesterase activation occurs after only a few collisions with activated transducins. Such a scheme is possible, perhaps even likely, but I do not believe it is necessarily correct and so do not neglect the rate of transducin accumulation as a separate step in the activation of the cyclic GMP cascade.

I make one more assumption about the cyclic GMP cascade. This is, that during the rising phase of the photoresponse, there is no lack of transducin and phosphodiesterase available for activation. My reasoning is thus. Frog rod disks are segmented into approximately 25 petals by incisures running radially from the edge of the disk to near the center, (Corless *et al.*, 1987). There are approximately 3.6×10^9 rhodopsin molecules and 2000 disks per frog rod (Liebman and Entine, 1968). One would expect, therefore, that there are approximately 3.6×10^4 rhodopsin molecules on each face of each petal. Hamm and Bownds (1986) have reported that the ratio of transducin enzymes to rhodopsin molecules is approximately 1:10 and Lamb and Pugh (1993) estimate in their review that in excess of 1000 transducins are activated per isomerized rhodopsin per second, although measured values vary over a wide range (Robinson *et al.*, 1986, Vuong *et al.*, 1984, Kahlert and Hoffman, 1991). During a rising phase of 200 milliseconds, one would therefore expect that approximately 200 transducin molecules would be activated, approximately 5% of the transducin that was present on the petal face when a photon was absorbed. I would expect a similar reduction in the availability of phosphodiesterase if the activation efficiencies are about the same for transducin and phosphodiesterase. The assumption that a constant amount of transducin and phosphodiesterase is available for

activation would, therefore, appear to be a reasonable one.

Combining the assumptions that there is no significant inactivation of rhodopsin or phosphodiesterase during the rising phase of the photoresponse and that a constant quantity of transducin and phosphodiesterase is available for activation, the Laplace transformations of a simplified Eqn. (B1) may be written as:

$$\tilde{R}^* \approx \frac{\tilde{I}}{s} = \frac{I}{s^2} \tag{B2}$$

$$\tilde{G}^* \approx \frac{k_G^* G \tilde{R}^*}{s + k_P^* P}$$

$$\tilde{P}^* \approx \frac{k_P^* P \tilde{G}^*}{s}$$

In this representation, I treat rhodopsin activation resulting from a step of illumination as a continuous function although I recognize that isomerizations are discrete events that are distributed over the entire rod outer segment. For the illuminating intensities that I use, however, rhodopsins will be isomerized rapidly with respect to their mean lifetime and the vast majority will act independently on non-overlapping domains. The step time-course should therefore be understood to represent the integration over time of individual photon captures.

The inverse Laplace transformation of Eqn (B2) is straightforward.

$$P^* \approx \frac{k_G^* G}{(k_P^* P)^2} I \left[1 - k_P^* P t + \frac{1}{2} (k_P^* P t)^2 - e^{-k_P^* P t} \right] \qquad \text{(B3a)}$$

When the exponential term is expanded into a series, we obtain:

This equation approximately describes the time course of active phosphodiesterase accumulation in response to a step of illumination. For an equivalent description for a flash, the series begins at $n = 2$ and n-3 is replaced by n-2.

Lamb and Pugh (1992) concluded that P^* is a linear function of time following a flash of illumination. This conclusion results from their assumption that transducin activation is synonymous with phosphodiesterase activation. This is equivalent to stating that $k^*_P Pt$ in Eqn (B3b) is large during the rising phase. In Fig. *B*1, I show scaled versions of the time course of phosphodiesterase accumulation expected during the first half-second of a step of illumination for three values of $k^*_P Pt$. The figure demonstrates that when phosphodiesterase is activated rapidly ($k^*_P P$ large) the time course of accumulation approaches parabolic, equivalent to a linear accumulation in the case of a flash. When activation is slow, the time course of accumulation is nearly cubic. For intermediate rates of activation, accumulation is initially cubic but then becomes parabolic. This behaviour can be expressed as:

$$\lim_{k_P^* P\, t \ll 1} \sum_{n=3}^{\infty} \frac{(k_P^* P\, t)^n}{n!} = \frac{(k_P^* P\, t)^3}{3!} \tag{B4}$$

$$\lim_{k_P^* P\, t \gg 1} \sum_{n=3}^{\infty} \frac{(k_P^* P\, t)^n}{n!} \rightarrow \frac{(k_P^* P\, t)^2}{2!}$$

In the derivation so far, I have assumed that each of the two transducins that are required for the full activation of a phosphodiesterase act independently and with equal efficiency. The primary motivation for this assumption is that cooperativity is difficult to model rigorously and Whalen *et al.* (1990) have observed non-cooperative activation of frog phosophodiesterase *in vitro*. On the other hand they and Bennet and Clerc (1990) have observed co-operative activation in bovine rods. One can, however, intuit the accumulation rate when phosphodiesterase activation is cooperative. If a quiescent phosphodiesterase is overwhelmingly surrounded by active transducin molecules and cooperative activation requires only a few collisions, then we may neglect transducin activation as an independent stage in the activation of the cyclic GMP cascade. This is again the same reasoning followed by Lamb and Pugh (1992) for non-cooperative activation. In the case of cooperative activation, we would therefore expect the accumulation of active phosphodiesterase to be proportional to the square of the accumulation of active transducin. On the other hand, if the activation stage is slow, one would expect instead that the rate of accumulation of active phosphodiesterase would be related to the square of the number of active transducins that is available, similar to the behaviour illustrated in Fig. *B*1. I have summarized these concepts in Table *B*1.

Table *B*1

G^* activation of *P*	Co-operativity	n
Rapid	No	> 2
Slow	No	< 3
Rapid	Yes	> 3
Slow	Yes	< 4

It is useful to describe the approximate time course of active phosphodiesterase accumulation as:

$$P^* \approx a_{\eta-1}\, k_G^*\, G\, k_P^*\, P\, I\, t^{\eta-1} \qquad \text{(B5)}$$

where I have approximated the series of Eqn (B3) by a single time factor according to the previous discussion. The term, η - 1, which is not necessarily an integer, is equivalent to *n* of Table *B*1 and the previous equations. I express this exponent as η-1 in anticipation of the final results. The significance of η is that it suggests the co-operativity and rate of phosphodiesterase activation when determined from experimental data. The constant term, $a_{\eta-1}$, replaces the factorial of previous equations.

The time course of phosphodiesterase accumulation is important only in so far as it can be used to describe the time course of the cyclic GMP concentration in the outer segment. Cyclic GMP metabolism may be written in terms of hydrolysis and

synthesis as:

$$\frac{d\ cGMP}{dt} = -k_h\ cGMP + v_s \tag{B6}$$

Here, *cGMP* is the cytosolic concentration of cyclic GMP, k_h is the hydrolysis rate constant and v_s is the rate of synthesis of cyclic GMP by guanylate cyclase. The solution to Eqn. (B4) is:

$$cGMP(t) = [cGMP(0) + \int_0^t v_s\ \kappa_h\ dt'\ ]\ \kappa_h^{-1} \approx cGMP(0)\ \kappa_h^{-1} \tag{B7}$$

where

$$\kappa_h = \exp(\int k_h\ dt')$$

On the right-hand side of this equation, I have neglected the integral within the brackets. This approximation is justified by noting, from Eqn. (B4) and Eqn. (B5), that during steady, bright illumination, when few cyclic GMP-gated channels are open:

$$cGMP(0) >> cGMP_{ss} = \frac{v_{s,ss}}{k_{h,ss}} \approx \kappa_h^{-1} \int_0^{t_{ss}} v_s\ \kappa_h\ dt' \tag{B8}$$

where the subscript, *ss*, refers to steady-state values in the light and t_{ss} refers to any time after steady-state conditions have been achieved.

Robinson *et al.* (1980) have found that the cyclic GMP concentration at which the rate of hydrolysis by phosphodiesterase is half-maximal is 900 μM. The cytosolic

concentration of free cyclic GMP in a dark-adapted rod is much lower - approximately 4 μM (Pugh and Lamb, 1990). Even if these values are not precise, k_h may be treated as independent of the cyclic GMP concentration and thus its dependence on active and inactive forms of phosphodiesterase may be written as:

$$k_h = \gamma_h^* P^* + \gamma_h^0 P \approx \gamma_h^* P^* \tag{B9}$$

Again an approximation is made on the right-hand side of the equation. The justification is that the catalytic rate of active phosphodiesterase has been observed to be more than 1500 times that of the quiescent form (Stryer, 1991) and the observation that illumination does, in fact, result in a complete suppression of the circulating current for a short period when fewer than one rhodopsin molecule per disk is isomerized (Chapter 5).

The final task is to put all of this together. But first, note that the cyclic GMP-gated channel is rapidly and co-operatively opened by three cyclic GMP molecules (Zimmerman and Baylor, 1986). Therefore:

$$\frac{J_g(t)}{J_g(0)} = \frac{cGMP^3(t)}{cGMP^3(0)} \tag{B10}$$

where J_g is the current flowing through the cyclic GMP-gated channel. Combining the right-most portions of Eqns (B5), (B7), (B9) and (B10), we obtain:

$$J_s(t) \approx J_s(0)\ e^{-k_I t^n} \qquad \text{(B11)}$$

$$k_I \propto k_h^* \ k_G^* \ G \ k_P^* \ P$$

The term, k_I, is the step illumination equivalent of the activation constant defined by Lamb and Pugh (1992).

Eqn (B11) is similar in form to the result obtained by Lamb and Pugh (1992). The term, k_I, is equivalent to their activation constant. A trivial difference between my result and the description by Lamb and Pugh (1992) is that mine describes the rising phase of the photoresponse elicited by a step of illumination while theirs is intended to describe a flash. My model describes flash responses when η-1 is substituted for η and k_I is divided by η. The more significant differences are the lack of a delay term and the fact that the rate of accumulation of phosphodiesterase in response to a flash of light may be as much as cubic in time rather than assuming it to be linear. A delay was not included because I am attempting to describe the effect of a large number of rhodopsin isomerizations. The individual delays experienced by solitary enzymes are distributed as in any stochastic process. The macroscopic behaviour reflects this and thus no explicit delay needs to be introduced. The difference in the time course of phosphodiesterase activation reflects the possibility that phosphodiesterase activation may not be extremely rapid and may require cooperative binding of activated transducins. I believe the final justification for my description of the rising phase of the photocurrent, and therefore the light-induced

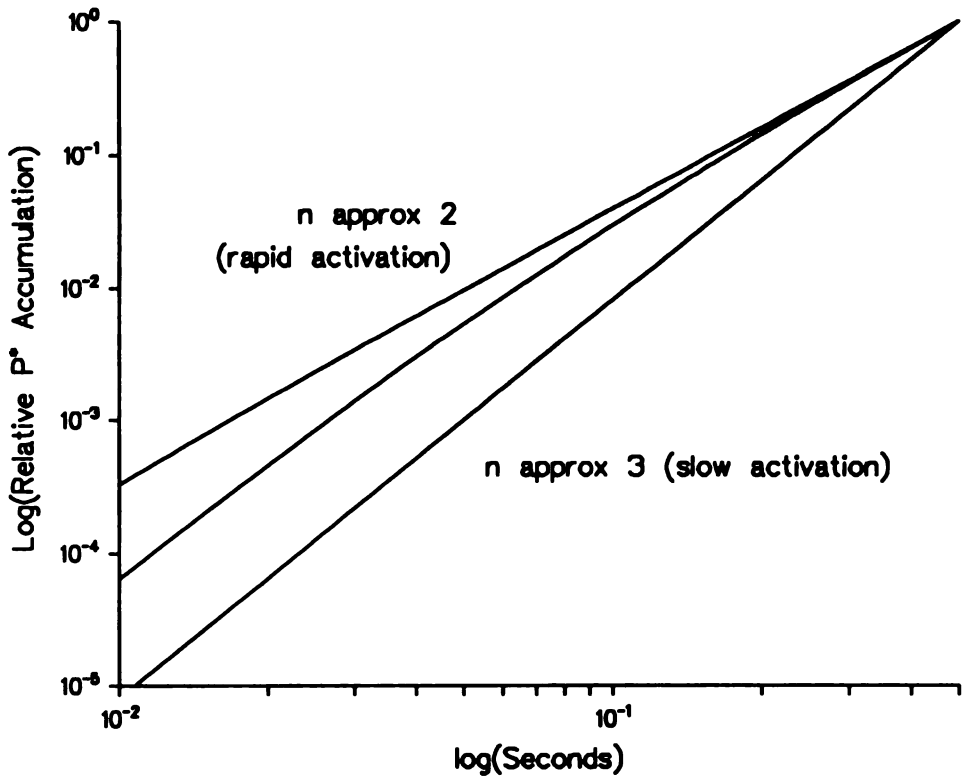

Figure B1. A comparison of the time dependence of phosphodiesterase accumulation when its activation is rapid (n = 2), slow (n = 3) and intermediate (2 < n < 3). All curves have been set to a value of 1 at 0.5 seconds for comparison.

APPENDIX C: HOMOGENEOUS RADIAL DIFFUSION

My solution to the homogeneous radial diffusion problem is described below. It is presented here for completeness and to make explicit the boundary conditions. It is not unique in terms of general principles; similar mathematical techniques are found in many texts on differential equations. The particular approach was inspired by analogous problems in electromagnetics (see for example Jackson, 1975). Useful properties of Bessel functions are neatly listed by Abramowitz and Stegun, 1972.

The rate of change in the total calcium concentration at any point in the rod is described by the diffusion equation.

$$\dot{Ca}_t(r,t) = \beta\ \dot{Ca}(r,t) = D\ \nabla^2\ Ca(r,t) \qquad \text{(C1)}$$

where Ca_t is the total calcium concentration which is equal to the buffering power, β, times the free concentration of calcium, Ca. The buffer is assumed to have a low affinity for calcium. The variable, D, is the intrinsic diffusion coefficient for calcium in the cytosol. I expect that its value will be similar to the value that is obtained in a standard salt solution of the same ionic strength, (Handbook of Chemistry and Physics, 1971). Cytoskeletal components and cytosolic viscosity may, however, be significant hindrances to calcium mobility; in which case, I would expect a lower value of D.

The general solution to the differential equation invokes the common technique

of separating the temporal and spatial dependence of the calcium distribution such that $Ca(r,t) = T(t)\,X(r)$ which results in a set of eigenfunctions which satisfy the relationship:

$$\frac{\dot{T}_m}{T_m} = \frac{D}{\beta}\frac{\nabla^2 X_m}{X_m} = -\frac{1}{\tau_m} \qquad \text{(C2)}$$

I have selected time constants, τ_m, to be the eigenvalues.

The solution to the diffusion equation can therefore be written as:

$$Ca(r,t) = Ca_0 \sum_m^{\infty} A_m\, J_0(r/\lambda_m)\, e^{-t/\tau_m} \qquad \text{(C3a)}$$

such that

$$\lambda_m^2 = \frac{D}{\beta}\tau_m \qquad \text{(C3b)}$$

where Ca_0 is the initial free calcium concentration, A_m are constants, $J_0(r/\lambda_m)$ is a zero-order Bessel function of the first kind, and λ_m are cylindrical length constants.

The first boundary condition that generates the specific solution to the problem is that the free calcium concentration is evenly distributed within the outer segment before the cyclic GMP-gated channels begin to close in response to illumination. That is:

$$\sum_m^{\infty} A_m\, J_0(r/\lambda_m) = 1 \qquad \text{(C4)}$$

for any $r < R$, the total radius of the rod. Making use of the orthogonal nature of Bessel functions;

$$\int_0^R r\, J_0(r/\lambda_n)\, J_0(r/\lambda_m)\, dr = \frac{R^2}{2} \left[J_0^2(R/\lambda_m) + J_1^2(R/\lambda_m) \right] \tag{C5}$$

when n = m and zero otherwise, to obtain:

$$A_m = 2\, \frac{\lambda_m^2}{R^2}\, \frac{(R/\lambda_m)\, J_0(R/\lambda_m)}{J_0^2(R/\lambda_m) + J_1^2(R/\lambda_m)} \tag{C6}$$

The second boundary condition requires that the rate of change of total calcium is equal to the rate at which it is extruded by the exchanger.

$$\int_V \dot{Ca}_i(r,t)\, dV = \frac{J_{ex}(t)}{eA_v} = \frac{J_{ex}(0)}{eA_v}\, \frac{Ca_i(R,t)}{Ca_o} \tag{C7}$$

where the integration is over the outer segment volume, V. $J_{ex}(t)$ is the exchange current which is proportional to the free calcium concentration at the plasma membrane, $Ca(R,t)$. A_v is Avagadro's Number and e is the quantal charge. This condition results in the requirement that:

$$\frac{(R/\lambda_m)\, J_1(R/\lambda_m)}{J_0(R/\lambda_m)} = \varepsilon \tag{C8a}$$

where a constant, ε, has been defined to simplify notation as:

$$\varepsilon = - \frac{J_{ex}(0)}{eA_v V Ca_i(0)} \frac{R^2 \beta}{2 D} \qquad \text{(C8b)}$$

Eqn (C8) may alternatively be considered a result of the requirement that the gradient of the free calcium concentration near the plasma membrane must be proportional to the flux across the membrane.

Eqns (C3), (C6) and (C8) may be combined to express the radial distribution of free calcium as:

$$Ca(r,t) = Ca_o \sum_m^{\infty} \frac{2 \varepsilon}{(R/\lambda_m)^2 + \varepsilon^2} \frac{J_0(r/\lambda_m)}{J_0(R/\lambda_m)} e^{-t/\tau_m} \qquad \text{(C9)}$$

from which the exchange current is obtained by setting $r = R$

$$J_{ex}(t) = J_{ex}(0) \sum_m^{\infty} \frac{2 \varepsilon}{(R/\lambda_m)^2 + \varepsilon^2} e^{-t/\tau_m} \qquad \text{(C10)}$$

and the space-averaged free calcium concentration is

$$\langle Ca(t) \rangle = \frac{1}{V} \int_V Ca(r,t)\, dv = Ca_o \sum_m^{\infty} \frac{2 \varepsilon}{(R/\lambda_m)^2 + \varepsilon^2} \frac{2 \varepsilon}{(R/\lambda_m)^2} e^{-t/\tau_m} \qquad \text{(C11)}$$

These are the equations presented in the text. Their numerical evaluation requires that the values of λ_m be determined. These parameters are constrained for any value of ε (Eqn (C8)) but there is no analytic solution. I relied on graphical estimates and regressive iteration to determine their values for the first few terms. For higher order

terms, λ_m are such the (R/λ_m) are very close to the zeroes of $J_0(R/\lambda_m)$

In the text, I state that the time course of the free calcium concentration could be represented as a series summation of exponentials for any well behaved spatial variation in the mobility of calcium ions. This is true when the buffering power, $\beta(r)$, and diffusion coefficient, $D(r)$, are time-invariant. A necessary but not sufficient condition of this property is that the dominant buffering system has a low affinity for calcium. If the condition is satisfied, the diffusion equation may be written as:

$$\beta(r)\ \dot{Ca}(r,t) = \nabla(\ D(r)\ \nabla Ca(r,t)) \tag{C12}$$

It should be clear that $Ca(r,t)$ may still be expressed as $T(t)X(r)$ to yield

$$Ca(r,t) = Ca_o \sum_m^{\infty} X_m(r)\ e^{-t/\tau_m} \tag{C13}$$

where $X_m(r)$ are the eigenfunction solutions of the Sturm-Liouville differential equation:

$$\nabla(D(r)\ \nabla X(r)) + \frac{\beta(r)}{\tau_m} X_m(r) = 0 \tag{C14}$$

The boundary conditions are the same as before, but $X_m(r)$ cannot be determined without knowing $D(r)$ and $\beta(r)$.

APPENDIX D - A TWO-COMPARTMENT MODEL FOR CALCIUM KINETICS

The compartmental model presented in the text is fundamentally a phenomenological model. It accurately predicts the magnitude and kinetics of the measured calcium concentrations but does not assume a specific physical process. It is always tempting, however, to ascribe a physical basis to such a model. There are several possible interpretations of the compartment model. I prefer to believe it is a reflection of radially non-uniform restrictions on calcium mobility arising from variations in the calcium buffering power, cytoskeletal components or the facilitation of diffusion that may be provided by disk incisures. I derive the parameters of the compartment model with this hypothesis in mind but recognize that the model has a value that is independent of the specific interpretation.

My interpretation of the compartment model grossly simplifies a realistic calcium distribution by assuming two idealized domains within the outer segment. One of these is considered to be adjacent to the plasma membrane. The free calcium concentration it contains is assumed to be proportional to the exchange current. The other, central domain, does not communicate directly with the plasma membrane. When calcium influx through the cyclic GMP-gated channels is abruptly halted by bright illumination, the rate of change of total calcium within each domain may be approximated as:

$$\beta_1 V_1 \dot{Ca}_1 = \frac{J_{ex}(0)}{eA_v} \frac{Ca_1}{Ca_o} + \alpha (Ca_2 - Ca_1) \qquad \text{(D1)}$$

$$\beta_2 V_2 \dot{Ca}_2 = - \alpha (Ca_2 - Ca_1)$$

where Ca_1 (Ca_2) is the free calcium concentration within the peripheral (central) domain with an idealized volume of V_1 (V_2) and a low-affinity buffering power of β_1 (β_2). The rate constant, α, describes how easily calcium may move between the domains. Intuitively, α depends on the diffusion coefficients of both domains. All other variables have their usual meaning (see Chapter 4 and Appendix C).

The Laplace transform solution of Eqn (D1) is:

$$\tilde{Ca}_1 = Ca_o \frac{s + \alpha_1 + \alpha_2}{s^2 + s(\alpha_1 + \alpha_2 + \alpha_{ex}) + \alpha_2 \alpha_{ex}} \qquad \text{(D2)}$$

$$\tilde{Ca}_2 = \frac{\alpha_2}{s + \alpha_2} (\tilde{Ca}_1 + Ca_o)$$

where

$$\alpha_1 = \frac{\alpha}{\beta_1 V_1} \qquad \alpha_2 = \frac{\alpha}{\beta_2 V_2} \qquad \alpha_{ex} = \frac{- J_{ex}(0)}{eA_v \beta_1 V_1 Ca_o} \qquad \text{(D3)}$$

Because I recognize the denominator of Eqn (D2), I make the substitutions:

$$\frac{1}{\tau_1} + \frac{1}{\tau_2} = \alpha_1 + \alpha_2 + \alpha_{ex} \tag{D4}$$

$$\frac{1}{\tau_1 \tau_2} = \alpha_2 \alpha_{ex}$$

The inverse Laplace transform is therefore:

$$Ca_1 = Ca_o \frac{\tau_1 (\alpha_{ex} \tau_2 - 1) e^{-t/\tau_1} + \tau_2 (1 - \alpha_{ex} \tau_1) e^{-t/\tau_2}}{\tau_2 - \tau_1} \tag{D5}$$

$$Ca_2 = Ca_o \frac{- \tau_1 e^{-t/\tau_1} + \tau_2 e^{-t/\tau_2}}{\tau_2 - \tau_1}$$

I show in the text that the exchange current is approximated by an empirical equation of the form:

$$\frac{Ca_1}{Ca_o} = \frac{J_{ex}}{J_{ex}(0)} = A_1 e^{-t/\tau_1} + A_2 e^{-t/\tau_2} \tag{D6}$$

where $A_1 + A_2 = 1$. I have equated the observed time constants with τ_1 and τ_2. In the same way, I make the connection that:

$$A_2 = \frac{\tau_2}{\tau_2 - \tau_1} (1 - \alpha_{ex} \tau_1) \tag{D7a}$$

which results in:

$$\alpha_{ex} = A_1/\tau_1 + A_2/\tau_2 \tag{D7b}$$

Eqn (D7b) and a rearrangement of Eqn (D4) are presented in Chapter 4 as Eqn (10). These are the most of the independent parameters of the compartment model.

The space-averaged calcium concentration is assumed to be a weighted average of the free calcium concentrations in the peripheral and central domains. I interpret the weighting factor to represent the fraction of the total volume of the outer segment that is associated with each domain. Therefore:

$$\langle Ca \rangle = a_1 \, Ca_1 + (1 - a_1) \, Ca_2 \qquad \text{where} \qquad a_1 = \frac{V_1}{V_1 + V_2} \tag{D8}$$

which results in:

$$\frac{\langle Ca \rangle}{Ca_o} = \frac{\tau_1 \, (\alpha_{ex} \, \tau_2 \, a_1 - 1) \, e^{-t/\tau_1} + \tau_2 \, (1 - \alpha_{ex} \, \tau_1 \, a_1) \, e^{-t/\tau_2}}{\tau_2 - \tau_1} \tag{D9}$$

Like the exchange current, the measured calcium concentration can be approximated by a function of the form:

$$\frac{\langle Ca \rangle}{Ca_o} = B_1 \, e^{-t/\tau_1} + B_2 \, e^{-t/\tau_2} \tag{D10a}$$

Solving for a_1, we obtain:

$$a_1 = \frac{B_1/\tau_1 + B_2/\tau_2}{A_1/\tau_1 + A_2/\tau_2} \tag{D10b}$$

where a substitution for α_{ex} has been made from Eqn (D7b).

Eqn (D10b) completes the determination of the compartment model parameters. Note that it was not necessary to assume specific buffering capacities of each domain or the magnitude of the flux between them. Nor was it strictly necessary to equate the weighting factor with a volume fraction although this is the interpretation that is most consistent with my original motivation.

The model as it stands at this point is simply descriptive of the exchange current and calcium concentration that are measured during bright illumination. I now include calcium influx through the cyclic GMP-gated channel to create a predictive model.

The rate of change of total calcium, independent of the distribution of calcium within the outer segment, can be written as:

$$\int_V \dot{Ca}_t \, dV = \int_V \beta(r) \, \dot{Ca}(r,t) \, dV = - \frac{1}{eA_v} \left[\frac{f}{2} J_g(t) - J_{ex}(t) \right] \qquad \text{(D11a)}$$

The right-hand side of this equation can be rewritten as:

$$\frac{f}{2} J_g(t) - J_{ex}(t) = \frac{J_{ex}(0) \, J_t(0)}{J_t(0) - J_{ex}(0)} \left[\frac{J_t(t)}{J_t(0)} - \frac{J_{ex}(t)}{J_{ex}(0)} \right] \qquad \text{(D11b)}$$

by noting that $f/2 = J_{ex}(0)/J_g(0)$ and $J_g(t) = J_t(t) - J_{ex}(t)$, where J_t is the total current flowing across the plasma membrane.

Comparing Eqn (D11) and Eqn (D1), it is clear that the complete compartmental model can be written as:

$$\dot{Ca}_1 = \alpha_{ex} \frac{J_r(0)}{J_r(0) - J_{ex}(0)} \left(\frac{J_r}{J_r(0)} - \frac{Ca_1}{Ca_o} \right) + \alpha_1 \left(Ca_2 - Ca_1 \right) \qquad \text{(D12)}$$

$$\dot{Ca}_2 = - \alpha_2 \left(Ca_2 - Ca_1 \right)$$

with

$$\frac{J_{ex}}{J_{ex}(0)} = \frac{Ca_1}{Ca_o} \qquad \text{and} \qquad \langle Ca \rangle = a_1 \, Ca + (1 - a_1) \, Ca_2 \qquad \text{(D6, D8)}$$

A general analytic solution of these equations is not, of course, possible without a complete analytic description of J_r. An evaluation by numeric integration allows, however, for the equating of J_r with the normalized photocurrents that are measured. Thus the exchange current and space-averaged calcium concentration are predicted from actual data - as complete a representation of the rod's response to illumination as is available.

I suggest that the compartment model is an approximate description of the spatial variation in calcium mobility within the outer segment. How different is the mobility in the central domain with respect to the periphery? From Eqn. (D3), the relative rate of change of free calcium within the central domain with respect to the peripheral domain due to movement of calcium between the domains can be written as:

$$\frac{\alpha_1}{\alpha_2} = \frac{\beta_2 \, V_2}{\beta_1 \, V_1} = \frac{\beta_2}{\beta_1} \frac{1 - a_1}{a_1} \qquad \text{(D13)}$$

This equation explicitly states that the relative mobility of calcium is proportional to the

relative effective buffering capacities of the domains. It may be that the actual buffering power is significantly different in each domain but I do not know this for sure. I do know, however, that the entire compartment model representation is a simplification. I also know that the effective diffusion coefficient in each domain can be approximated as:

$$D_{eff,1} = D_1/\beta_1 \qquad \text{and} \qquad D_{eff,2} = D_2/\beta_2 \tag{D14}$$

where $D_{eff,1}$ ($D_{eff,2}$) is the effective diffusion coefficient in the periphery (center). I therefore consider that the ratio β_1/β_2 is more informatively written as $D_{eff,2}/D_{eff,1}$. The mobility of calcium ions in the peripheral domain with respect to their mobility in the central domain can therefore be written as:

$$\frac{D_{eff,1}}{D_{eff,2}} = \frac{\alpha_1}{\alpha_2} \frac{a_1}{1 - a_1} \tag{D15}$$